Elettra Sincrotrone Trieste

Chemical and magnetic imaging with x-ray photoemission electron microscopy (XPEEM)

Andrea Locatelli

Andrea.locatelli@elettra.eu

Why do we need photoelectron microscopy?

- To combine SPECTROSCOPY and MICROSCOPY to characterise the structural, chemical and magnetic properties of surfaces, interfaces and thin films
- Applications in diverse fields such as surface science, catalysis, material science, magnetism but also geology, soil sciences, biology and medicine.

Surface Science

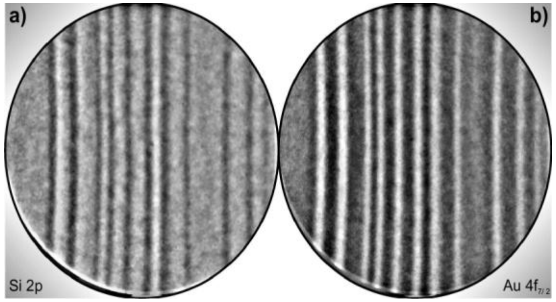

DOI: 10.1103/PhysRevLett.86.5088

Magnetism

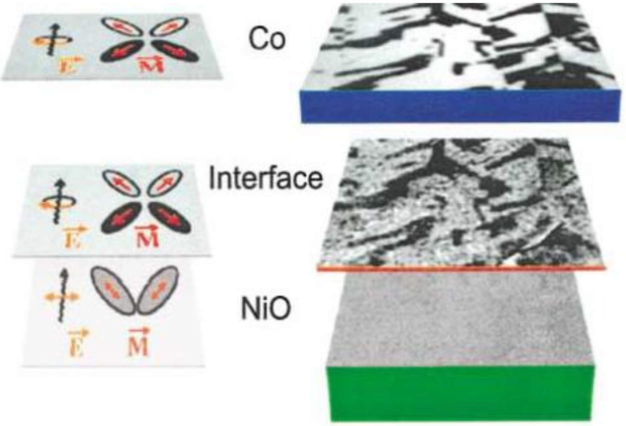

DOI: 10.1103/PhysRevLett.87.247201

Biology

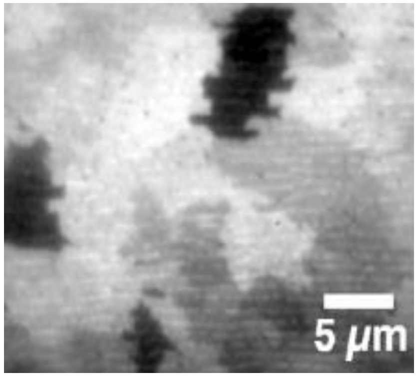

PRL **98,** 268102 (2007)

Outline

- Synchrotron radiation and x-ray spectro-microscopy: basics
- Cathode lens microscopy: methods
- Applications
  - Chemical imaging of micro- structured materials
  - Graphene research.
  - Biology
  - Magnetism
  - Time-resolved XPEEM

Why does PEEM need synchrotron radiation?

- High intensity of SR makes measurements faster
- Tuneability – very broad and continuous spectral range from IR to hard X-Rays
- Narrow angular collimation
- Coherence!
- High degree of polarization
- Pulsed time structure of SR – This adds time resolution to photoelectron spectroscopy!
- Quantitative control on SR parameters allows spectroscopy:
  - Absorption Spectroscopy (XAS and variants)
  - Photoemission Spectroscopies (XPS, UPS, ARPES, ARUPS)

$$J = f(h\nu, \varepsilon, \Theta, \Phi; E^{e}_{kin}, \sigma, \theta_e, \varphi_e)$$

Cathode lens microscopy methods

PEEM, LEEM, SPELEEM, AC-PEEM/LEEM

PEEM basics

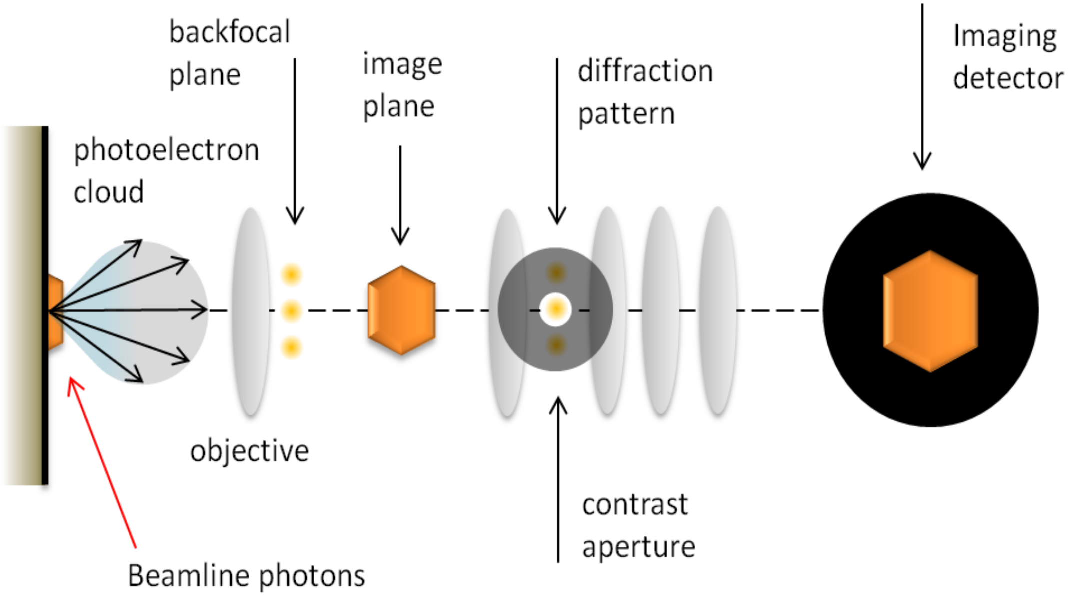

- Direct imaging, parallel detection
- Lateral resolution determined by electron optics: with AC, few nm possible
- Elemental sensitivity (XAS)
- Spectroscopic ability (energy filter)
- $P_{max} < 5 \cdot 10^{-5}$ mbar

PEEM is a full-field technique. The microscope images a restricted portion of the specimen area illuminated by x-ray beam. Photoemitted electrons are collected at the same time by the optics setup, which produces a magnified image of the surface. The key element of the microscope is the objective lens, also known as cathode or immersion lens, of which the sample is part

Cathode lens operation principle

Elettra Sincrotrone Trieste

1. In emission microscopy θ (emission angle) is large. Electron lenses can accept only small θ because of large chromatic and spherical aberrations

2. Solution of problem: accelerate electrons to high energy before lens $\rightarrow$ Immersion objective lens or cathode lens

$n \sin\theta = \text{const}$

$n \sim \sqrt{E}$

$\theta \rightarrow \alpha$

$\sin \alpha / \sin \alpha_0 = \sqrt{E_0/E}$

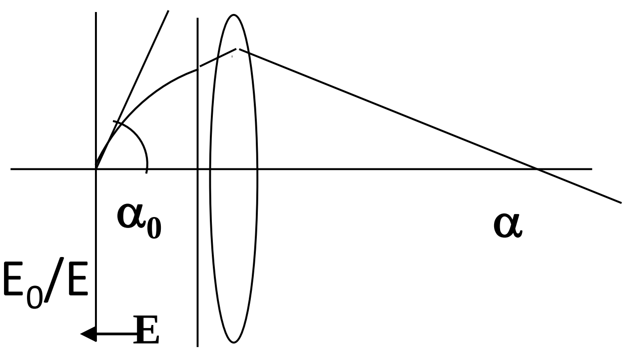

Example for E = 20000 eV:

E_0	2 eV	200 eV
α for $\alpha_0 = 45^o$	0.4^o	4.5^o

3. The aberrations of the objective lens and the contrast aperture size determine the lateral resolution

$$d = \sqrt{d_{SP}^2 + d_{CH}^2 + d_D^2}$$

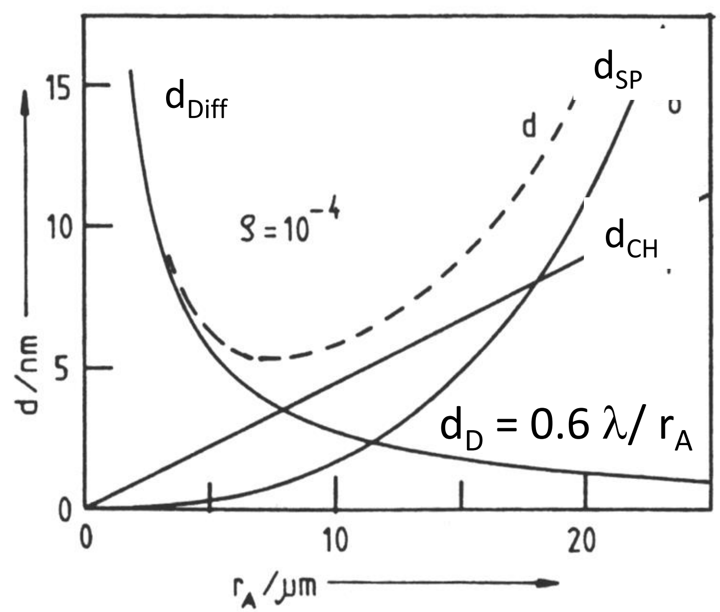

The different types of PEEM measurements

Elettra Sincrotrone Trieste

	PEEM	Probe	Measurement
•	threshold microscopy	Hg lamp	photoelectrons
•	Laterally resolved XPS, micro-spectroscopy	X-ray	core levels or VB ph.el.
•	Laterally resolved UPS, microprobe ARUPS /ARPES	X-rays, He lamp	VB photoelectrons
•	Auger Spectroscopy	X-ray, or electrons	secondary electrons
•	XAS-PEEM (XMC/LD-PEEM)	X rays	secondary electrons

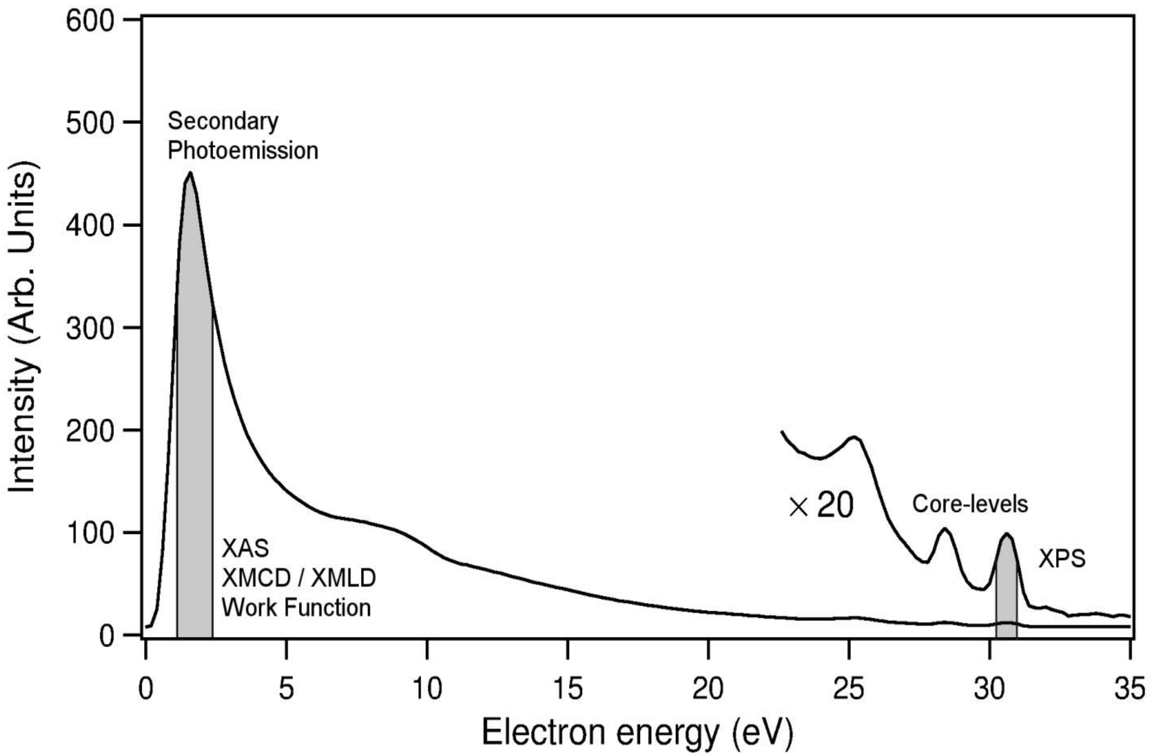

Require energy filter

Simple PEEM instruments

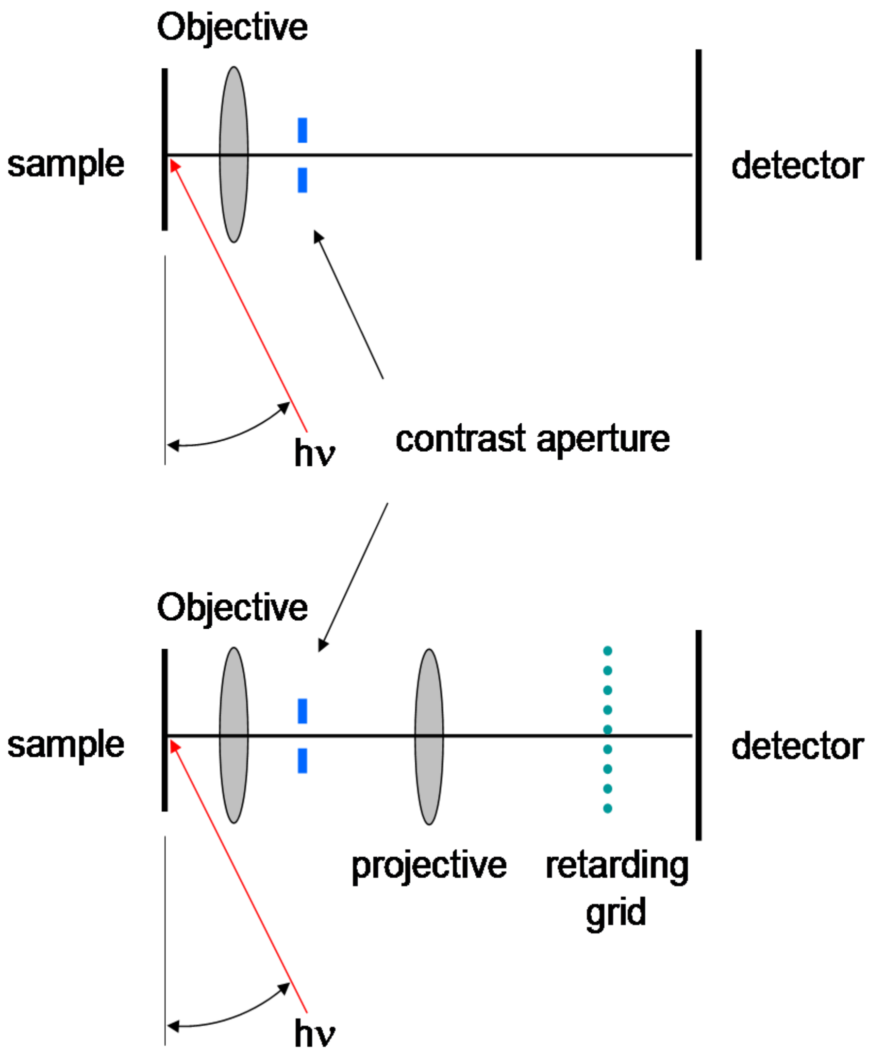

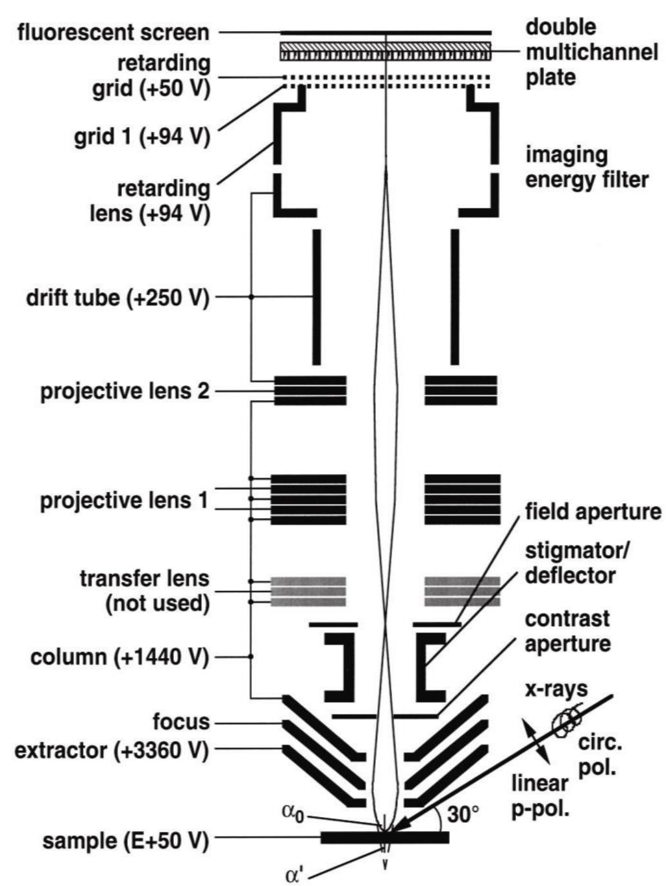

PEEM instrments with energy filter: NanoESCA

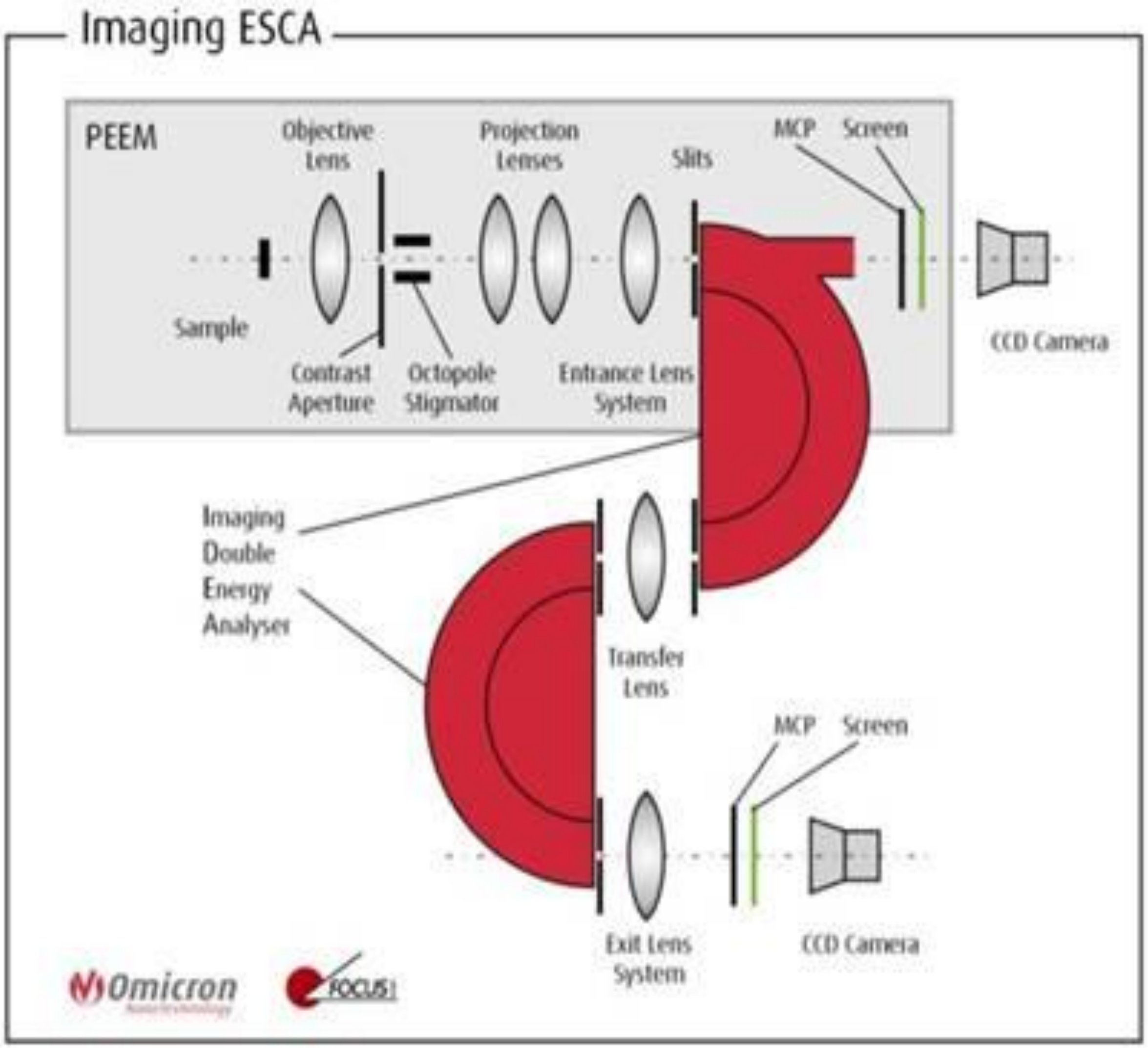

Low energy electron microscopy (LEEM)

Elettra Sincrotrone Trieste

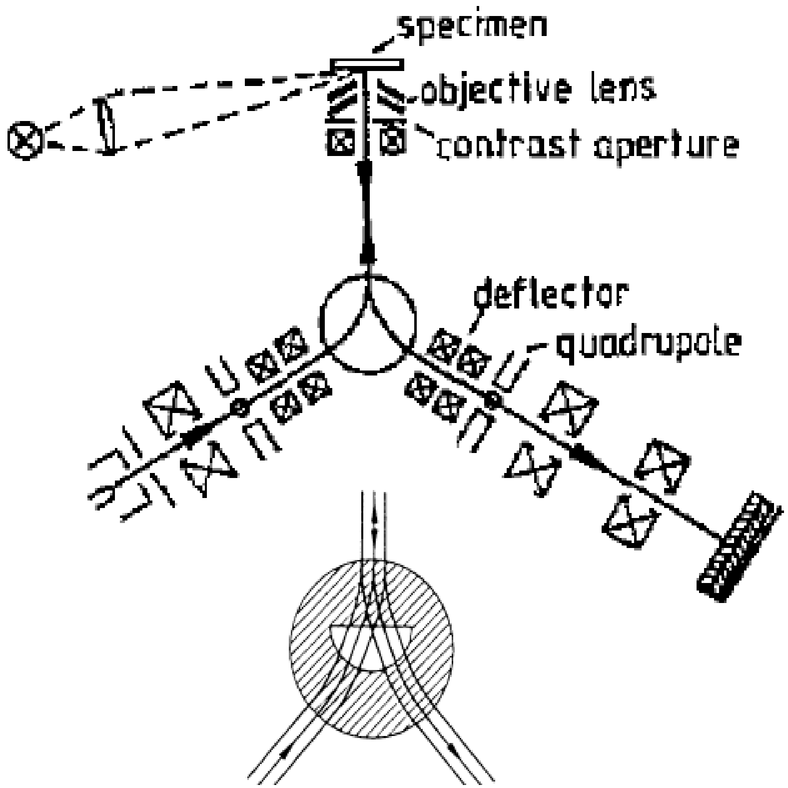

Backscattering cross section

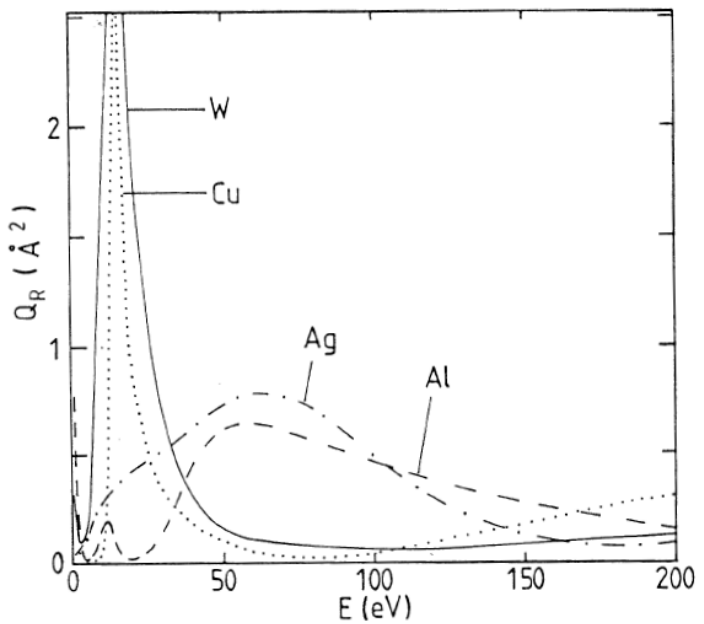

E. Bauer, Rep. Prog. Phys. 57 (1994) 895-938.

- LEEM probes surfaces with low energy electrons, using the elastically backscattered beam for imaging.
- Direct imaging and diffraction imaging modes

- High structure sensitivity
- High surface sensitivity
- Video rate: reconstructions, growth, step dynamics, self-organization

Imaging dynamic processes in LEEM

Elettra Sincrotrone Trieste

540 < T < 750 C

[001]

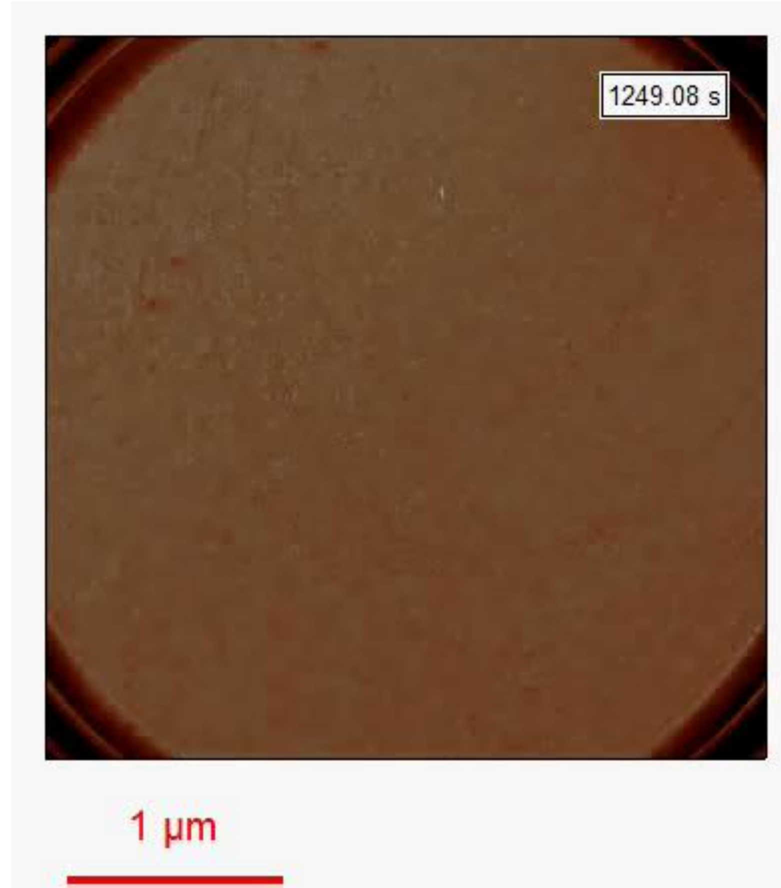

Ni growth on W(110): step flow and completion of ps ML

Ni growth on W(110): formation of a striped phase above 1 ps ML Ni

Image contrast in LEEM

Different contrast mechanisms are available for strucutre characterization

SURFACE STRUCTURE

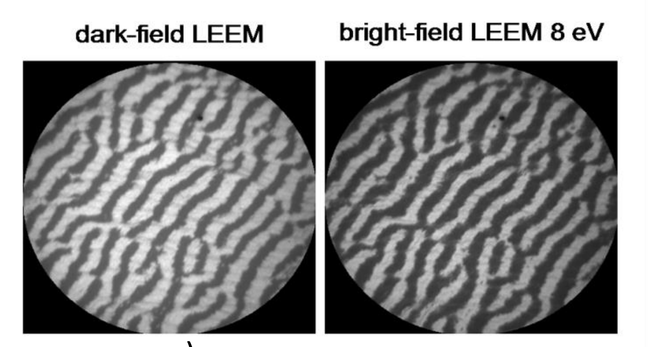

diffraction contrast

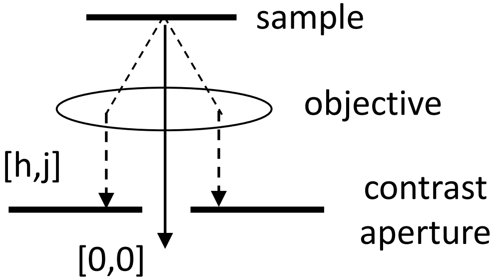

FILM THICKNESS

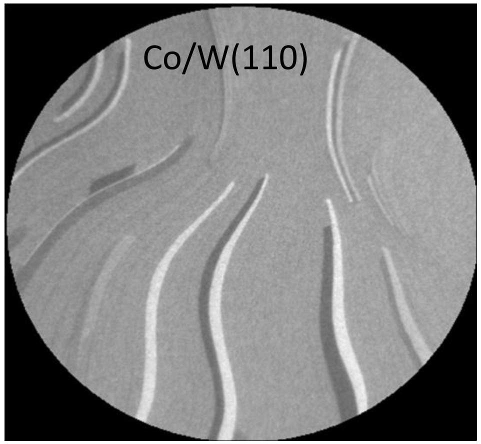

quantum size contrast

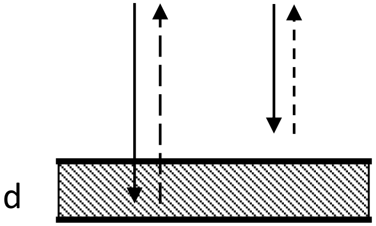

STEP MORPHOLOGY

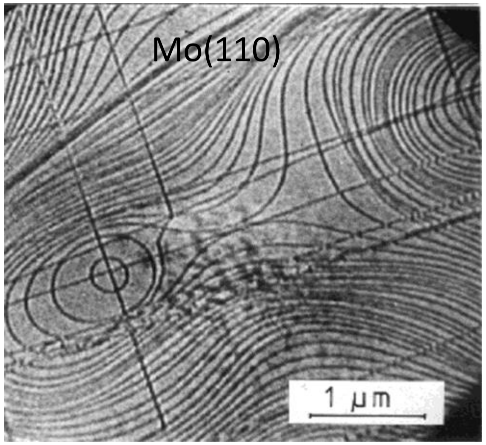

geometric phase contrast

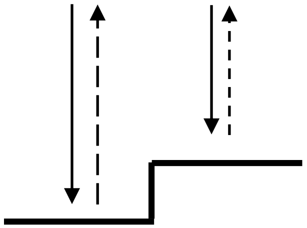

SPELEEM = LEEM + PEEM

Elettra Sincrotrone Trieste

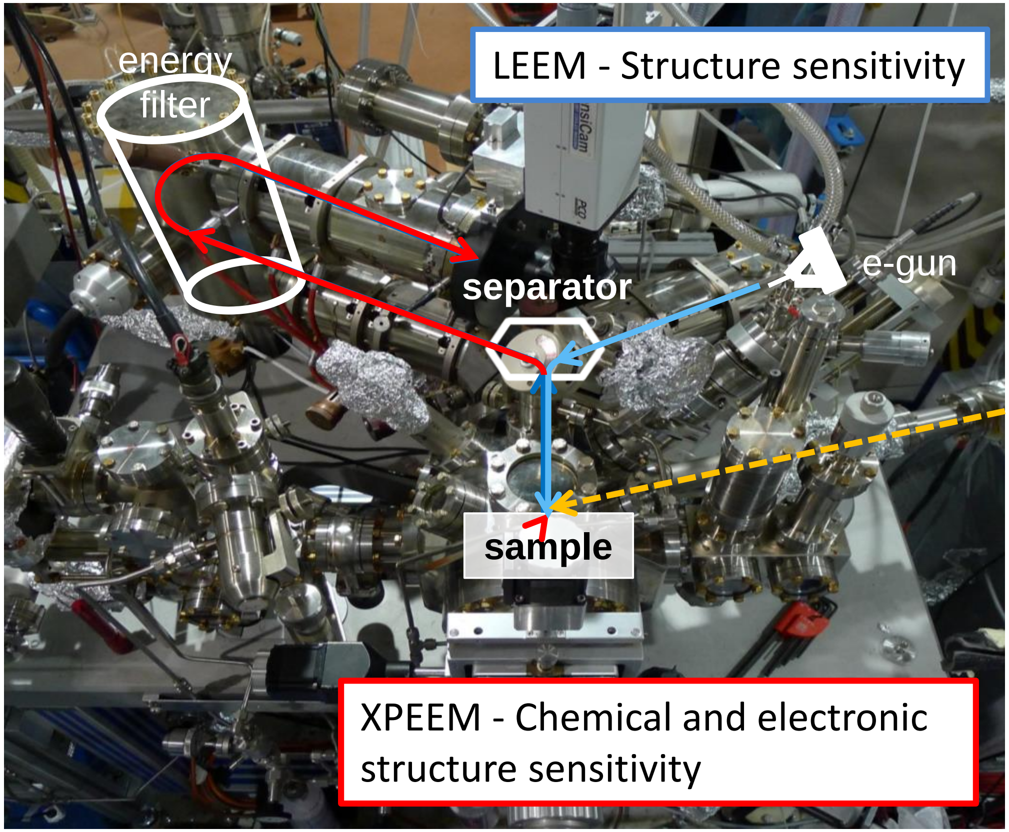

The Nanospectroscopy beamline@Elettra

Flux on the sample: 10^{13}ph/sec (microspot) intermediate energy resolution.

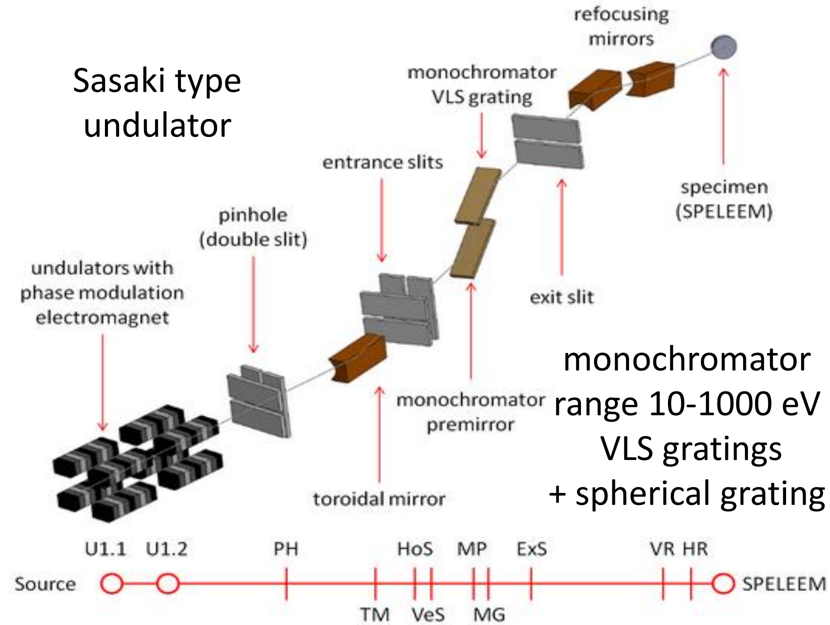

Applications:
characterization of materials at microscopic level, magnetic imaging of micro-structures
Imaging of dynamical processes

A. Locatelli, L. Aballe, T.O. Menteş, M. Kiskinova, E. Bauer, Surf. Interface Anal. 38, 1554-1557 (2006)

T. O. Menteş, G. Zamborlini, A. Sala, A. Locatelli; Beilstein J. Nanotechnol. 5, 1873–1886 (2014)

SPELEEM many methods analysis

Elettra Sincrotrone Trieste

Spectroscopic imaging	microprobe-diffraction	microprobe-spectroscopy
XAS-PEEM / XPEEM / LEEM	ARPES / LEED	XPS

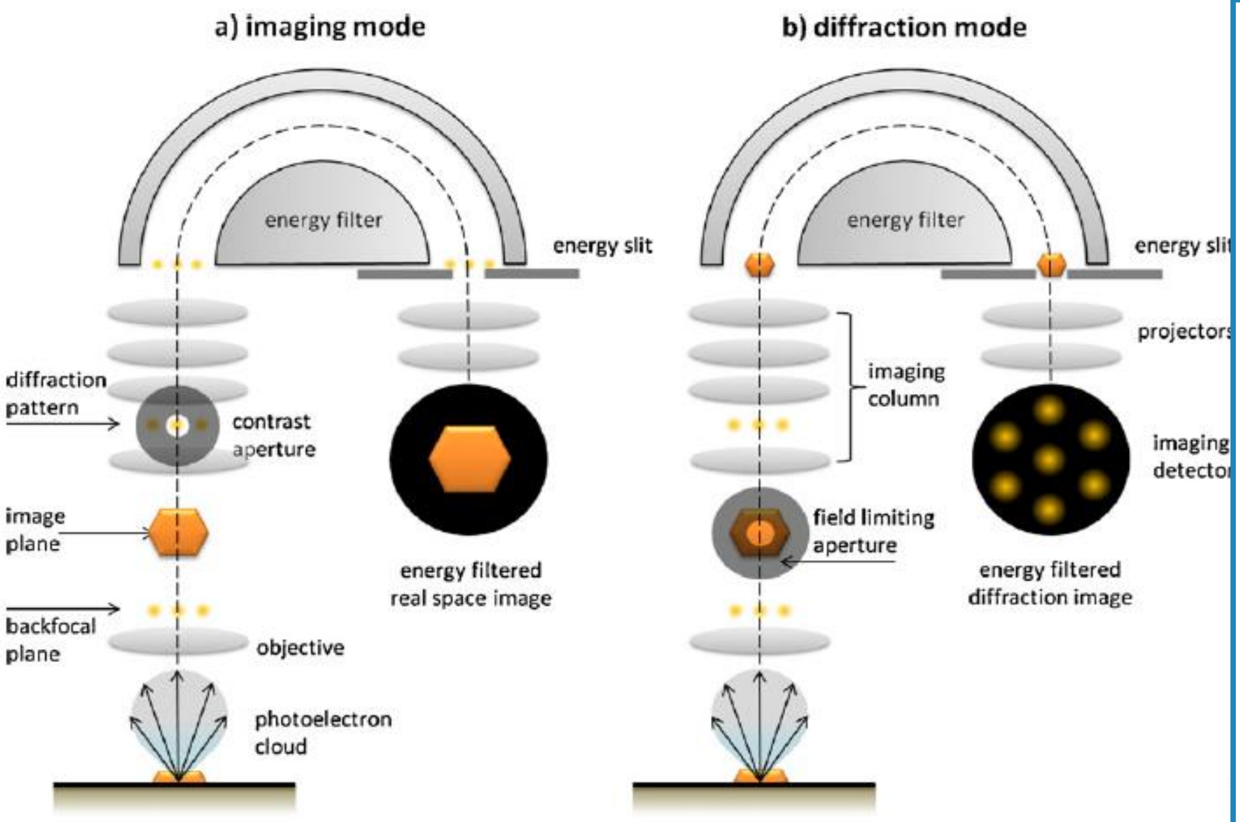

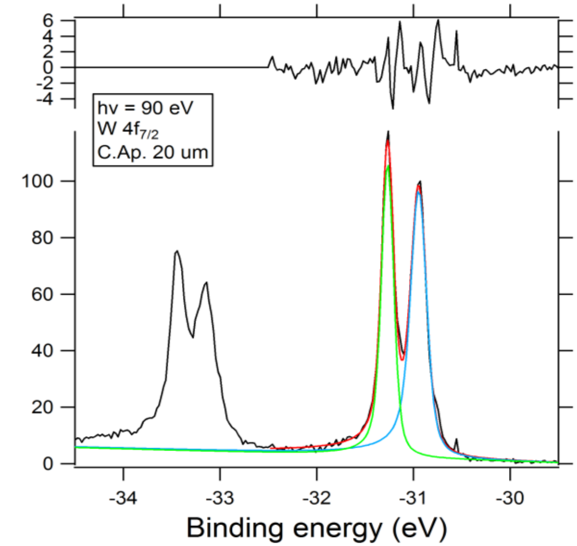

T. O. Menteş et al.
Beilstein J. Nanotechnol. 5, 1873–1886 (2014).

energy resolution
µXPS : 0.11 eV

spatial resolution
LEEM : 10 nm
XPEEM : 25 nm

energy resolution
XPEEM : 0.3 eV

Limited: to 2 microns in dia.
angular resolution
transfer width: 0.01 Å^{-1}

SPELEEM summary

Elettra Sincrotrone Trieste

Performance: lateral resolution in imaging: 10nm (LEEM)
30 nm (XPEEM)
energy resolution: 0.3 eV (0.1 eV muXPS)

Key feature: multi-method instrument to the study of surfaces and interfaces offering *imaging* and *diffraction* techniques.

Probe: *low energy e-* (0-500 eV) ⟷ structure sensitivity
soft X-rays (50-1000 eV) ⟷ chemical state, magnetic state, electronic struct.

Applications: *characterization* of materials at microscopic level
magnetic imaging of microstrucutres
dynamical processes

Correction of spherical and chromatic aberrations

Electron optics

Round **convex** lenses

Round **concave** lenses

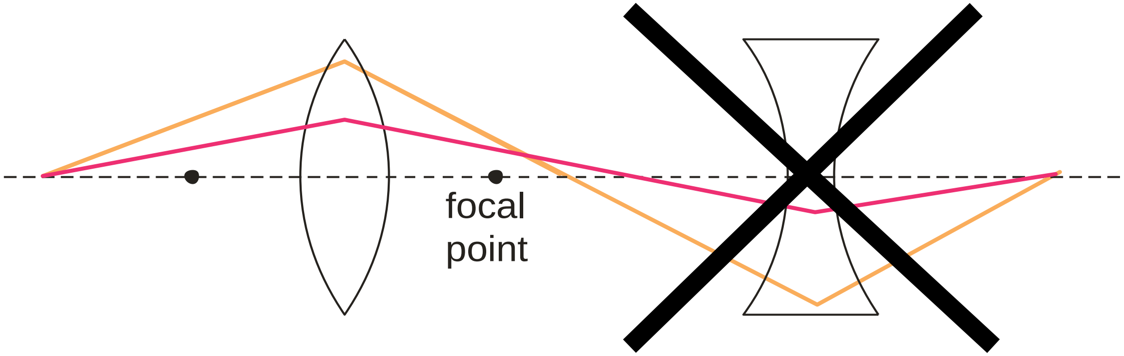

Spherical aberration

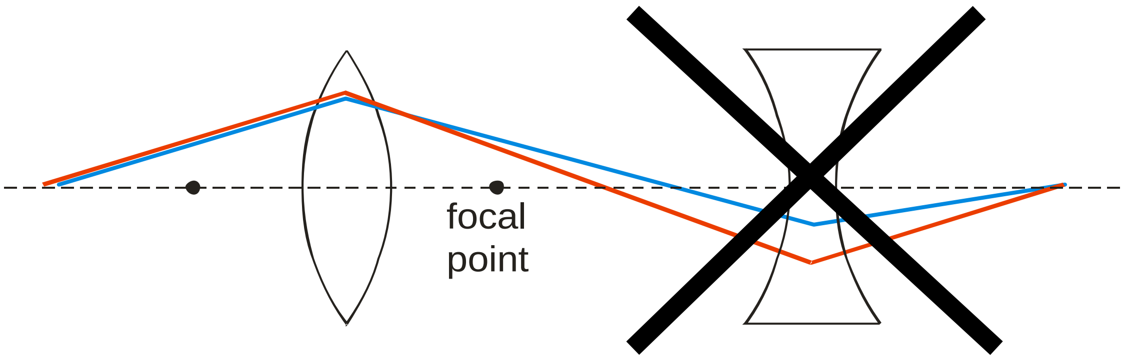

Chromatic aberration

Electron Mirror

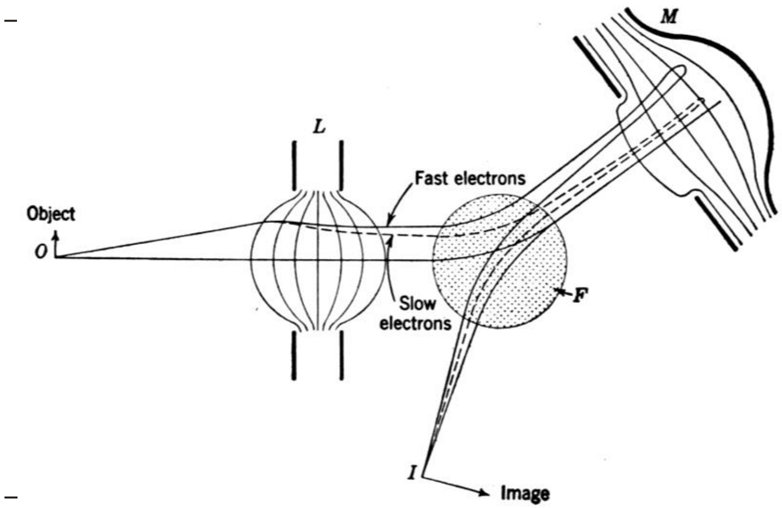

V.K. Zworykin et al, Electron Optics and the Electron Microscope, John Wiley, New York 1945

The SMART AC microscope: calculation

Elettra Sincrotrone Trieste

Simultaneous improvement in Transmission and Resolution!!!

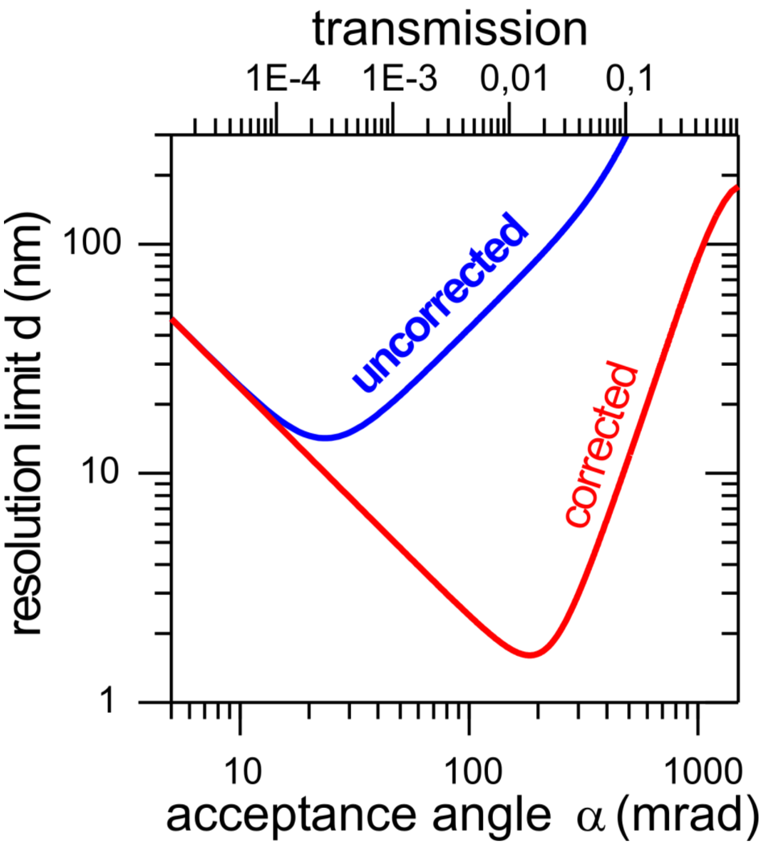

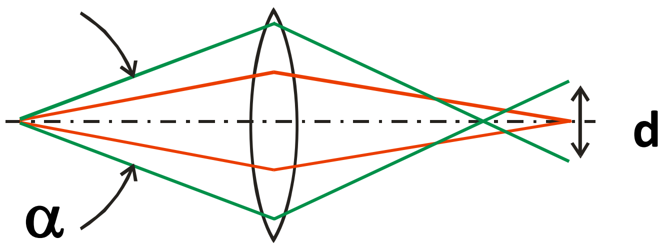

Resolution limit	without correction	with correction
Spherical	$\alpha^3 + \ldots$	α^5
Chromatic	$\Delta E\ \alpha + \ldots$	$\Delta E\ \alpha^2 + \Delta E^2\ \alpha$
Diffraction	$1/\alpha$	$1/\alpha$

D. Preikszas, H. Rose, J. Electr. Micr. 1 (1997) 1

Th. Schmidt, D. Preikszas, H. Rose et al., Surf.Rev.Lett 9 (2002) 223

First results of the SMART microscope @BESSY

Atomic steps on Au(111),
LEEM 16 eV, FoV = 444 nm x 444 nm
(18.09.06)

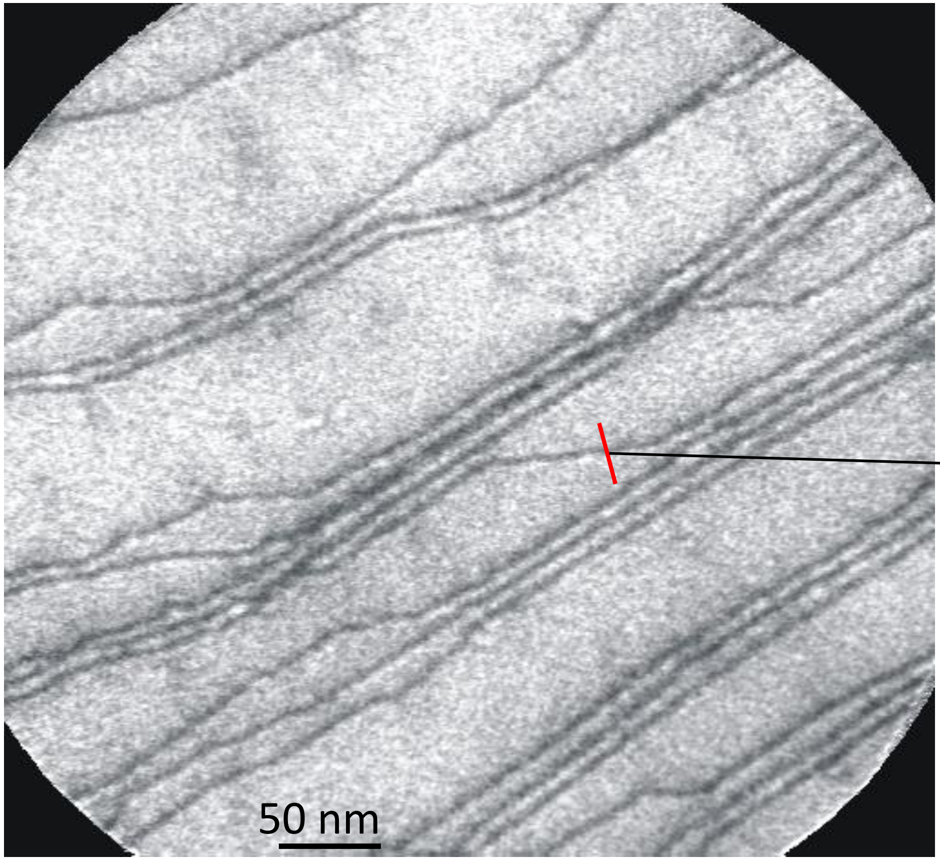

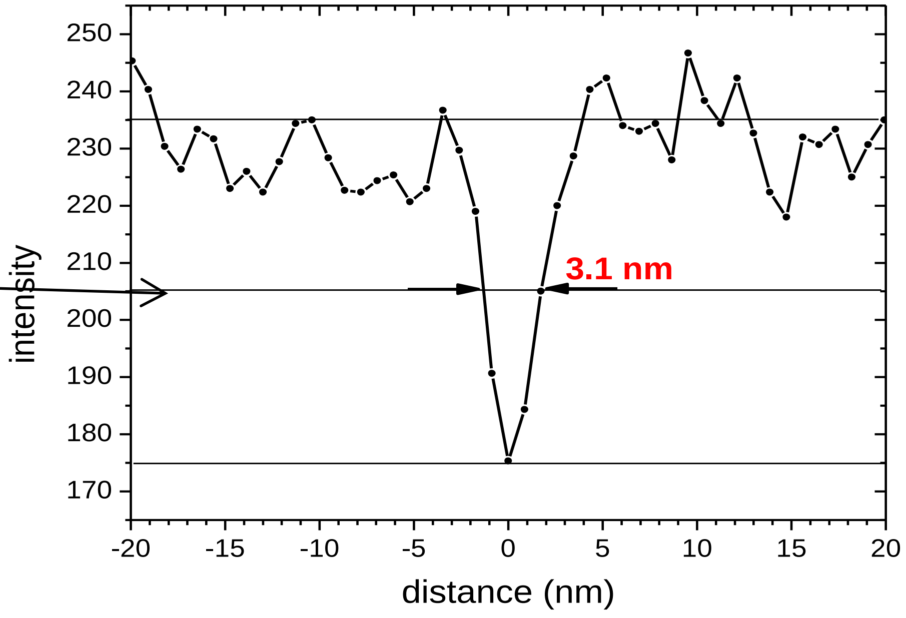

Courtesy of Th. Schmidt et al.; 5th Int. Conf. LEEM/PEEM, Himeji, 15.-19. Oct. 2006

Lateral resolution limitations: space charge

Elettra Sincrotrone Trieste

Ni/W(100) hv = 181 eV

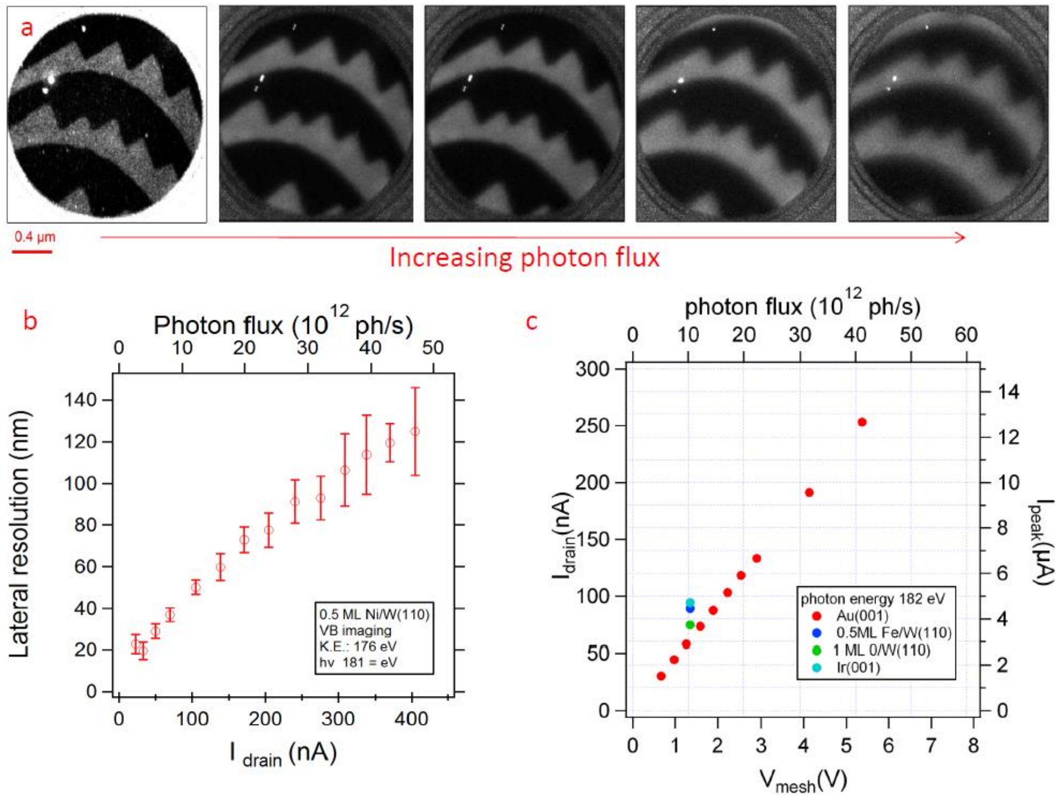

photocurrent estimate for SPELEEM@Elettra; Au/W(110)

- 440 bunches
  rev. frequency: 1.157 MHz
  bunch length: 42 ps (2GeV)
- 1 10^{13} ph./s on sample =
  = 20000 ph./bunch
- Total photoionization yield: about 2% photons result in a photoemission event
- $I_{peak} \approx 400\ e^-/ 42$ ps
  ≈ 1.5µA vs 20 nA (LEEM)

13 pA/µm² versus 20 nA/µm²

1. Image blur can be observed with SR but only under very high photon fluxes. Must Keep into account in beamline design. No space charge in LEEM
2. Both the lateral and energy resolution are strongly degraded by Boersch and Loeffler effects occurring in the first part of optical path.

Ultramicroscopy **111**, 1447 (2011).

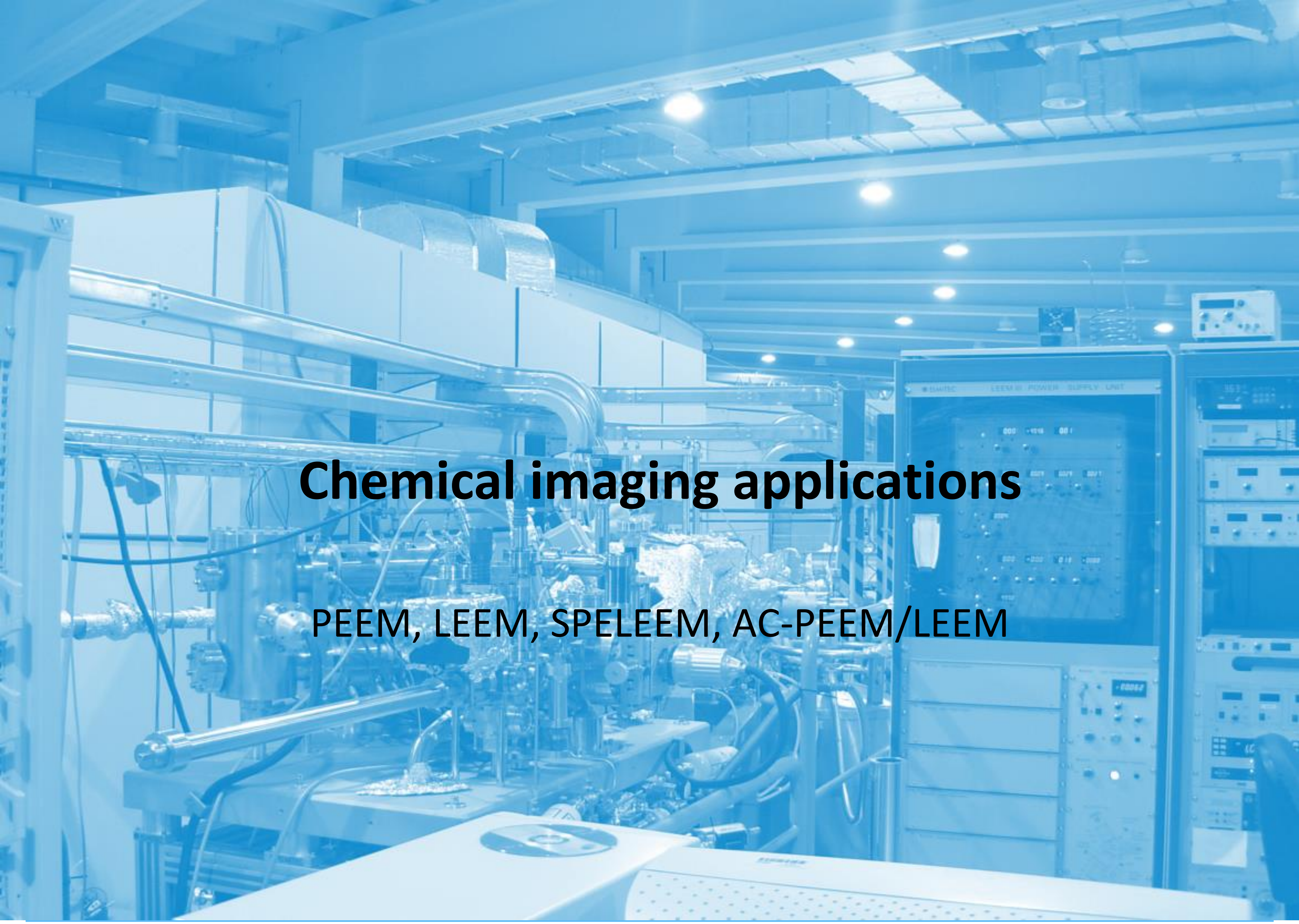

Chemical imaging applications

PEEM, LEEM, SPELEEM, AC-PEEM/LEEM

Au/TiO_2(110): controlling growth by vacancies

Creation of ordered oxygen vacancies

MEM
Work Function

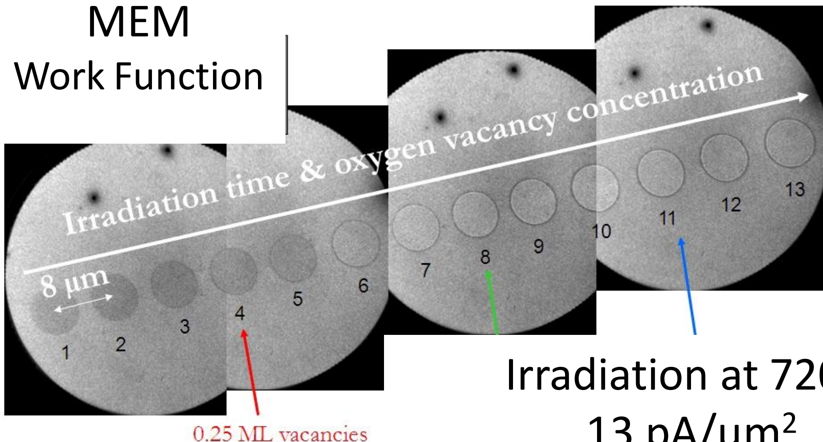

Irradiation at 720 K
13 pA/µm^2

Au growth on TiO_2(110)

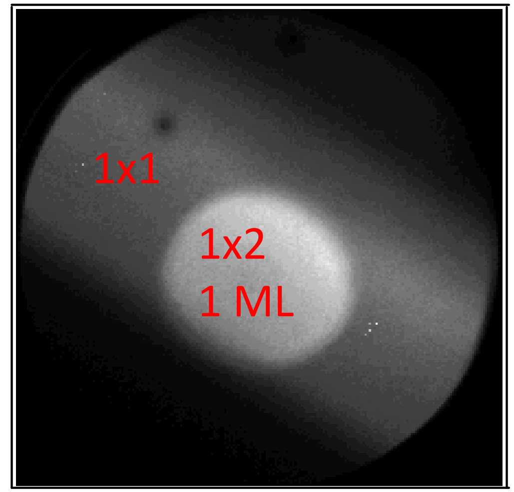

XPEEM
@ Au 4f

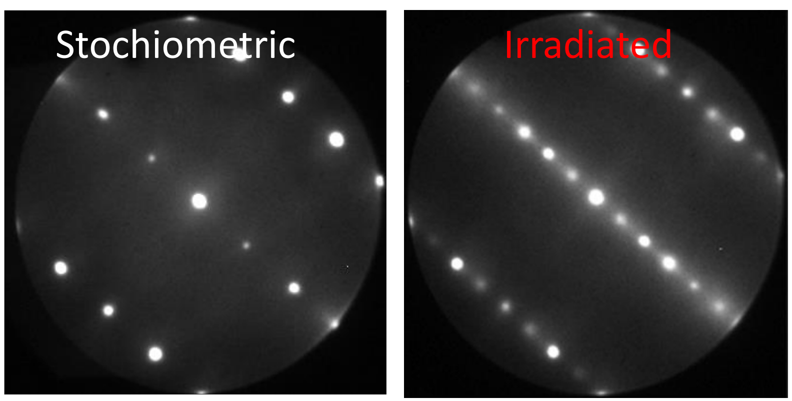

(1x1) (1x2)

µ-LE
struc

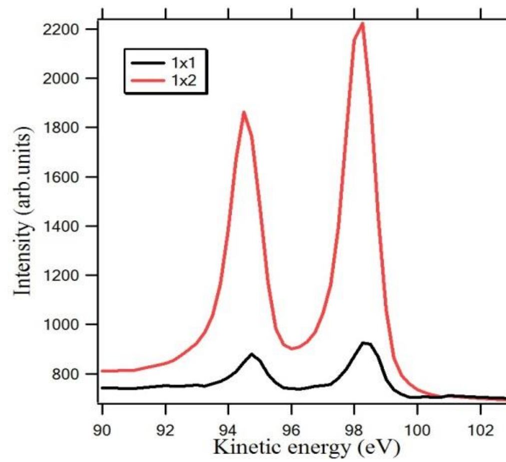

µ-XPS

Surface Oxygen on Ag : *e-beam "Lithography"*

Elettra Sincrotrone Trieste

Full oxidation of Ag using NO_2 does not occur:

$$NO_2 \rightarrow NO_{ad} + O_{ad}$$

Instead: e-beam (60 eV) stimulated desorption of NO_{ad} works at RT!

Low T: NO_{ad} stays, prevents oxidation.

High T: NO_{ad} desorbs, but Ag_2O unstable.

LEED reveals path towards Ag_2O under e-beam

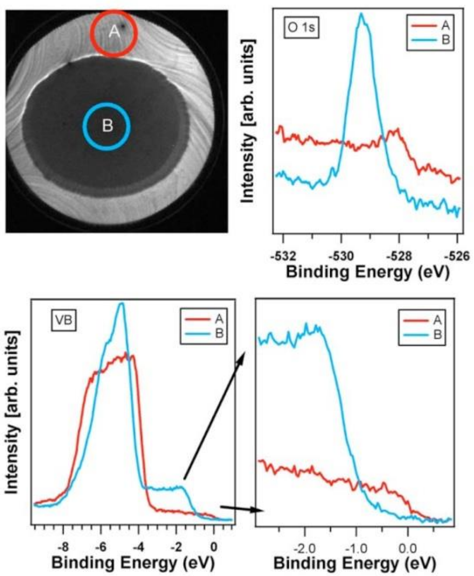

A: metallic Ag
B: Ag_2O

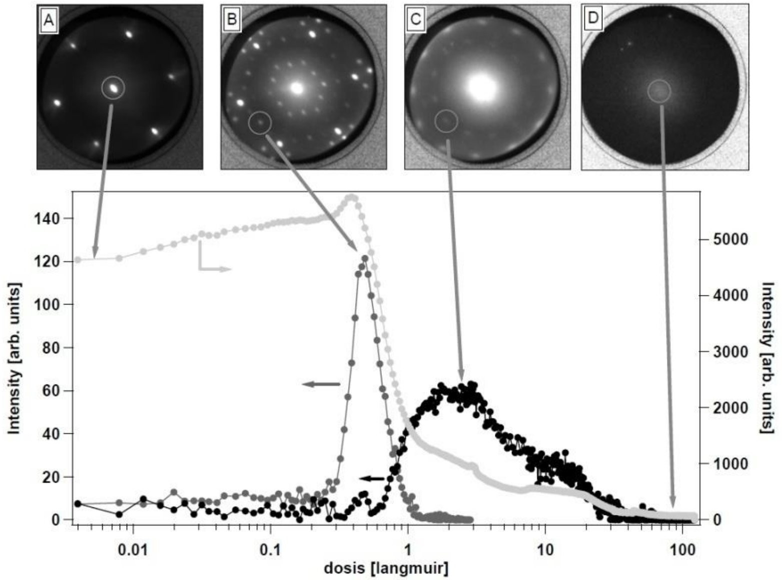

S. Günther *et al., App. Phys. Lett.* 93, 233117 (2008).

S. Günther *et al., Chem. Phys. Chem.* 2010.

Thickness dependent reactivity in Mg

Elettra Sincrotrone Trieste

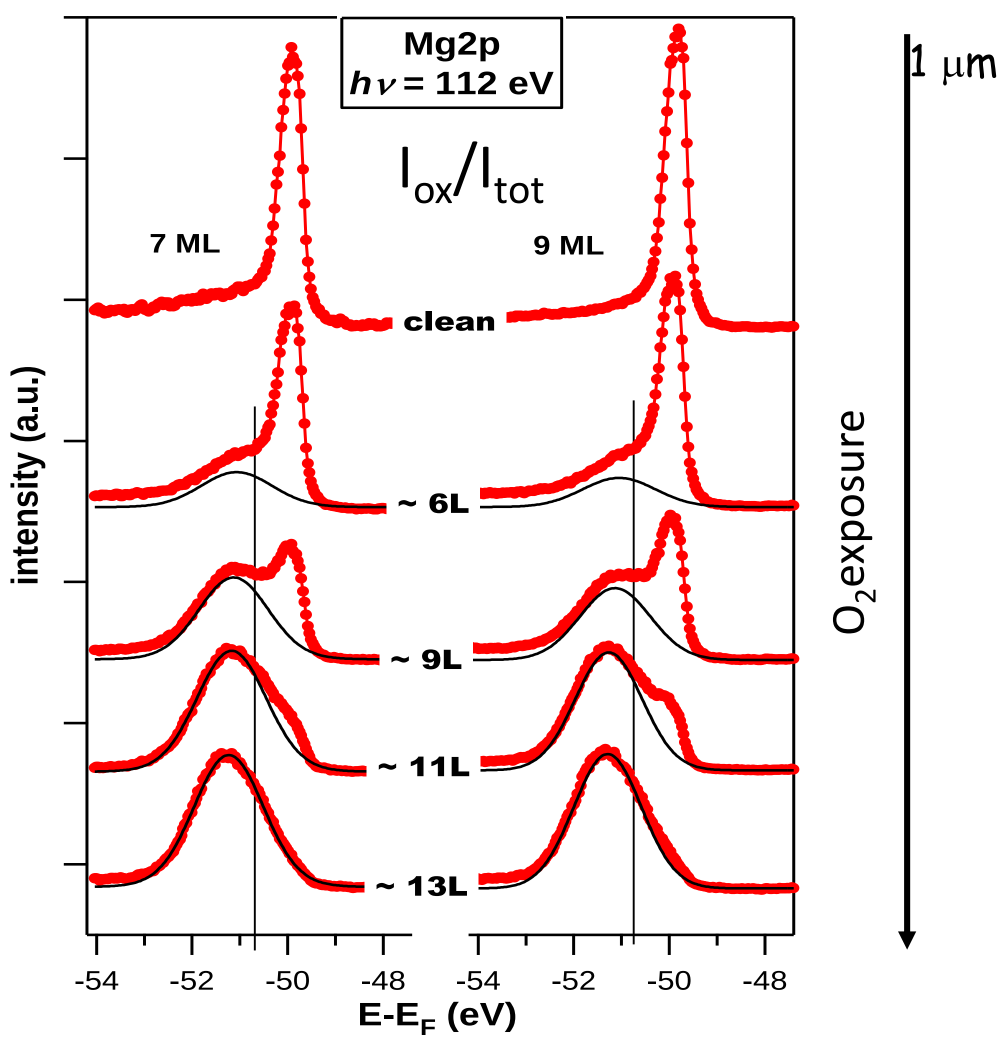

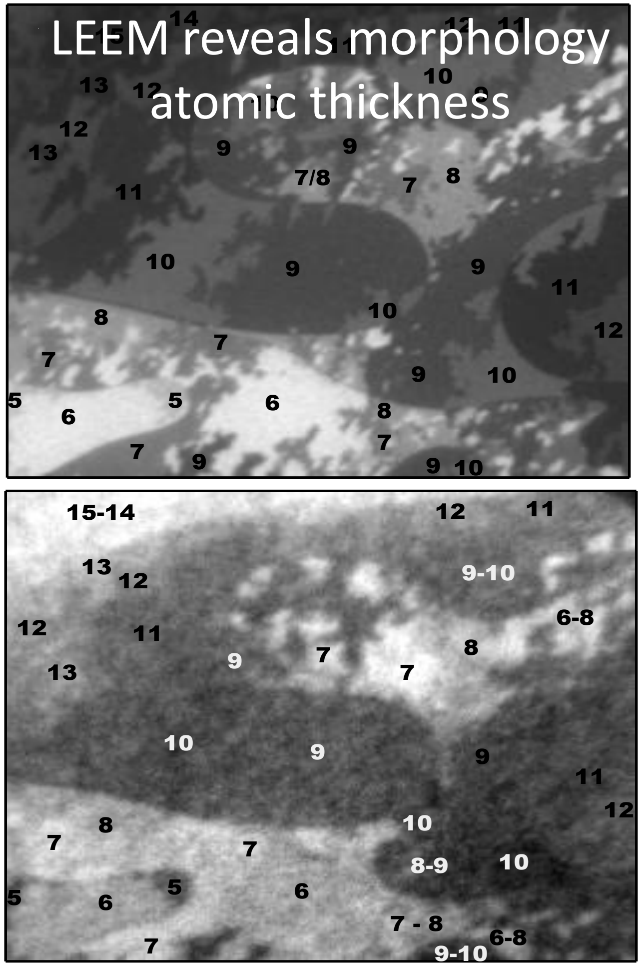

Oxide component reveals chemistry!

L. Aballe *et al.*, Phys. Rev. Lett. **93**, 196103 (2004)

Oxidation of Mg film and QWR

Elettra Sincrotrone Trieste

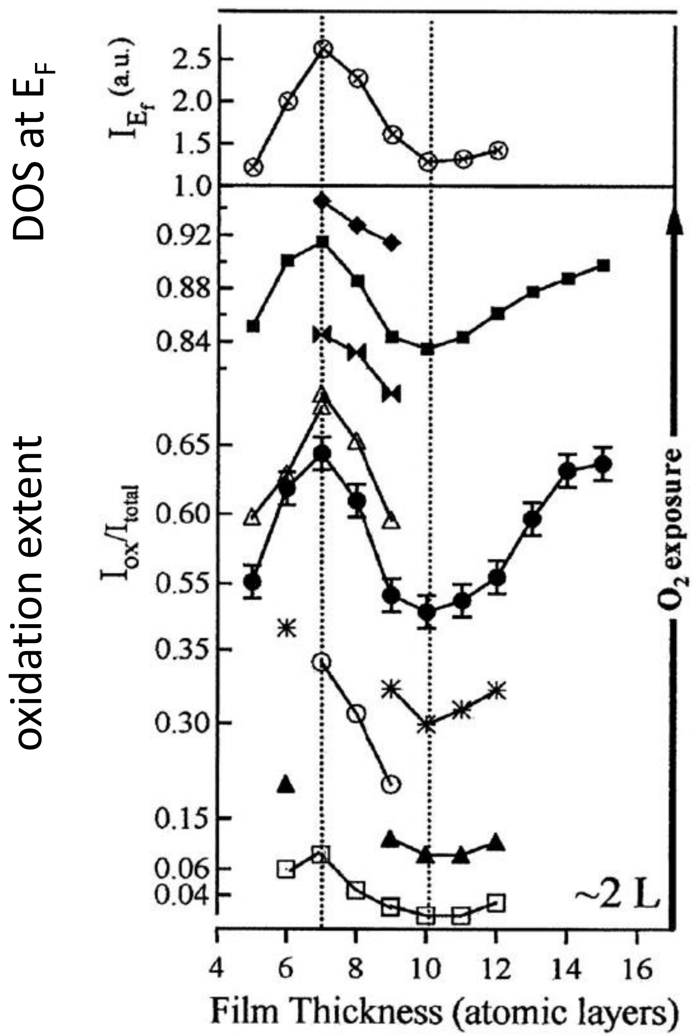

FACTS

- ✓ Strong variations in the oxidation extent are correleted to thickness and to the density of states at E_F
- ✓ XPEEM is a powerful technique for correlating chemistry and electronic structure information

SIGNIFICANCE OF THE EXPERIMENTS

- ✓ Control on film thickness enables modifying the molecule-surface interaction
- ✓ Theoretical explanation: Decay length of QWS into vacuum is critical: it reproduces peak of reactivity in experimental data. See Binggeli and M. Altarelli, Phys.Rev.Lett. 96, 036805 (2005)

L. Aballe *et al.*, Phys. Rev. Lett. 93, 196103 (2004)

The complexity of the metal-graphene interface

Elettra Sincrotrone Trieste

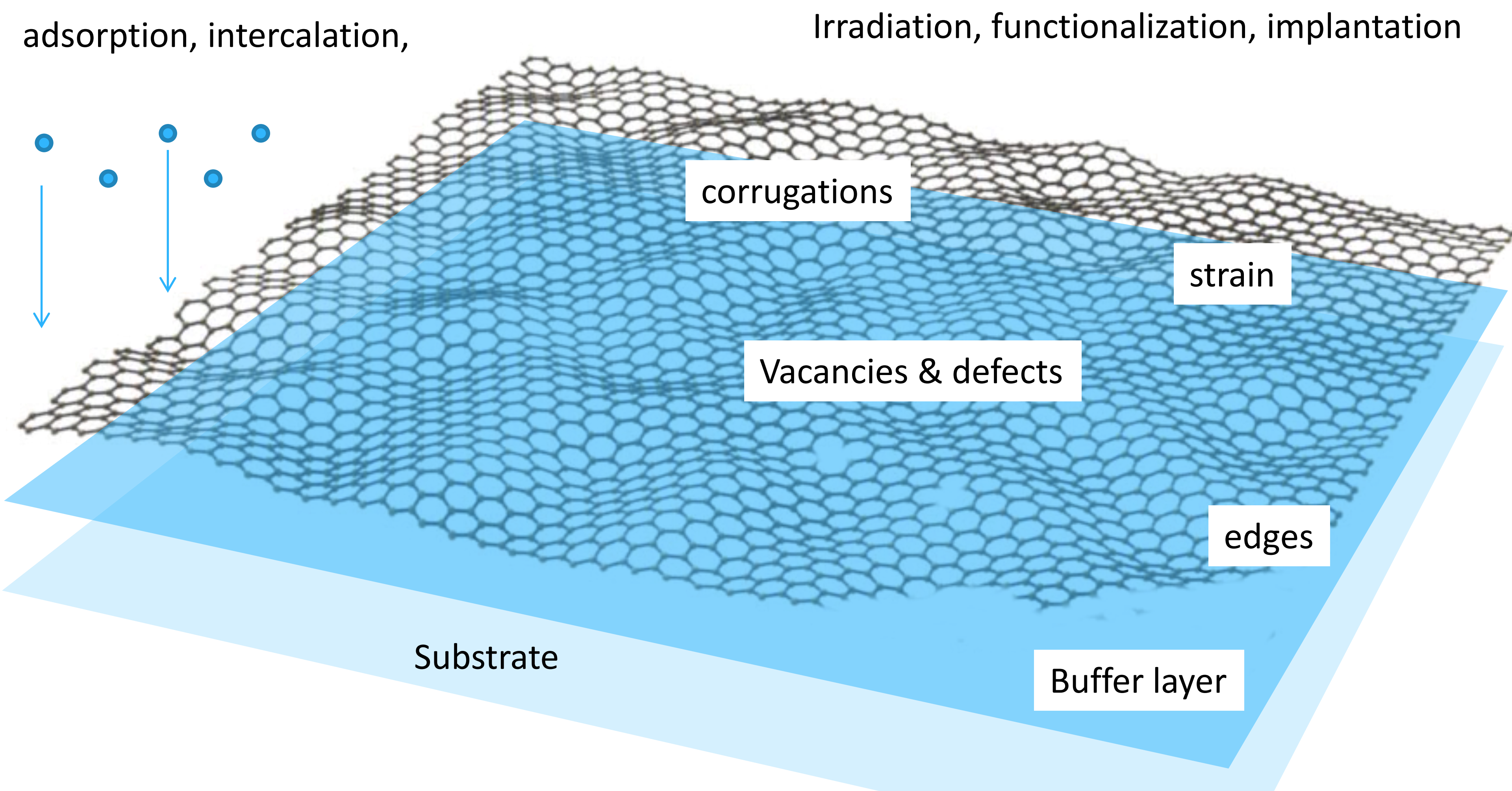

- Understand and control the fundamental interactions occurring at the interface
- verify the properties (crystal quality, stoichiometry, electronic structure) at the mesoscale!

XPEEM studies of graphene

- Effect of substrate’ symmetry
  - The complex structure of g/Ir(100)
- Buffers
  - Au Intercalation
  - Carbides in graphene on Ni(111)
- Irradiation/implantation
  - [Low energy N+ ion irradiation of g/Ir(111)]
  - Irradiation with noble gases of g/Ir(100)

graphene growth on Ir(001)

Growth 600°C < T < 670°Cb

$P_{C2H4} = 2 \cdot 10^{-8}$ mbar

growth at T > 800°C

microprobe-LEED: graphene

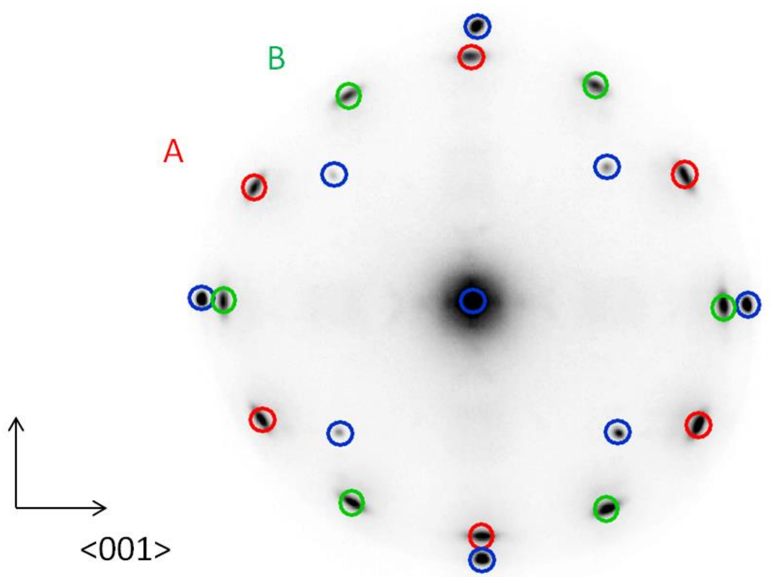

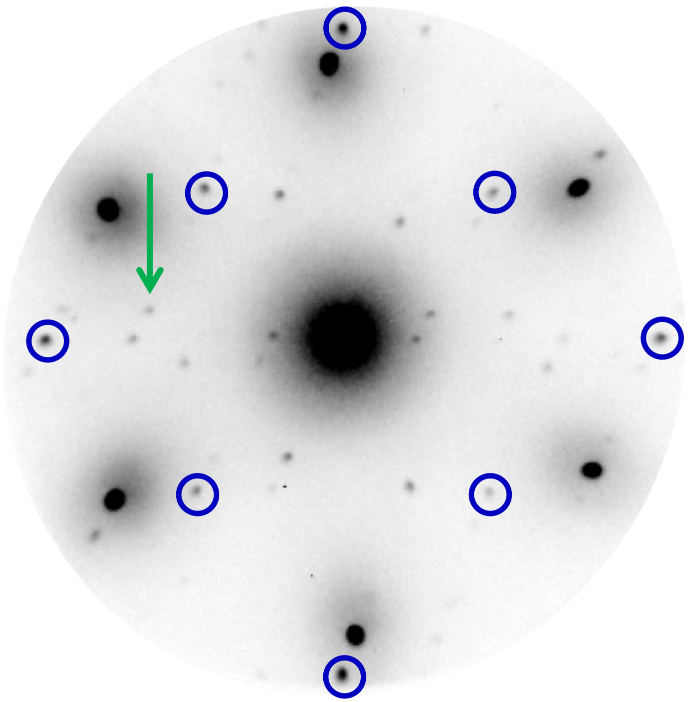

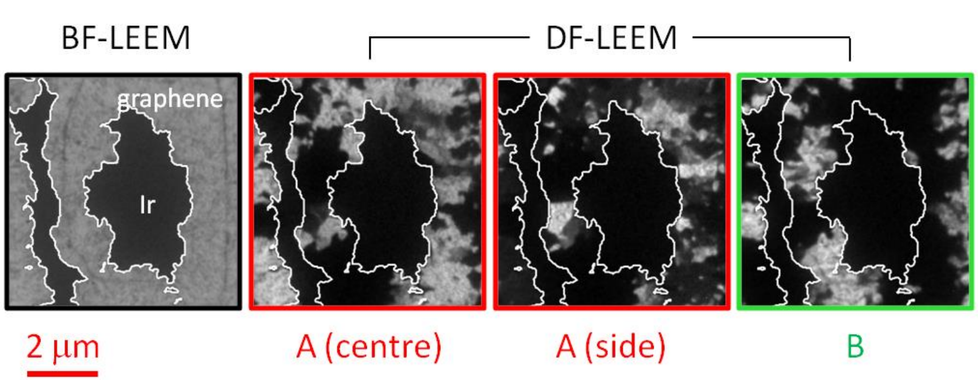

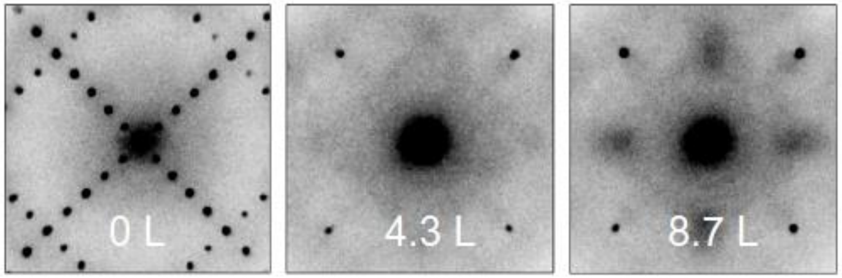

A. Locatelli, G. Zamborlini, T.O. Menteş; Carbon 74, 237–248 (2014);

Reversible phase transformation in graphene

Elettra Sincrotrone Trieste

Upon cooling a new graphene phase nucleates (dark stripes)

The stripes disappear upon annealing to high temperature.

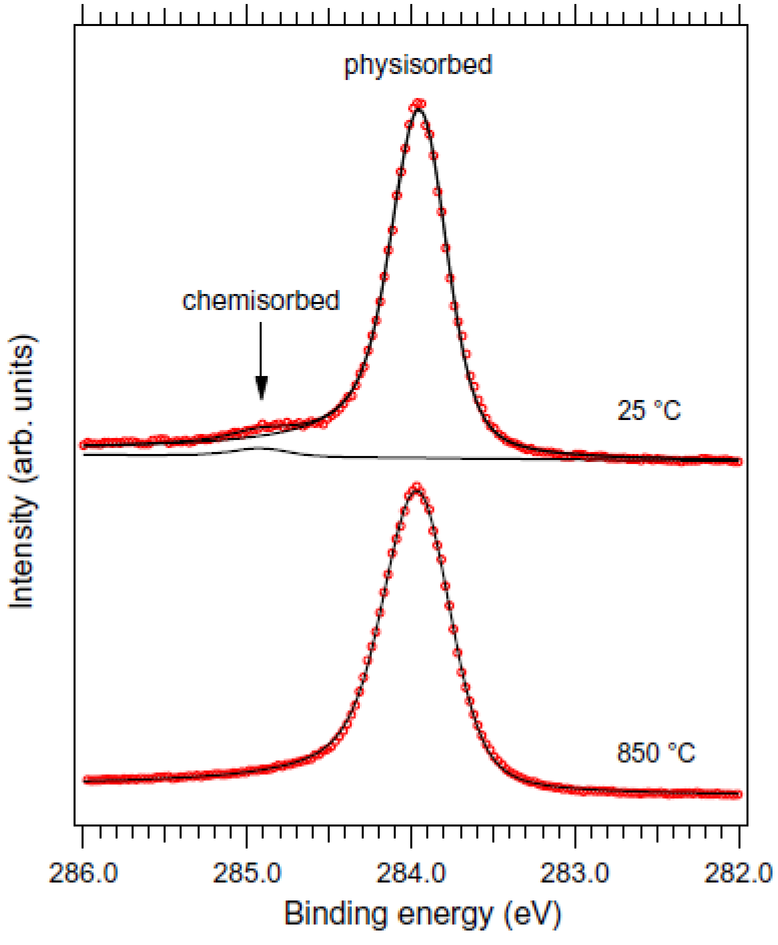

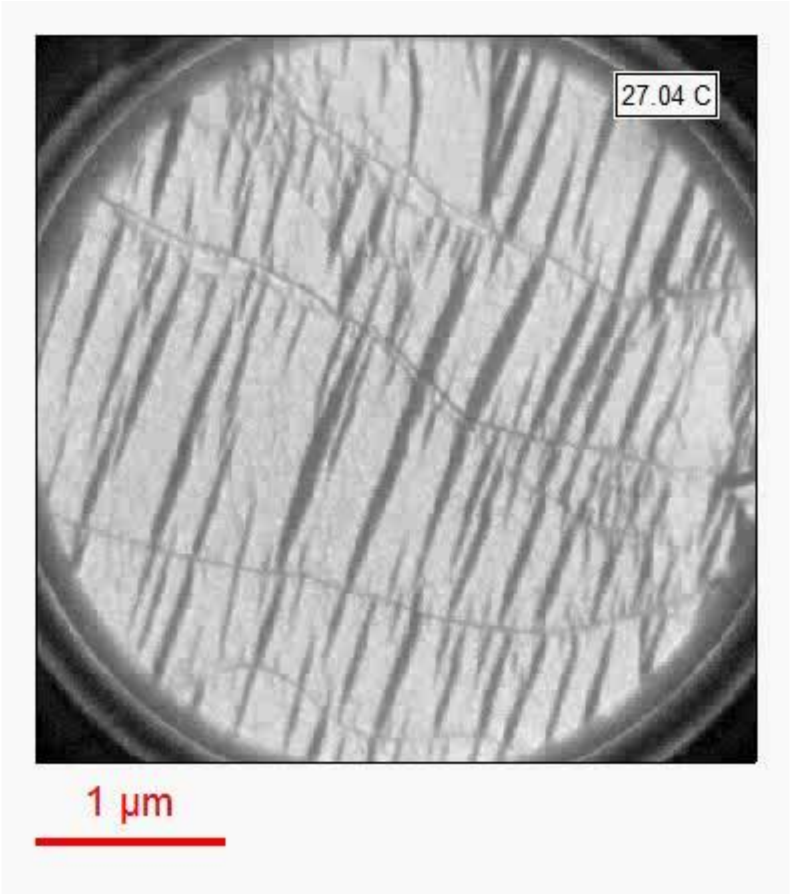

Graphene/Ir(100): strucutre of FG and BG

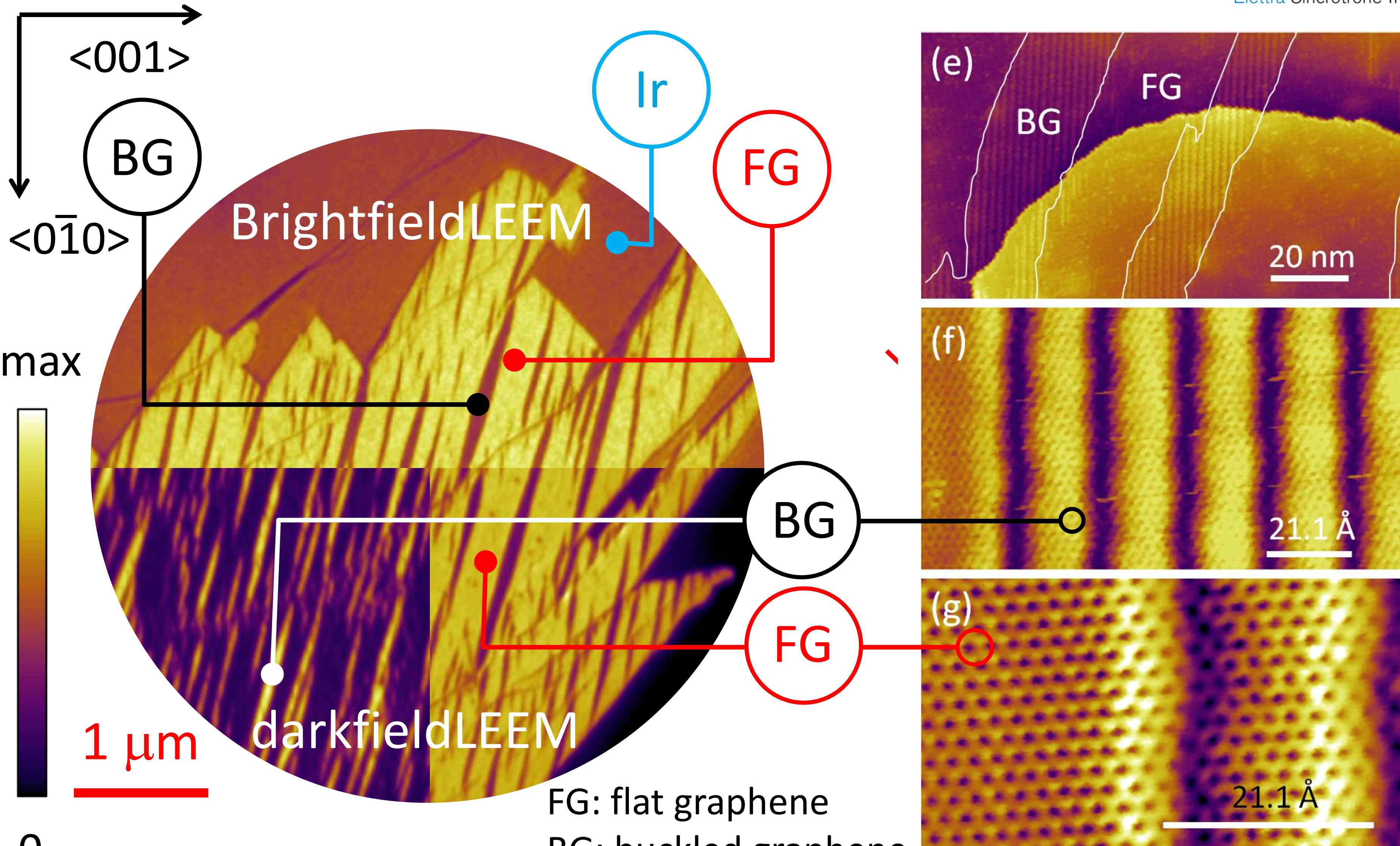

Room temperature

FG: flat graphene

BG: buckled graphene

Buckled graphene unit cell by ab-initio

buckled graphene unit cell

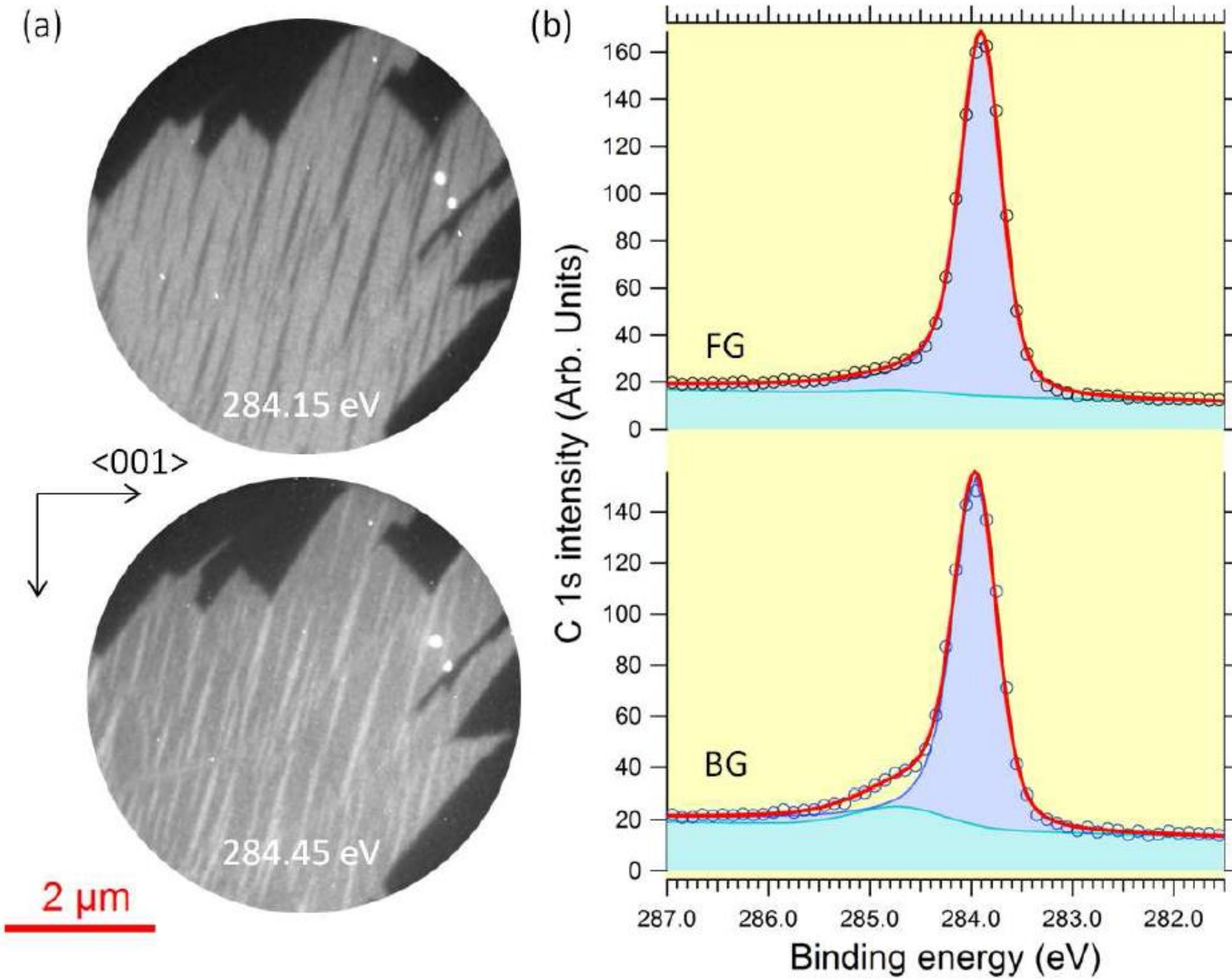

Buckled Graphene

<u>Exceptionally large buckling</u>

GGA:

- Min Ir-C distance of 1.9 Å
- Max Ir-C distance of 4.0 Å

DFT-D:

- Min Ir-C distance of 2.1 Å
- Max Ir-C distance of 3.7 Å

- 18 atoms over 160 (i.e. 11%) are **chemisorbed**, the others are physisorbed

Buckled graphene shows regular one-dimensional ripples with periodicity of 2.1nm.

Electronic structure: graphene doping

Elettra Sincrotrone Trieste

what is the difference in electronic structure between FG and BG?

do they both show the same Dirac-like dispersion?

Diffraction Imaging

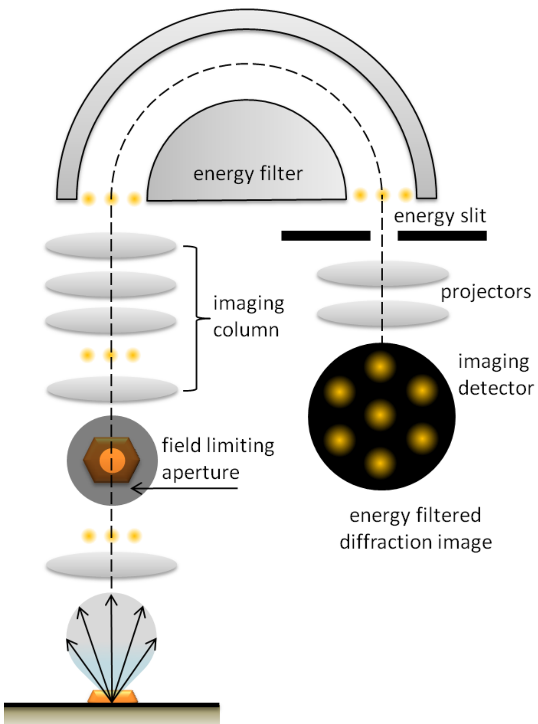

measurements limited to 2 um in dia.

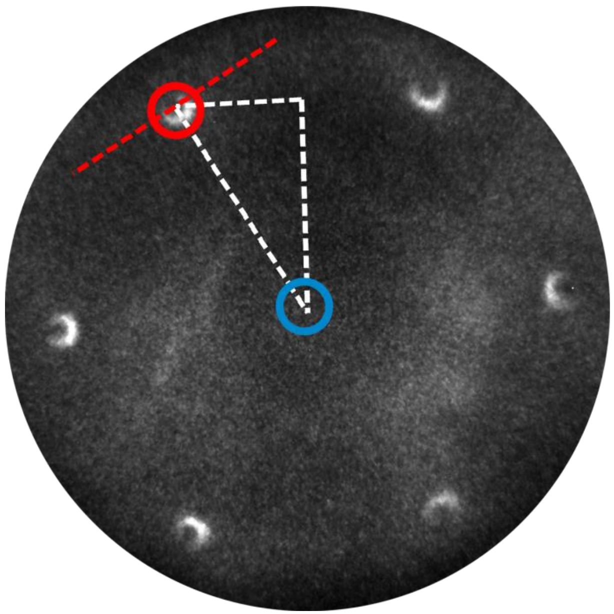

μ-ARPES at E_F

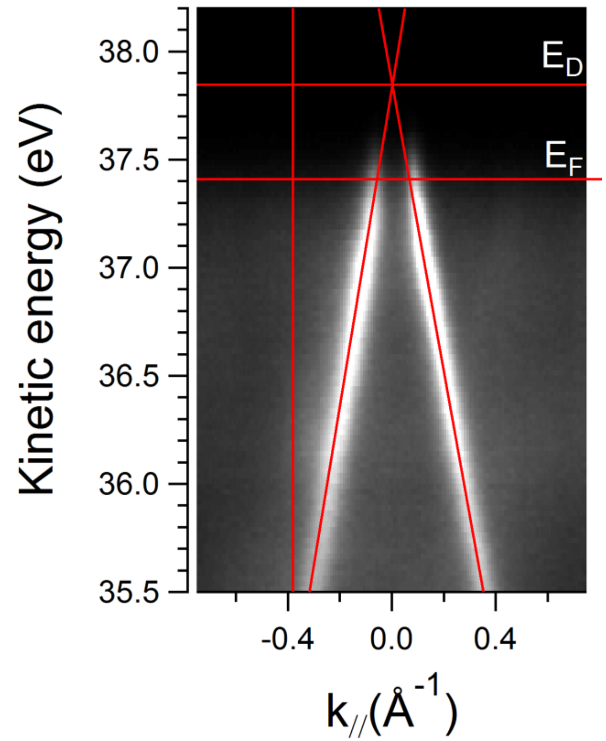

$E_D = 0.42$ eV

A. Locatelli et al; ACS Nano, ACS Nano, 7, 6955–6963 (2013)

Different character of FG and BG

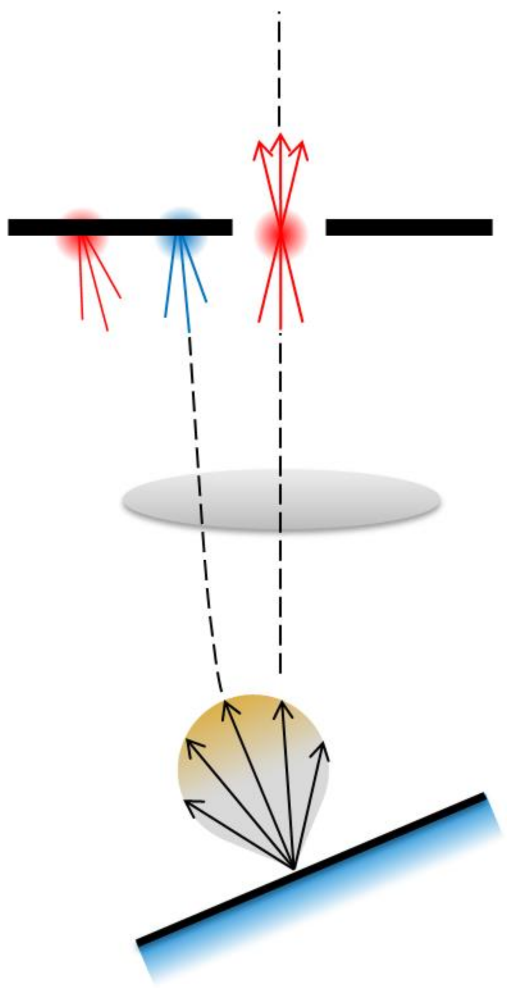

Image intensity proportional to local DOS!

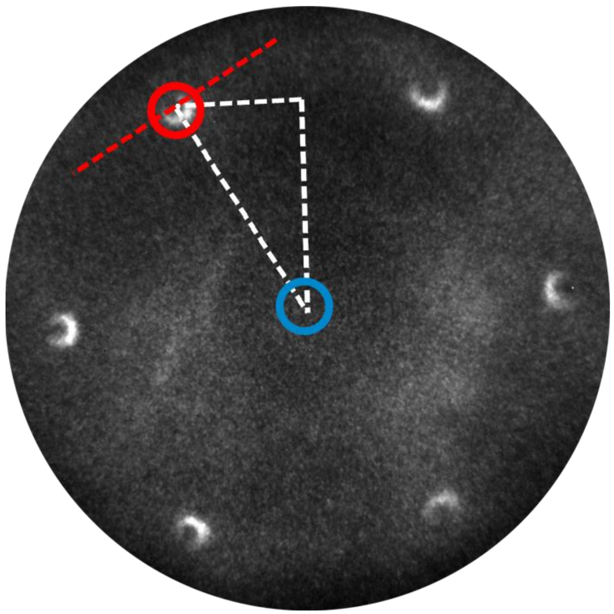

μ-ARPES at E_F

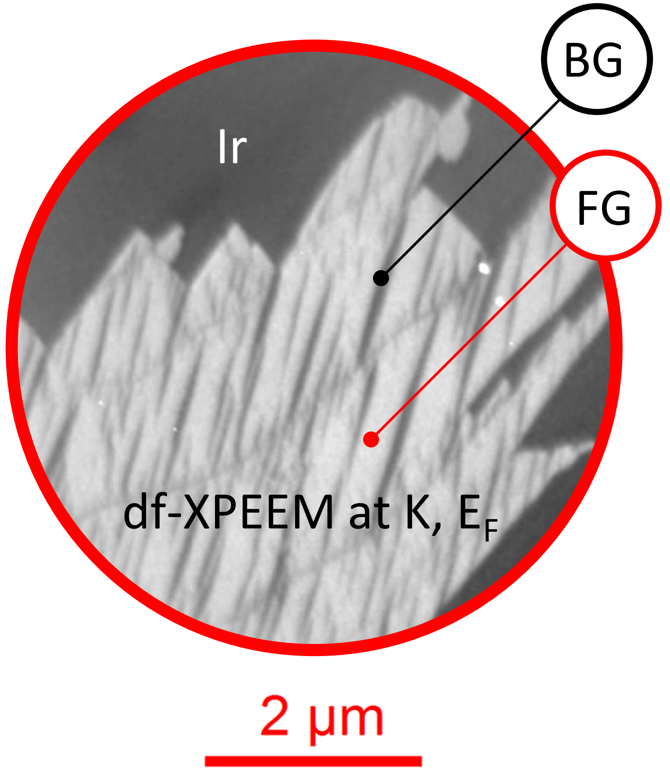

FG: high DOS at K → Dirac cones intact

BG hybridized, metalllic-like DOS

Decoupling graphene from substrate:

- **Intercalated Au/g/Ir(100)**
- **Switchable formation of carbides in g/Ni(111)**

Tuning the interaction by Au intercalation

Real time LEEM imaging during Au intercalation at 600 °C

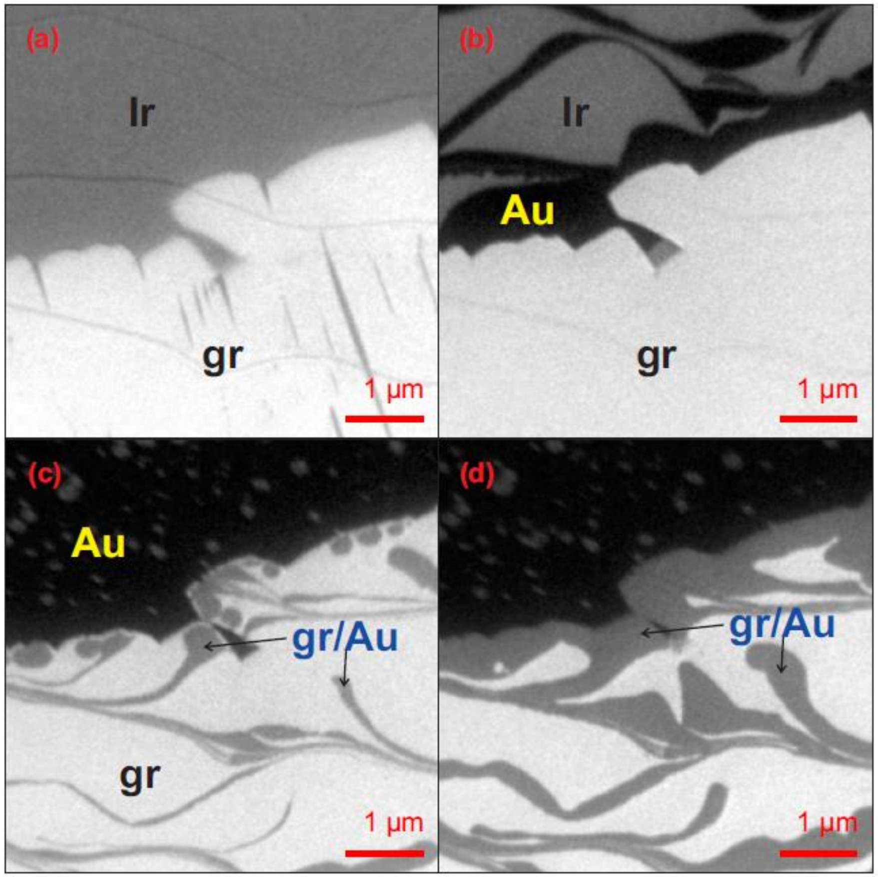

Electonic structure by microprobe ARPES

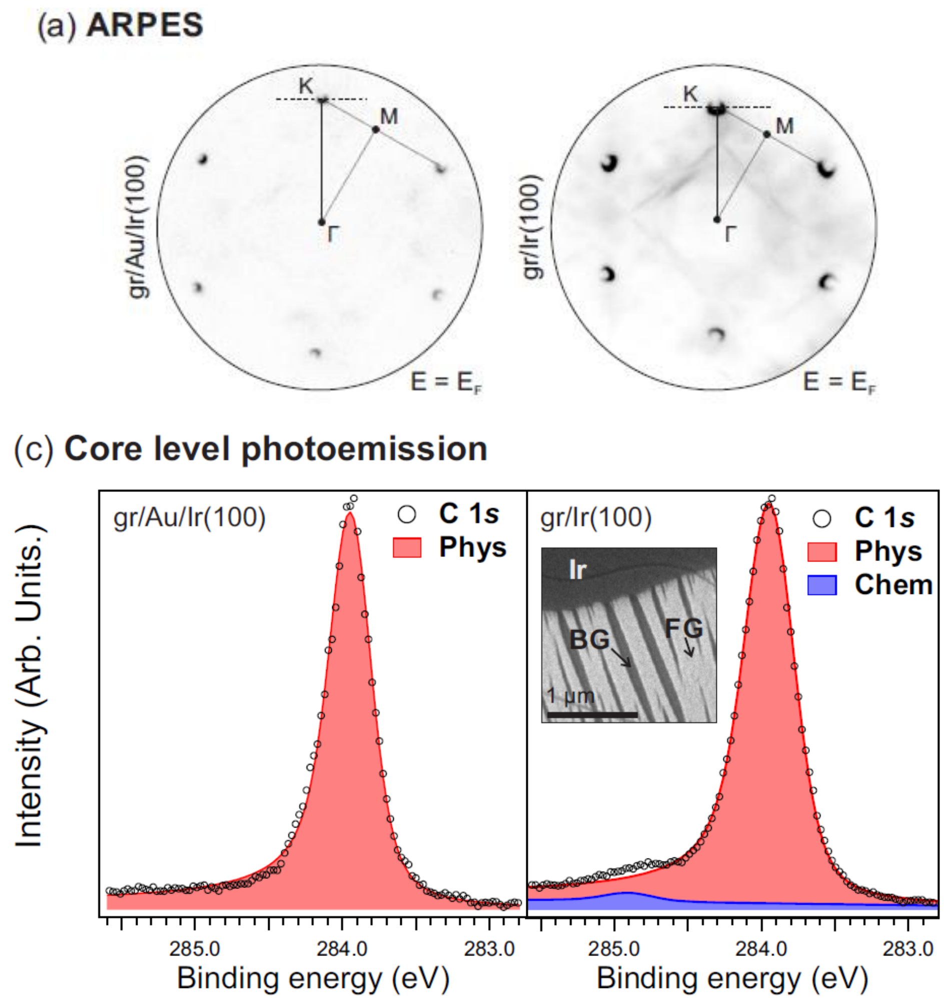

Beilstein J. Nanotechnol. 5, 1873–1886 (2014)

Identifying crystal grains in graphene/Ni(111)

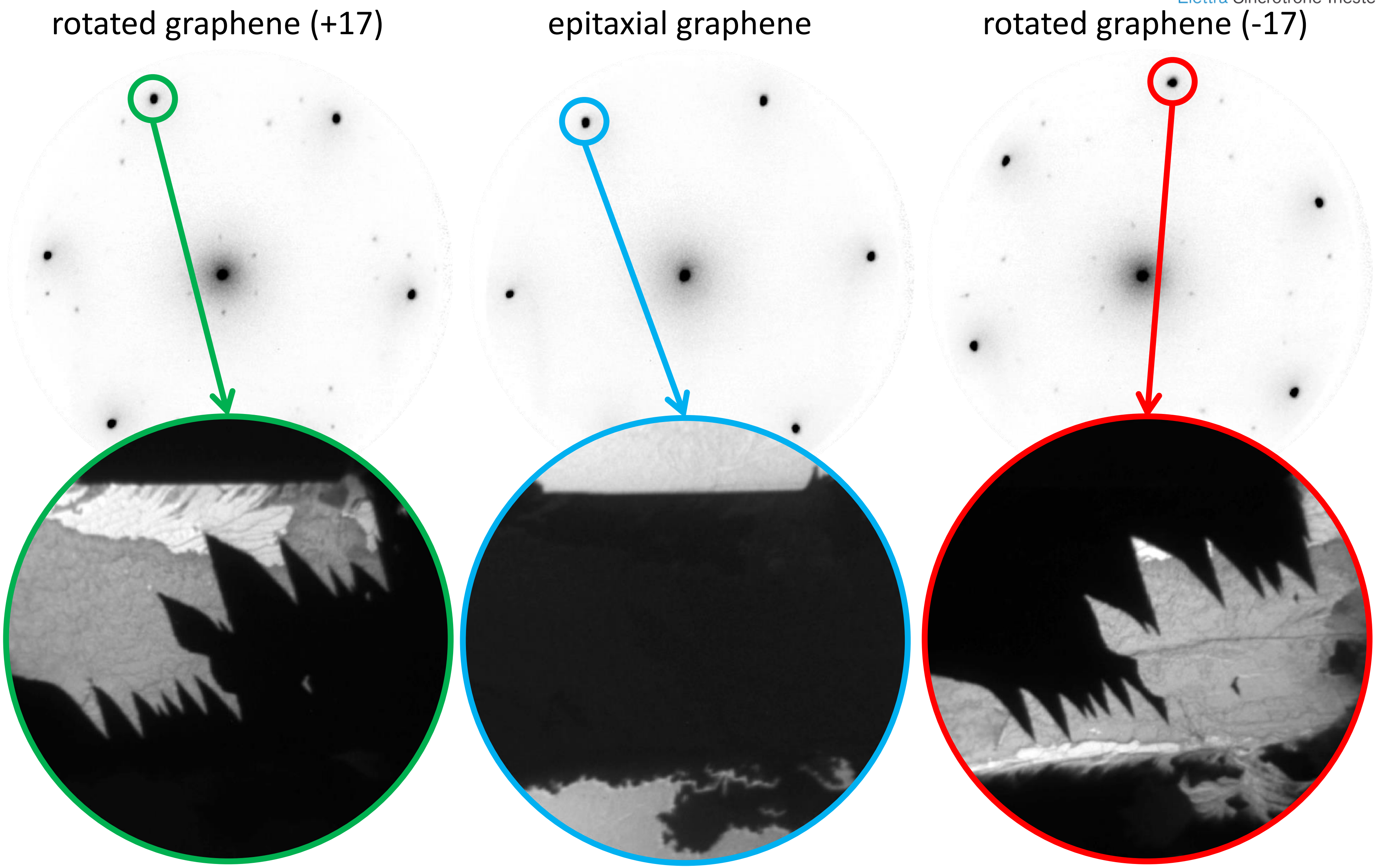

C. Africh, C. Cepek, L.Paterq. et al, Scientific Reports **6**, 19734 (2016)

Formation/dissolution of carbides under rg/Ni(111)

Elettra Sincrotrone Trieste

1: carbide nucleation

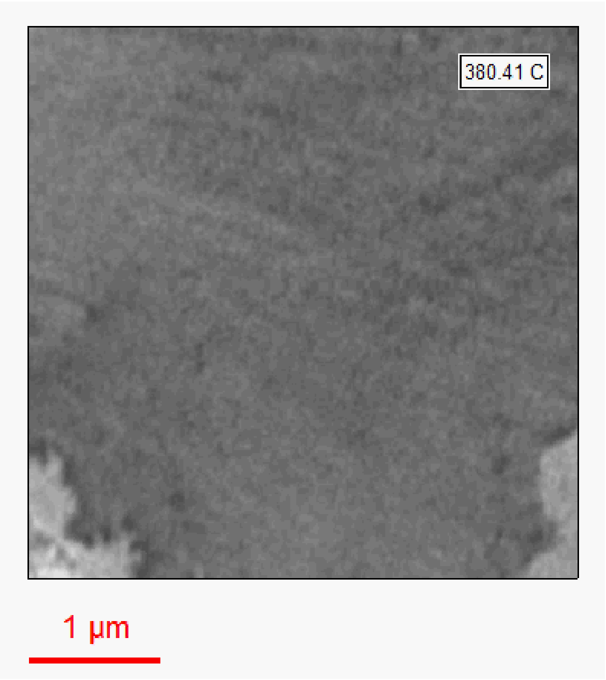

The Ni-carbide nucleates exclusively under rotated graphene, starting at temperatures below 340°C

Different electron reflectivity explains change of contrast

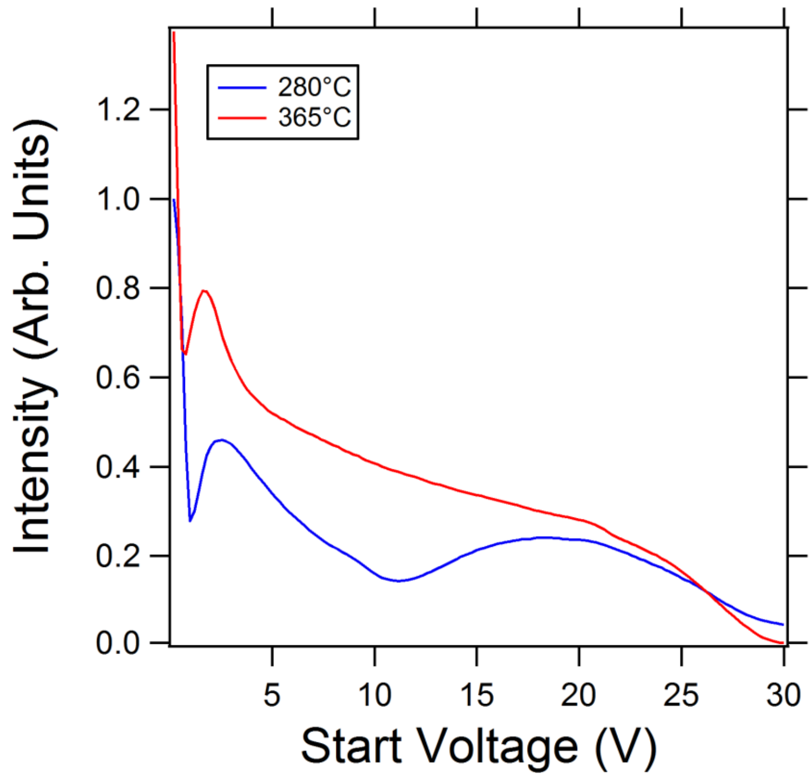

All movies: LEEM FoV 6 um, electron energy: 11 eV

Coupling-decoupling is revealed by μ-ARPES

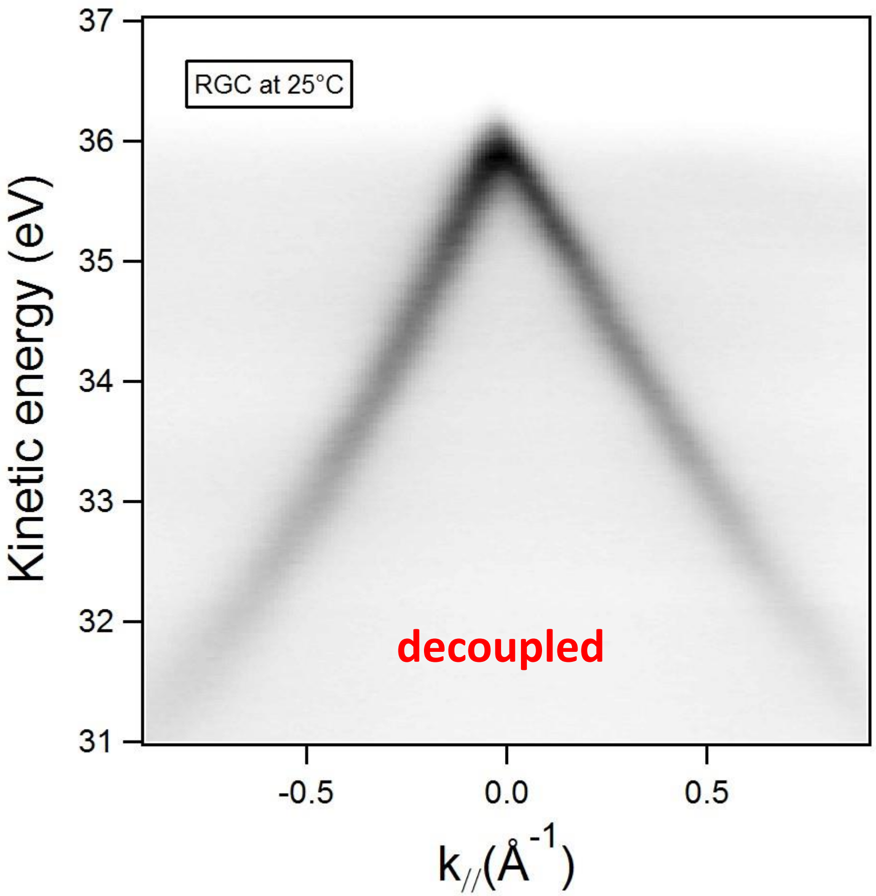

Rotated graphene with Ni-carbide underneath at room temperature; There's no double layer

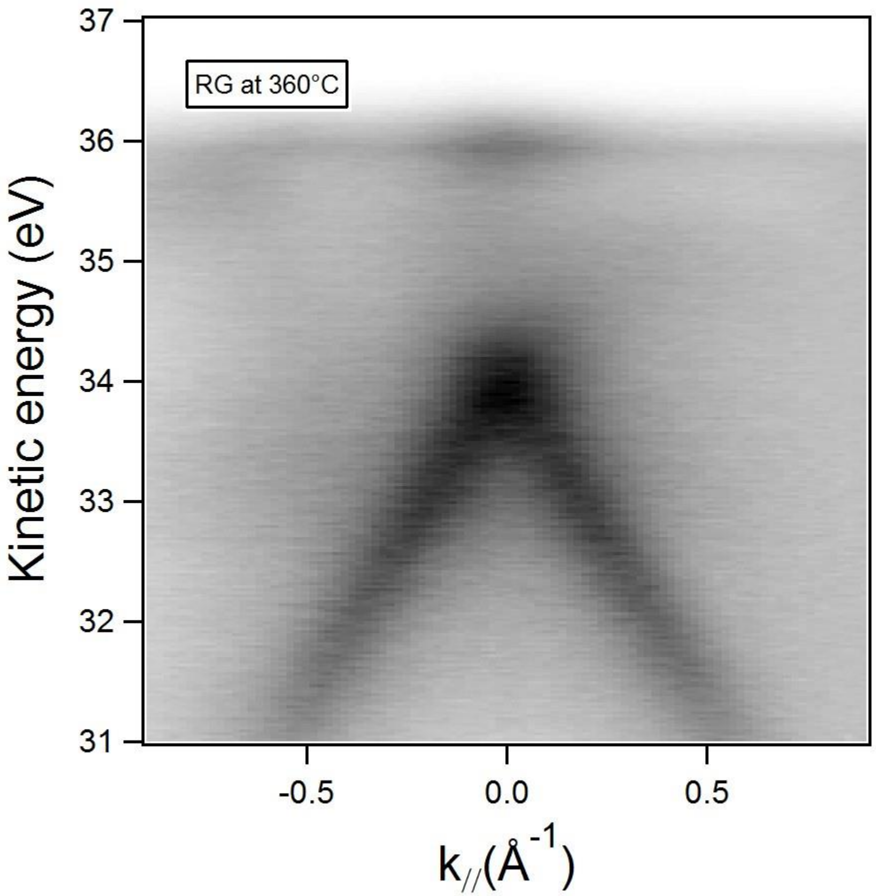

Rotated graphene without Ni-carbide underneath at 365°C

C. Africh, C. Cepek, L.Paterq. et al, Scientific Reports **6**, 19734 (2016)

Ion irradiation of graphene

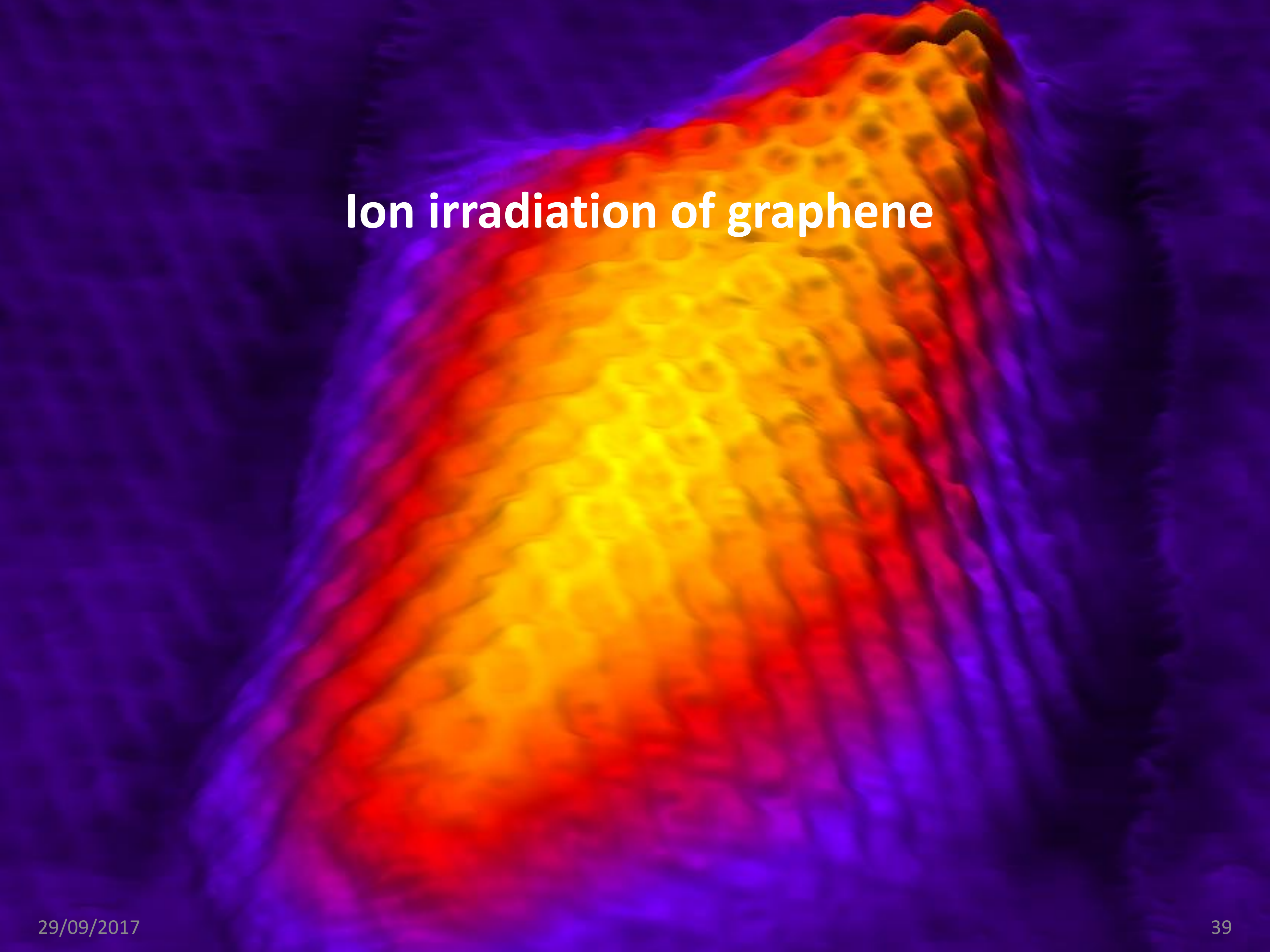

Example: Nitrogen-ion irradiated gr/Ir(111)

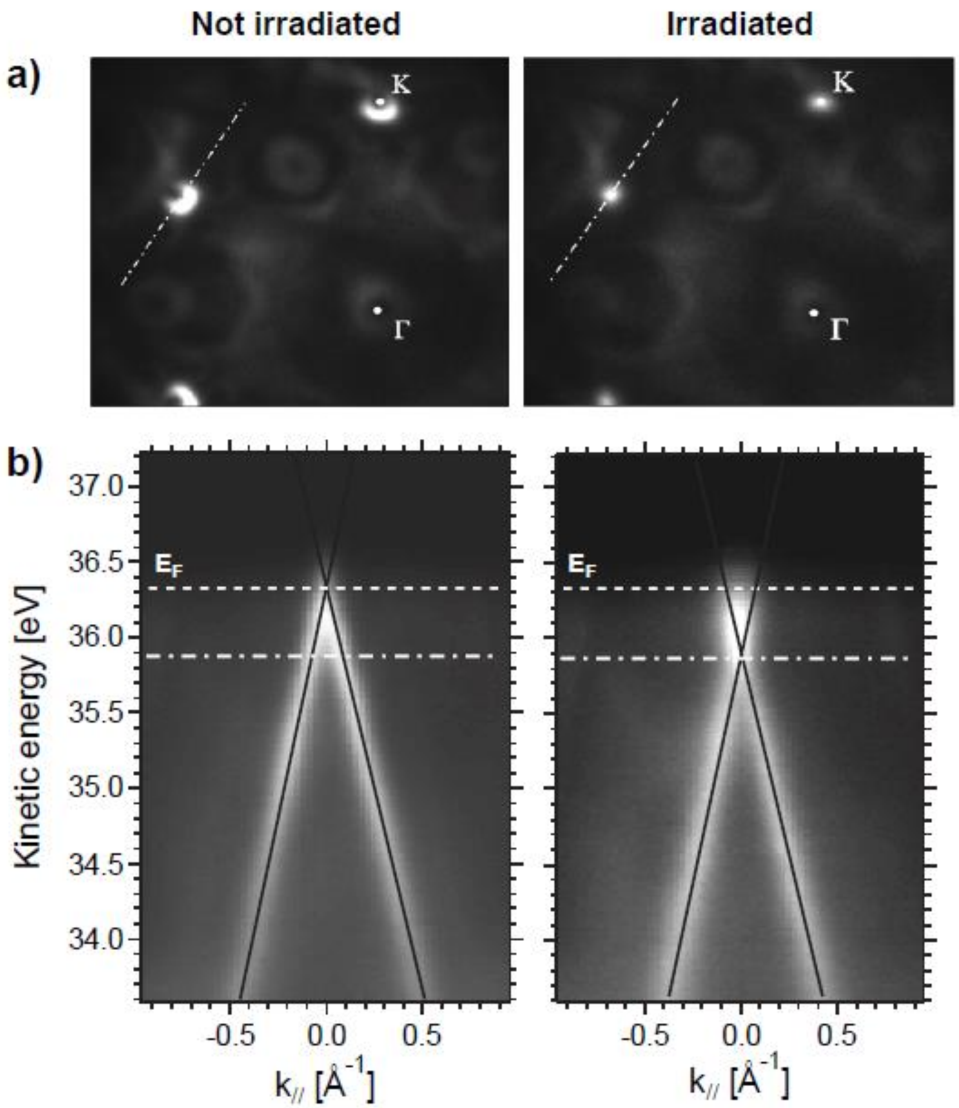

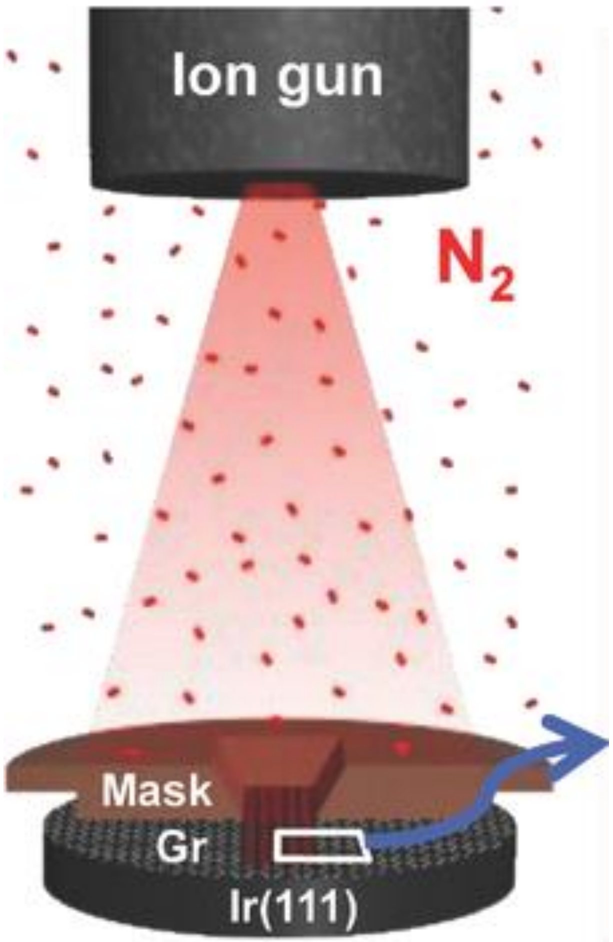

A. Sala et al., Small 11(44), 5927-5931 (2015)

Example: Nitrogen-ion irradiated gr/Ir(111)

Elettra Sincrotrone Trieste

M. Scardamaglia *et al.*, Carbon **73** (2014), 371-381

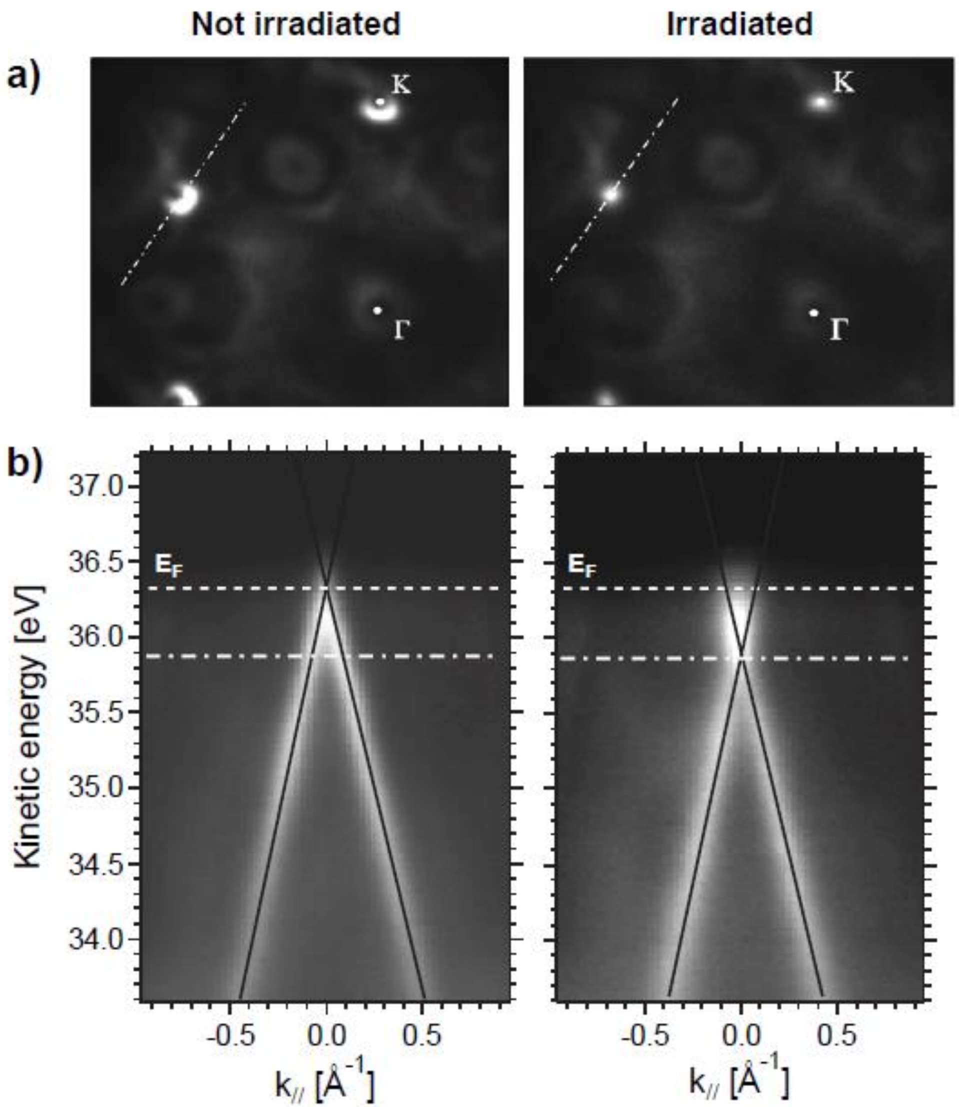

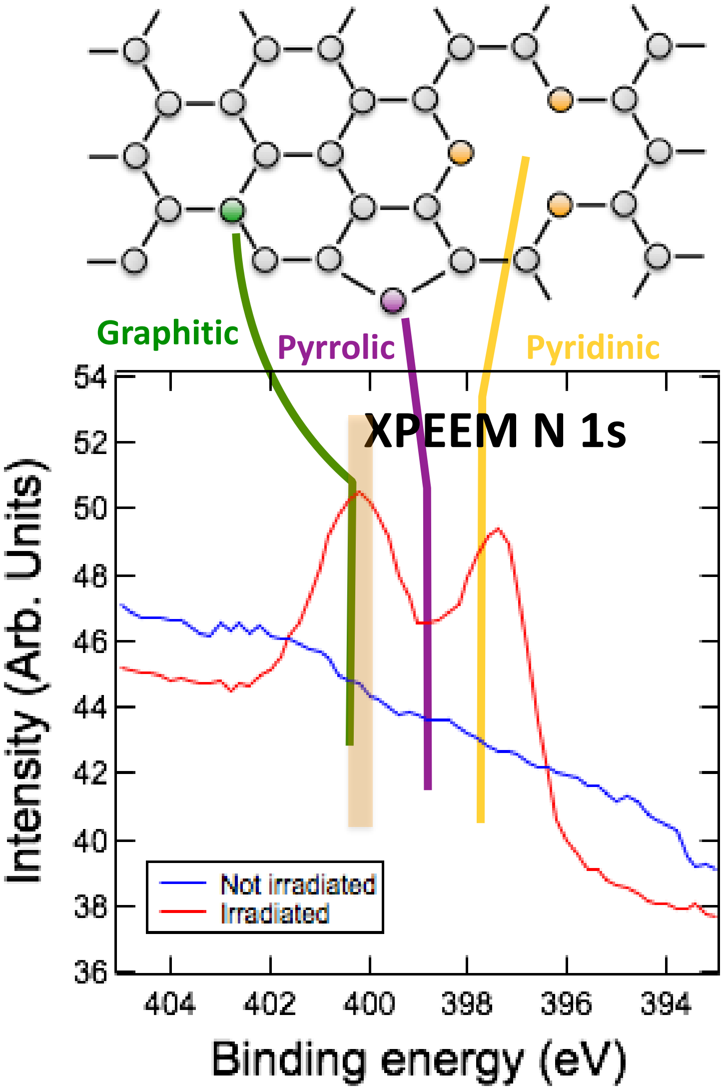

A. Sala et al., Small 11(44), 5927-5931 (2015)

Morphology of Ar^+ irradiated graphene/Ir(100)

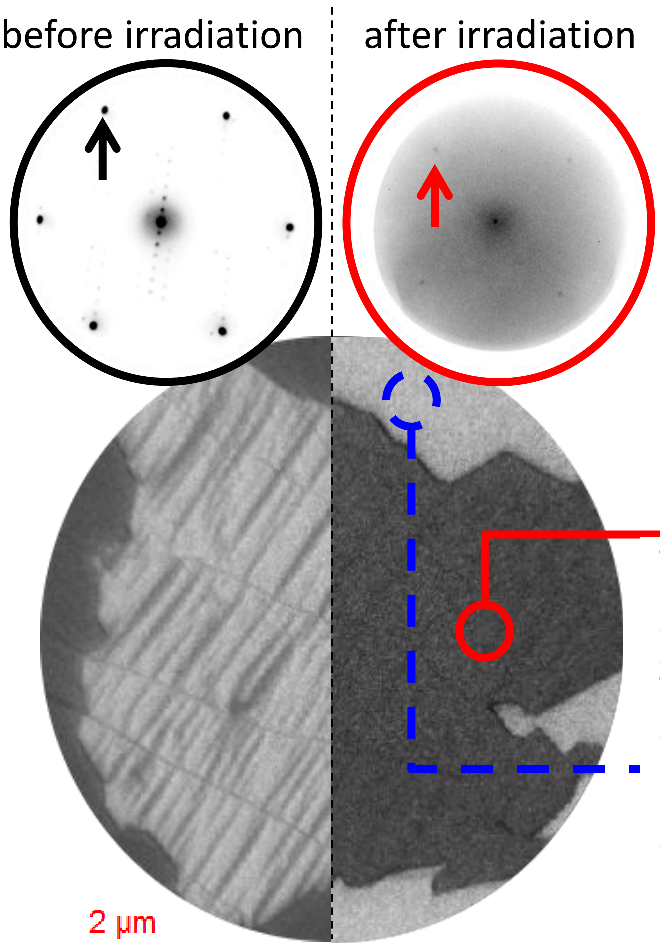

LEEM 12 eV
0.5keV Ar^+ , 1.5 10^{-5} mbar, 7 s

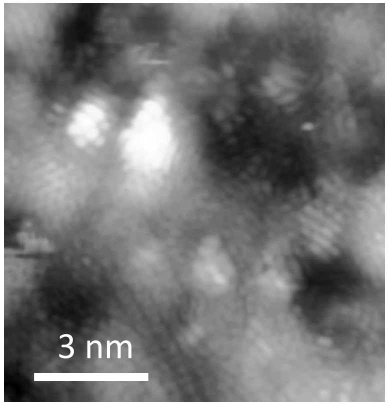

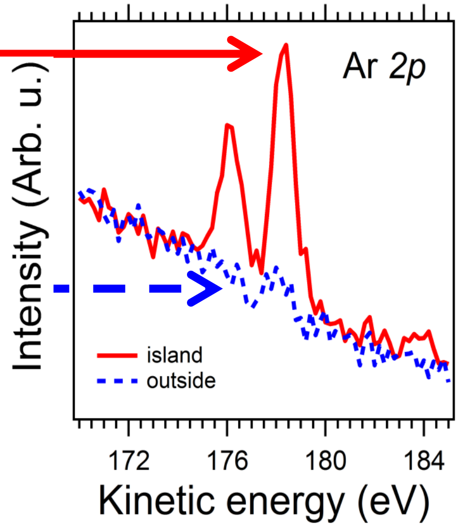

Rough morphology, but ...
graphene is <u>continuous</u>
average height 0.1 nm!

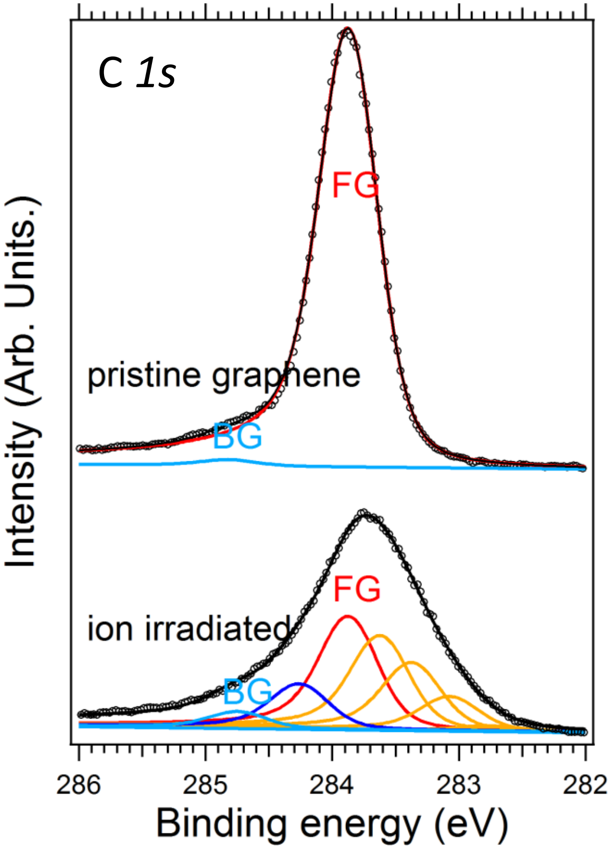

G. Zamborlini et al., *Nano Lett.*, 2015, 15 (9), pp 6162–616

LEEM & XPEEM formation of Ar nanobubbles

LEEM movie 12 eV

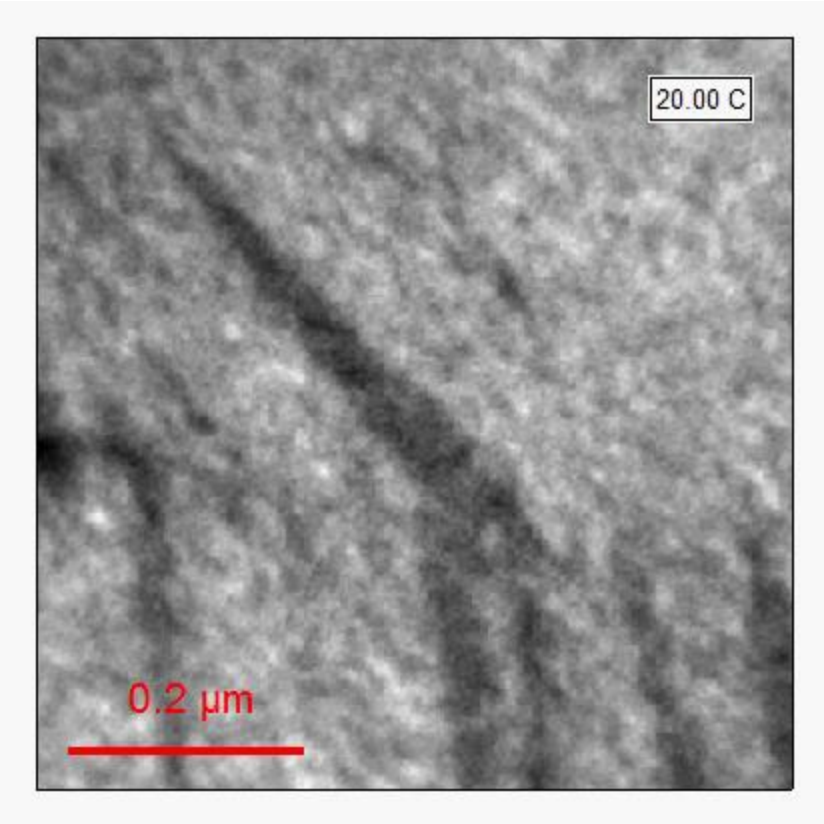

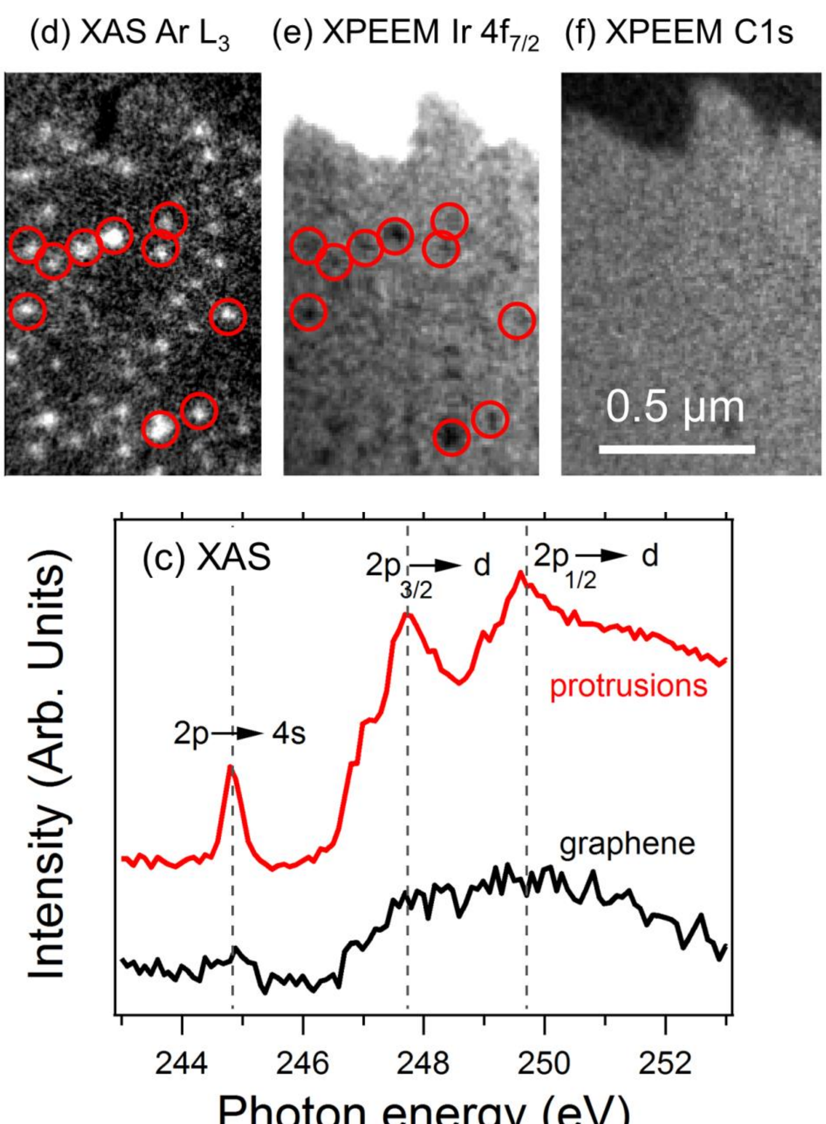

G. Zamborlini et al., *Nano Lett.*, 2015, 15 (9), pp 6162–616

NB formation for g/Ne/Ir(100)

100 eV Ne+ ion irradiation was followed by 5 min annealing to 650 °C and subsequent cooling to RT

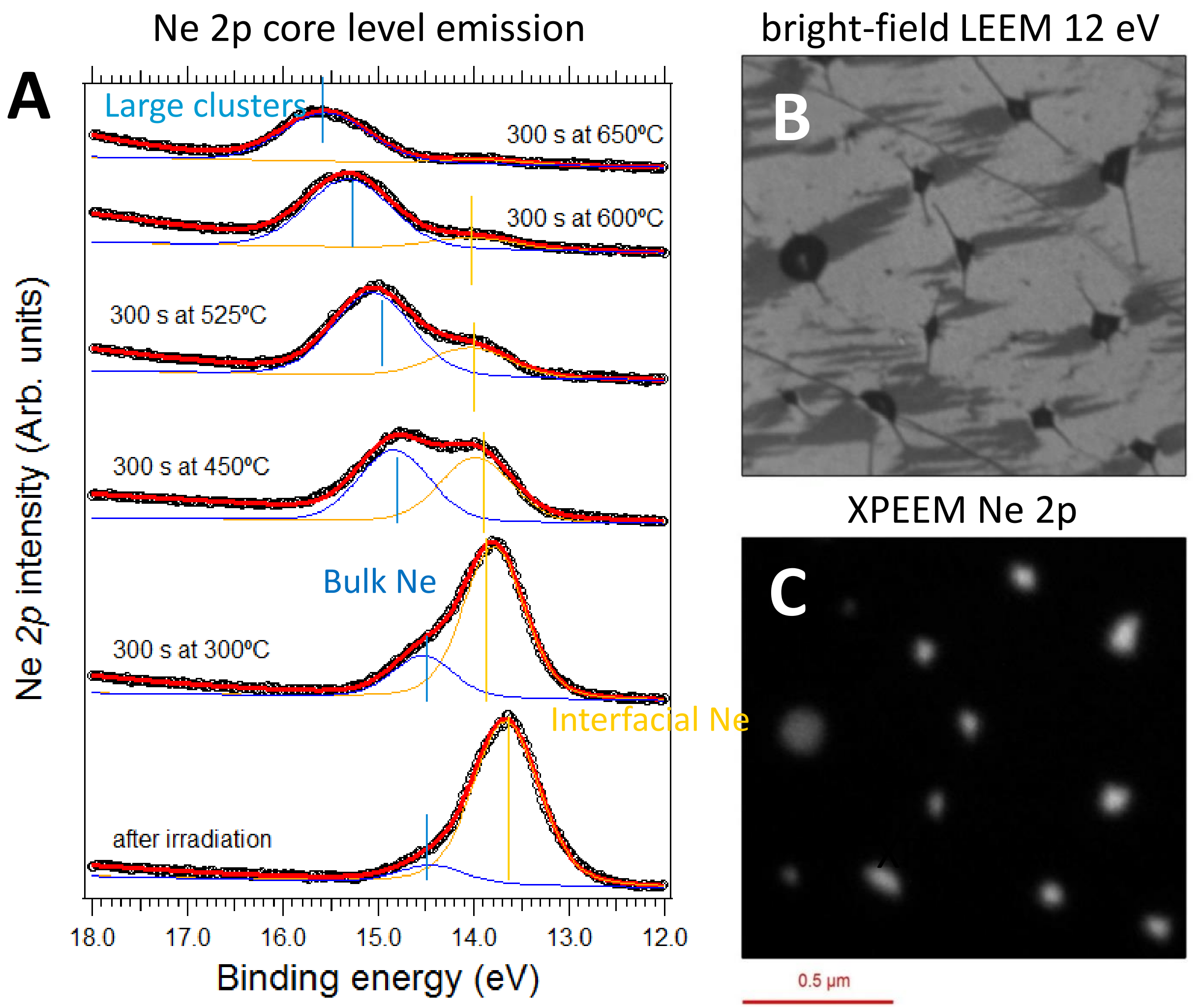

A. Locatelli et al, in preparation

Ne state: XAS-PEEM

Elettra Sincrotrone Trieste

Ne NB K shell XAS-PEEM

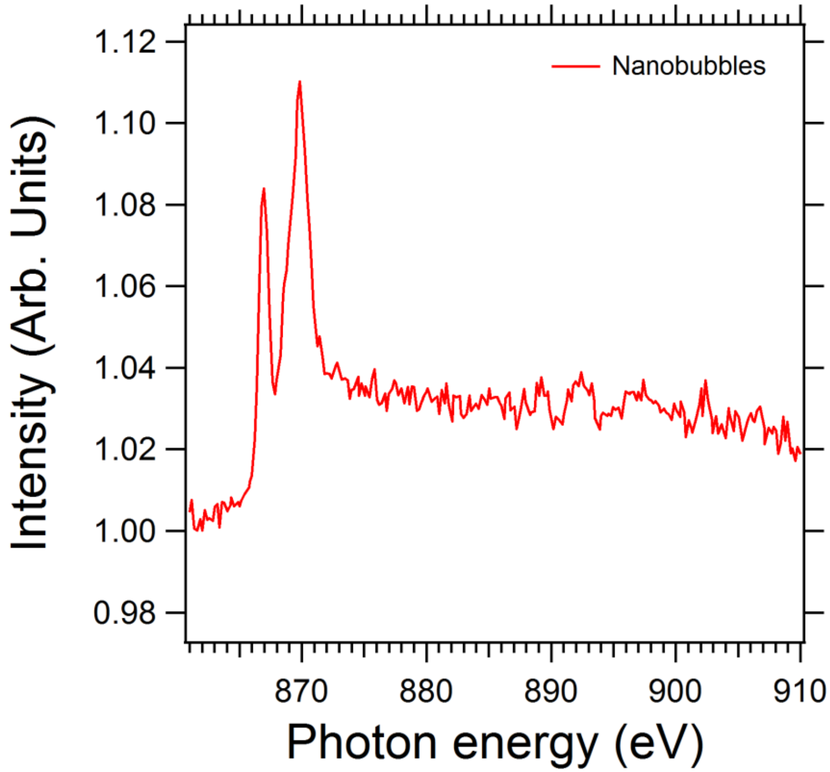

- 1s → 3p,4p transition visible
- Spectrum is featureless at high energy

Large Ne NB are not solid!

Ne NB gas phase XPS data

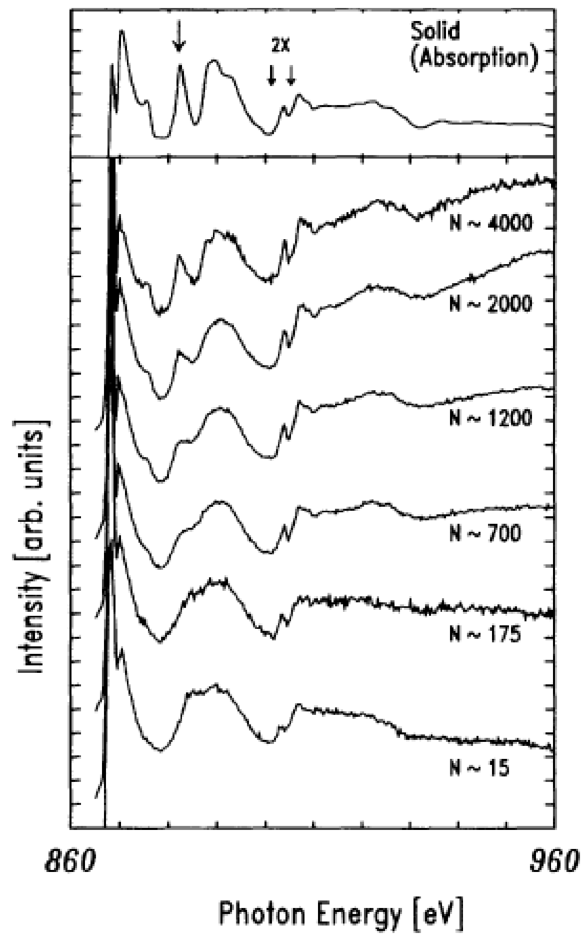

F. Federmann *et al.*,
Phys. Rev. Lett. **73**, 1549 (1994)

XAS-PEEM applications to biosciences

biomineralization

Applications of XAS in biology: biomineralization

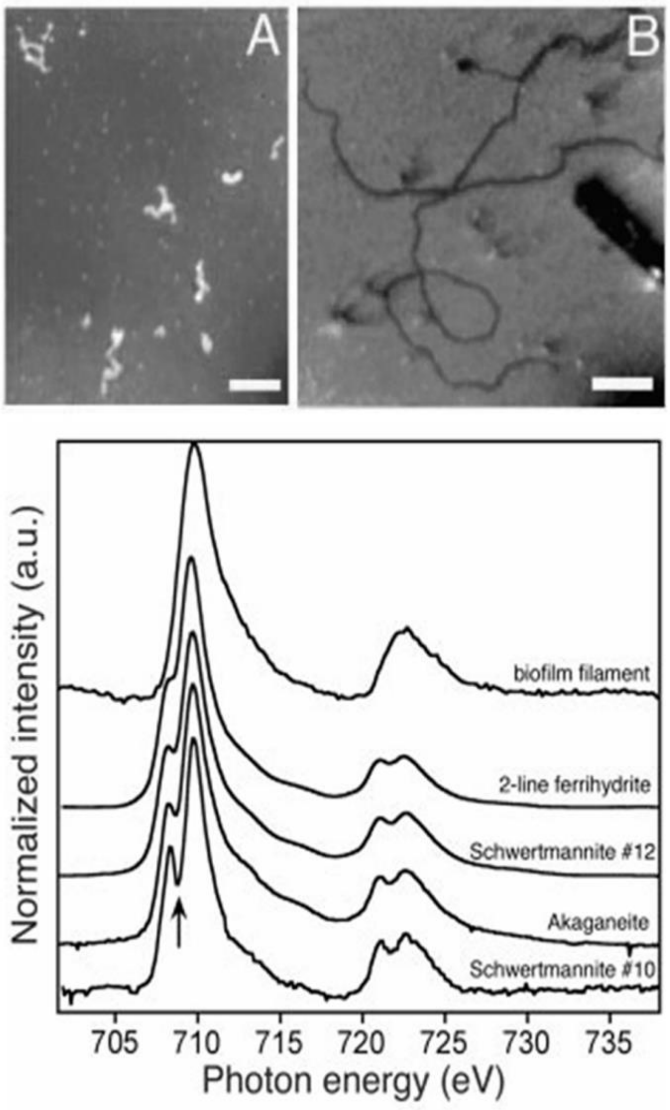

- Bio-mineralization resulting from microbal activity
- X-PEEM images of (A) non mineralized fibrils from the cloudy water above the biofilm (scale bar, 5 um)
- (B) mineralized filaments and a sheath from the biofilm (scale bar, 1 um); (bottom)
- X-PEEM Fe L-edge XANES spectra of the FeOOH mineralized looped filament shown in (B), compared with iron oxyhydroxide standards, arranged (bottom to top) in order of decreasing crystallinity.

P.U.P.A Gilbert *et al. (ALS group)*, *Science* **303** 1656-1658, 2004.

Nano-scale architecture of Nacre

Carbon K-edge image Carbon K-edge XANES

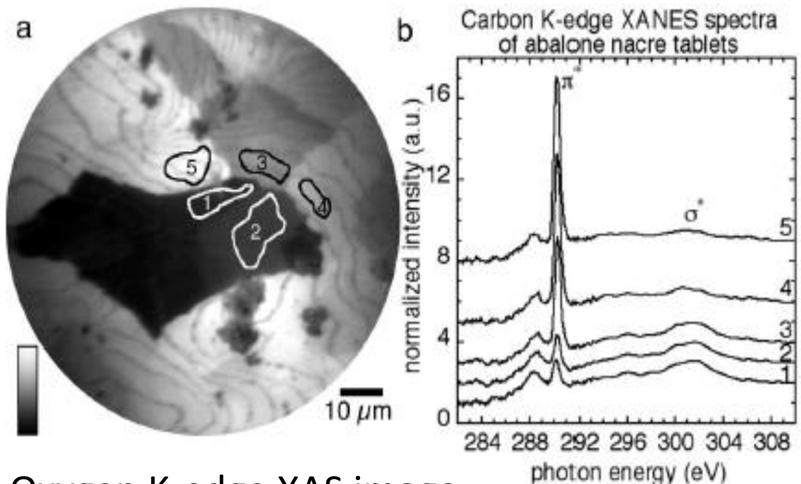

Oxygen K-edge XAS image

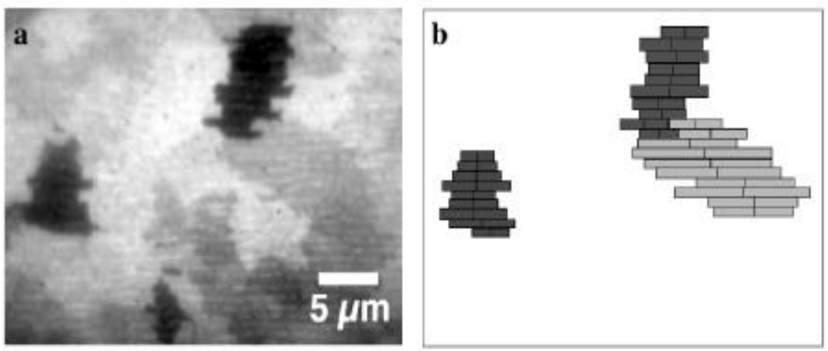

$$I(\vartheta, \theta, T) = a + b(3\cos^2\vartheta - 1)\langle Q_{zz}\rangle + c(3\cos^2\theta - 1)\langle M^2\rangle_T + d\sum_{i,j}\langle \hat{s}_i \cdot \hat{s}_j\rangle_T$$

Contrast is observed between adjacent individual nacre tablets, arising because different tablets have different crystal orientations with respect to the radiation's polarization vector.

The 290.3 eV peak corresponds to the C 1*s* → *Pi** transition of the CO bond. Synchrotron radiation is linearly polarized in the orbit plane. Under such illumination, the

intensity of the peak depends on the crystallographic orientation of each nacre tablet with respect to the polarization. This was the first observation of x-ray linear dichroism in a bio-mineral.

R.A. Metzler *et al.*, *Phys.Rev.Lett.* **98**, 268102 (2007)

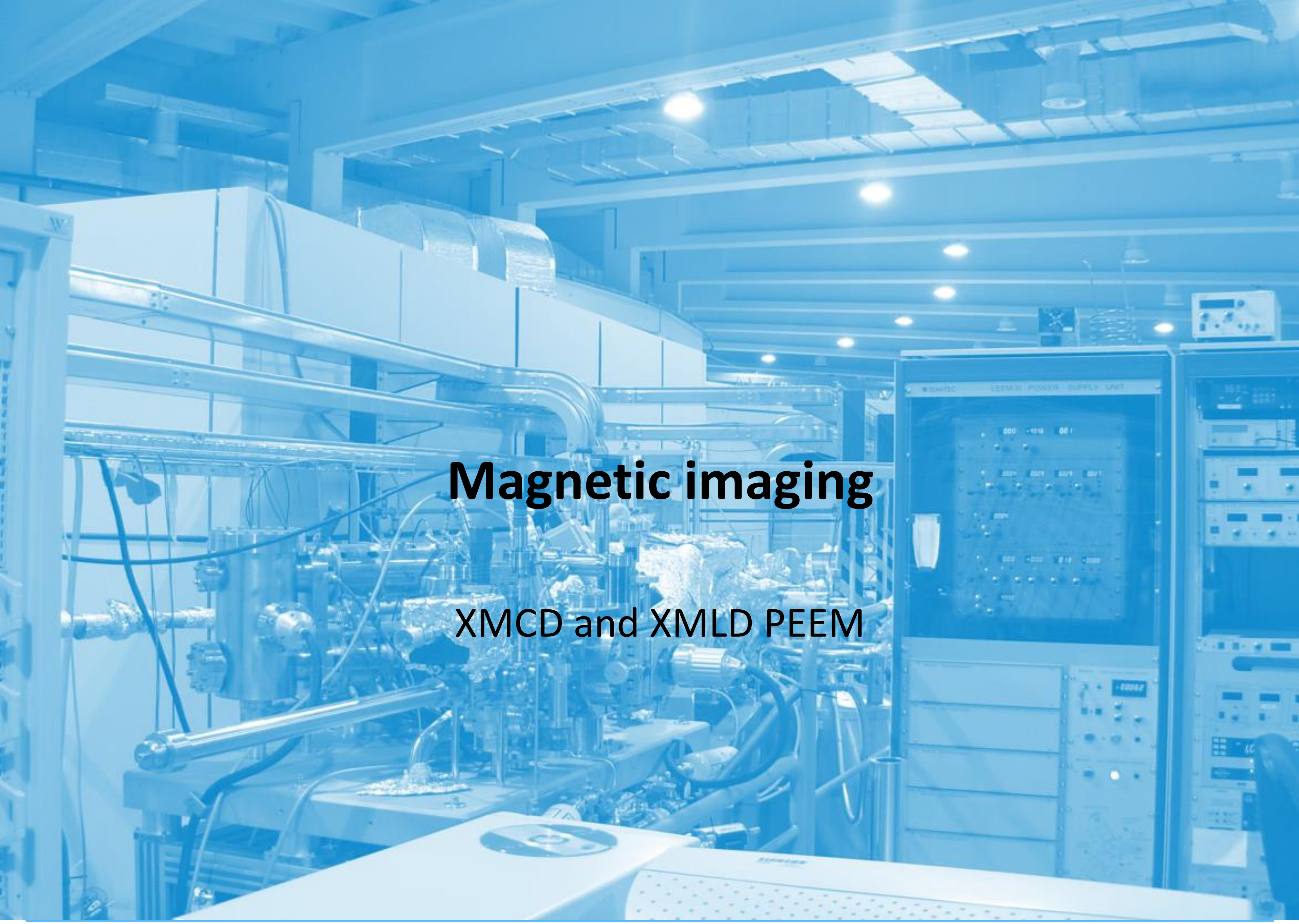

Magnetic imaging

XMCD and XMLD PEEM

Magnetic domain imaging by XMCD

Elettra Sincrotrone Trieste

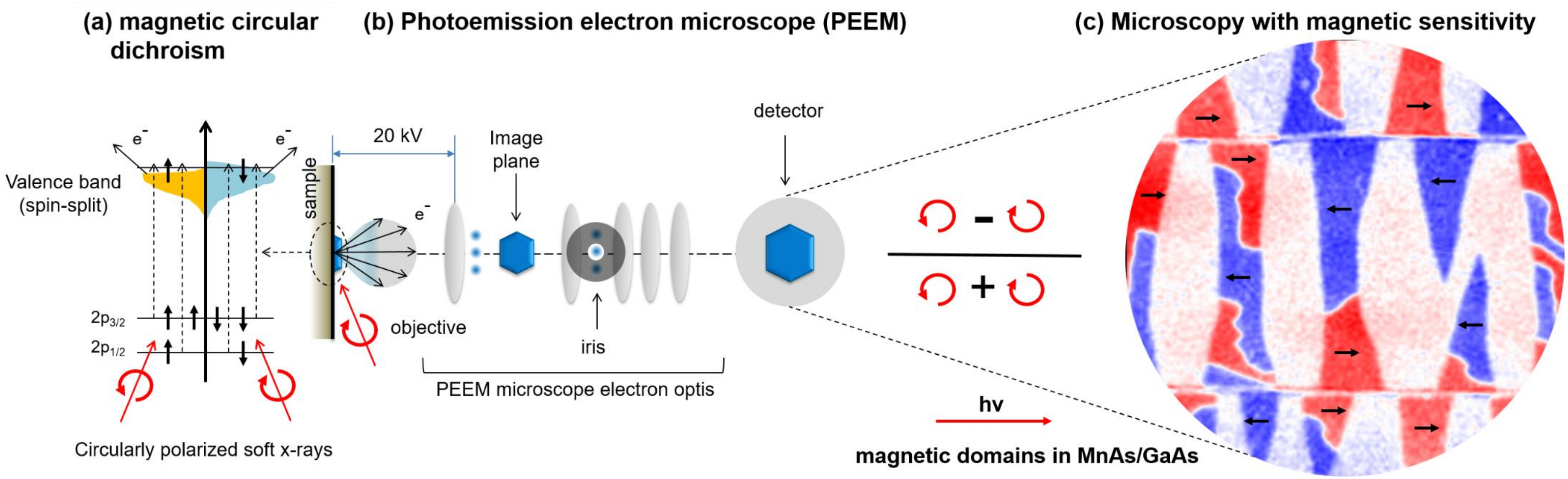

- We **PROBE** 3d elements by exciting 2p into unfilled 3d states
- Dominant channel: 2p → 3d
- White line intensity of the L3 and L2 resonances goes with number of empty d states (holes).
- Photoelectrons with opposite spins are created in the cases of left and right handed polarization. Spin polarization is opposite also for $p_{3/2}$ (L_3) and $p_{1/2}$ (L2) levels.
- The spin-split valence shell is a detector for the spin of the excited photoelectron. The size of the dichroism effect scales like cosθ, where θ is the angle between the photon spin and the magnetization direction.

Magnetic domain imaging by XMCD

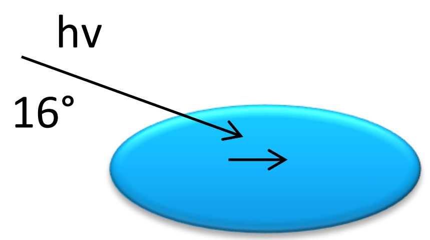

the illumination geometry, → *in plane* component of M

(d) Chemical image of a magnetic nanostructure

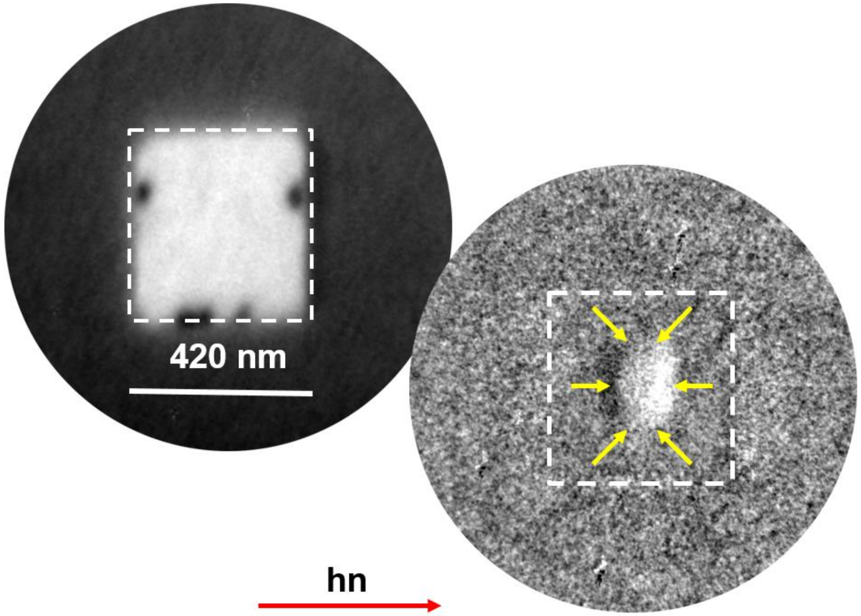

(e) Magnetic image of a skyrmion

- The spin-split valence shell is a detector for the spin of the excited photoelectron. The size of the dichroism effect scales like cosθ, where θ is the angle between the photon spin and the magnetization direction.

Examples of XMCD-PEEM applications

Elettra Sincrotrone Trieste

IMAGING OF MAGNETIC DOMAINS & DOMAIN WALLS

Co nanodots on Si-Ge

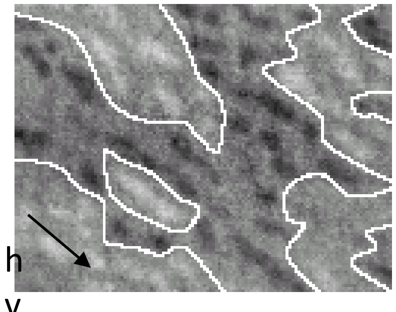

A. Mulders et al, Phys. Rev. B 71, 214422 (2005).

patterned structures

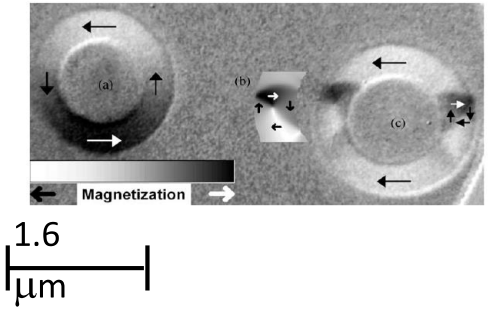

pulse injection

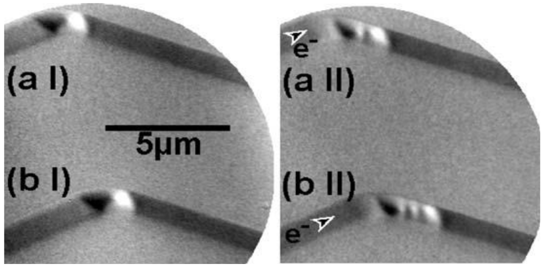

M. Klaeui et al, PRL , PRB 2003 - 2010

domain wall motion induced by spin currents

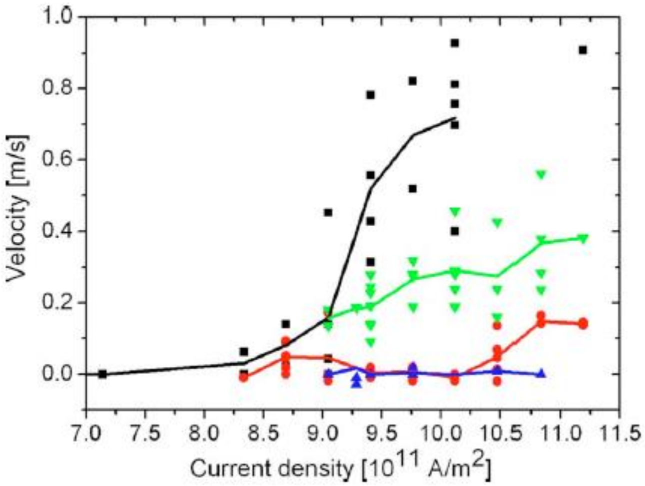

Laufemberg et al, APL 88, 232507(2006).

Examples of XMCD-PEEM applications

Elettra Sincrotrone Trieste

nano-magnetism of (Ga,Fe)N films

Fe L3 edge (chemical)

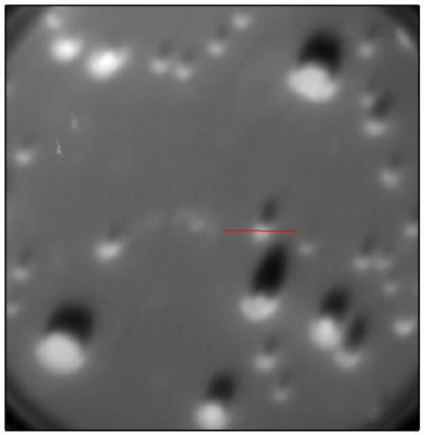

Fe L3 edge (XMCD)

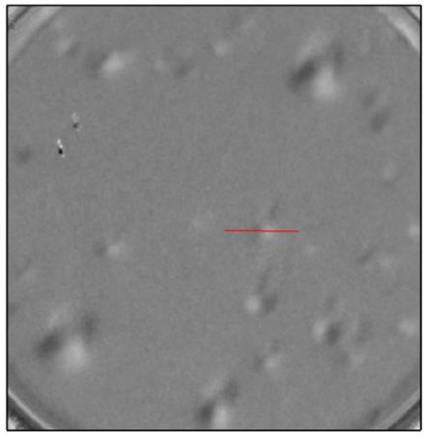

0.4 µm

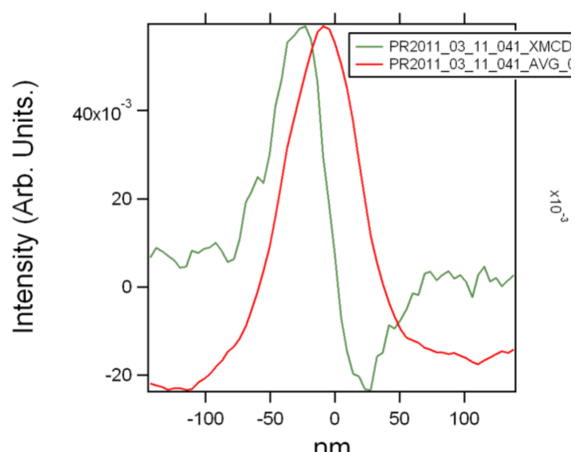

Flux closure domains in some particles

Magnetization in NiPd nanostructures

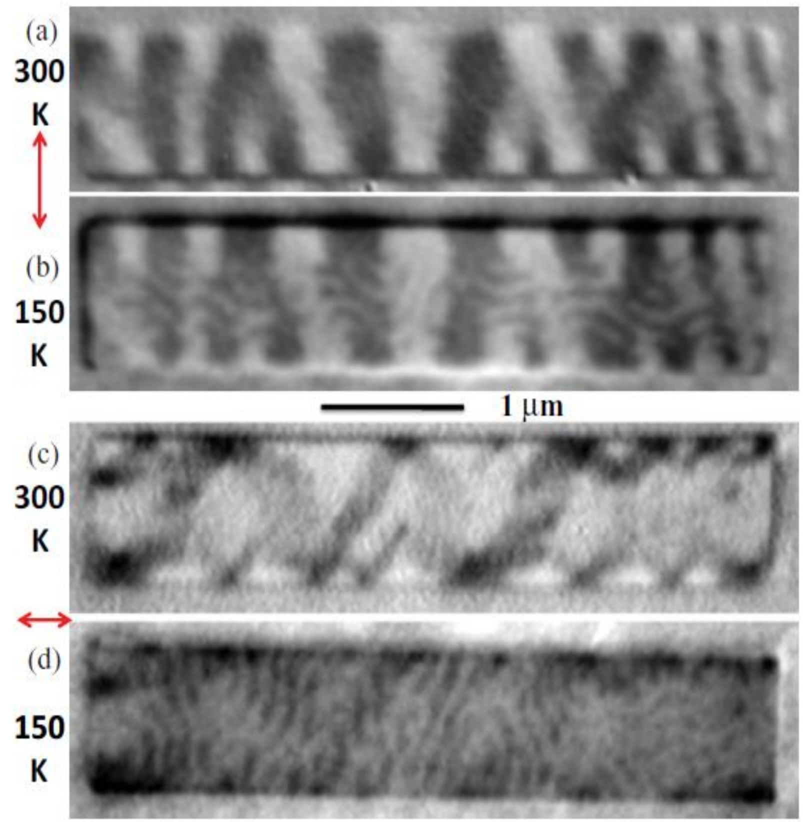

Canted configurations at low temperatures

J.-Y. Chauleau, Phys. Rev. B 84, 094416 (2011)

Time evolution by XMCD-PEEM

Elettra Sincrotrone Trieste

Beamline settings

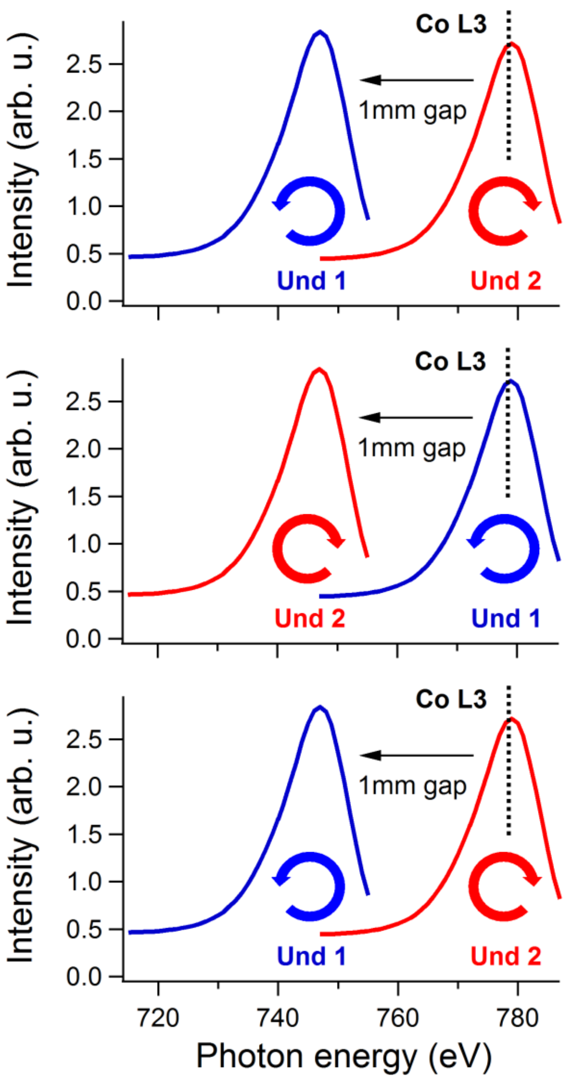

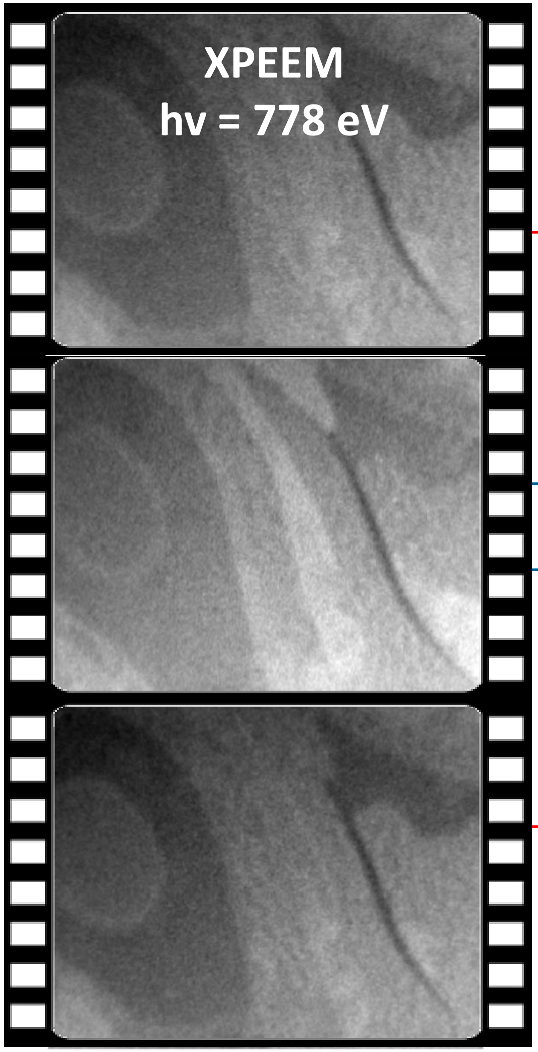

FoV 6 um; 12 sec/frame

$$I^{XMCD} = \frac{I^{-} - I^{+}}{I^{-} + I^{+}}$$

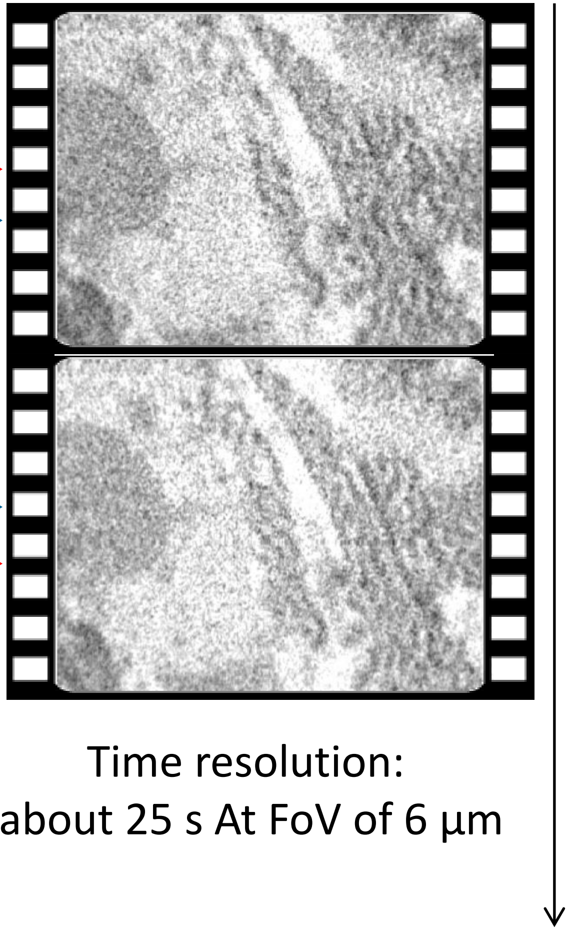

Time resolution:
about 25 s At FoV of 6 µm

SRT upon CO uptake under photon irradiation

Elettra Sincrotrone Trieste

Magnetic configuration of cobalt thin films on Re(0001) upon CO uptake

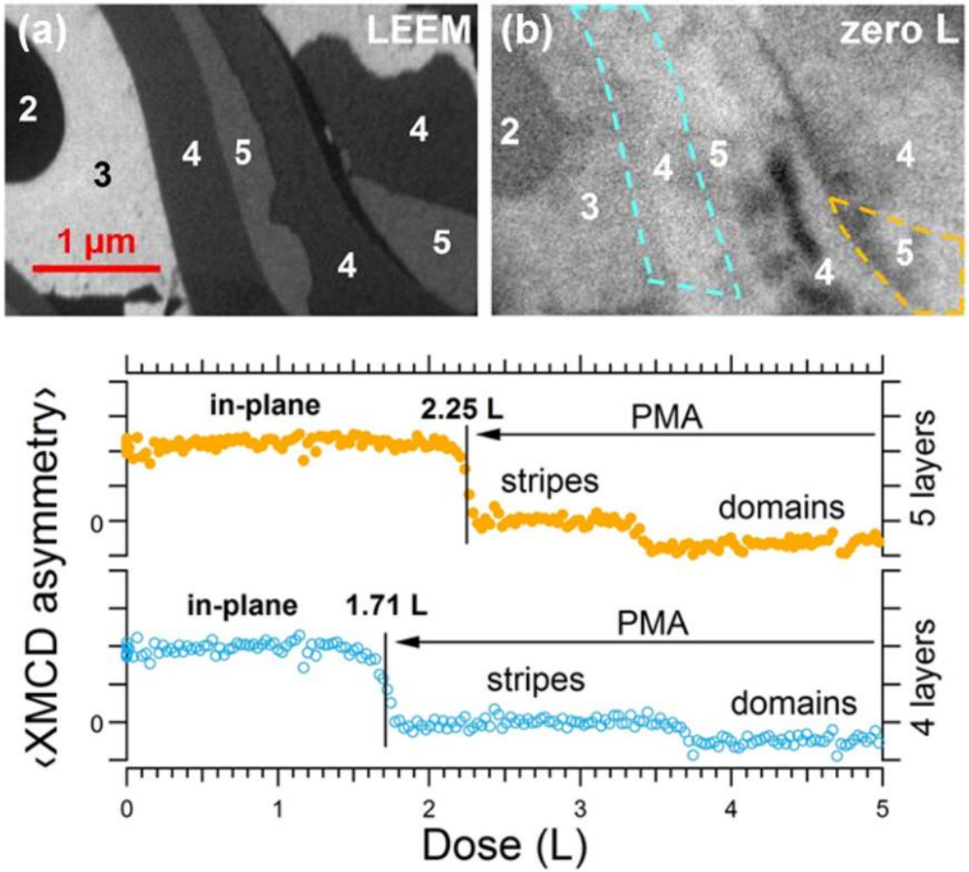

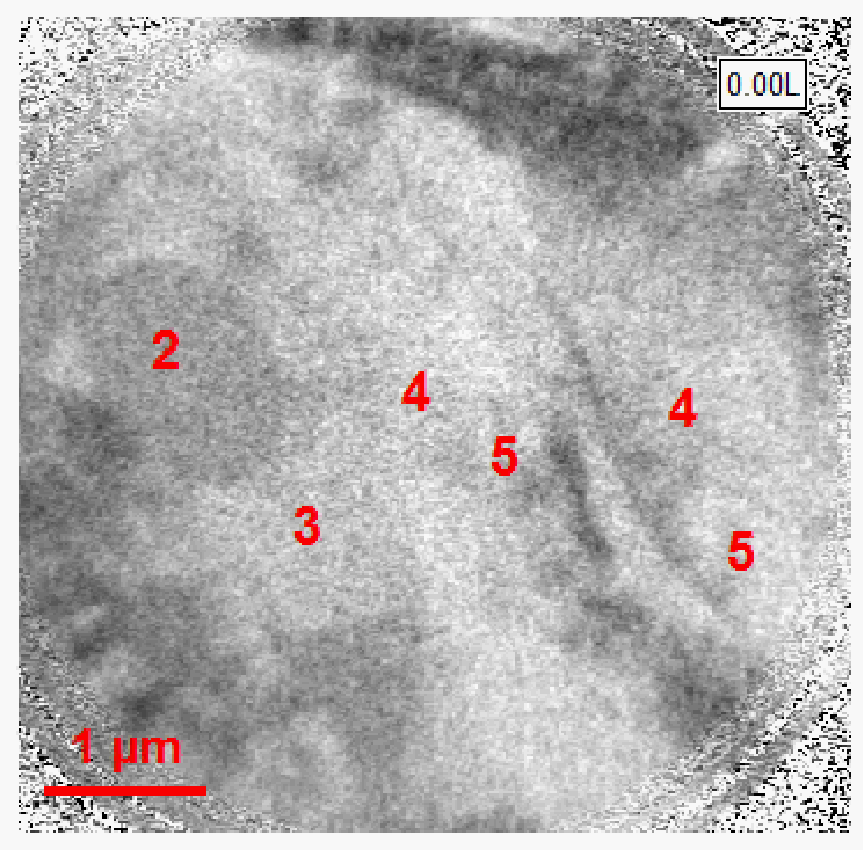

XMCD movie @ Co L_3 edge (780 eV); $P_{CO}=2\cdot10^{-9}$ mbar; frame acquisition 12 s, FoV 6 µm

Magnetic imaging basics: XMLD

Elettra Sincrotrone Trieste

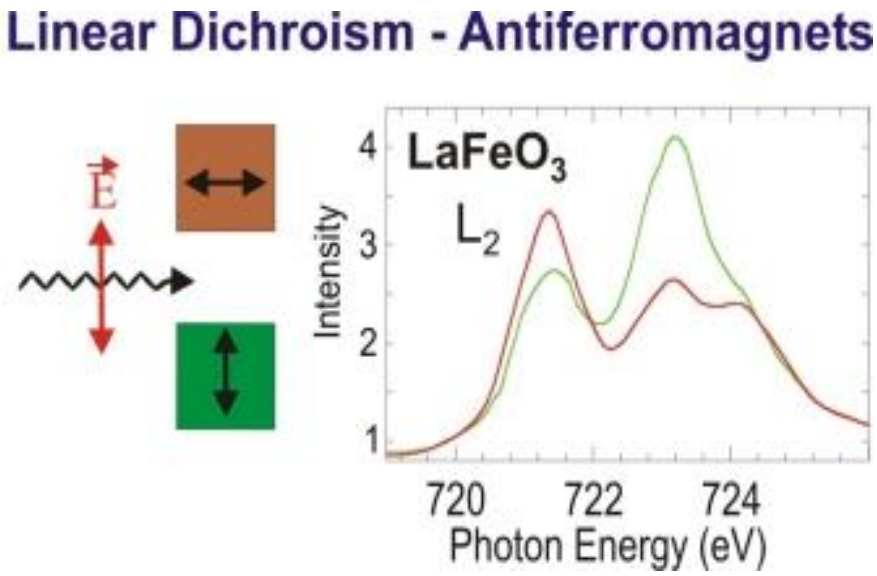

In the presence of spin order the spin-orbit coupling leads to preferential charge order relative to the spin direction, which is exploited to determine the spin axis in antiferromagnetic systems.

✓Element sensitive technique

✓ Secondary imaging with PEEM determine large probing depth (10 nm), buried interfaces.

✓Applied in AFM systems (oxides such as NiO)

Absorption intensity at resonance

$$I(\vartheta,\theta,T) = a + b(3\cos^2\vartheta - 1)\langle Q_{zz}\rangle + c(3\cos^2\theta - 1)\langle M^2\rangle_T + d\sum_{i,j}\langle \hat{s}_i \cdot \hat{s}_j\rangle_T$$

1st term: quadrupole moment, i.e.electronic charge (not magnetic!)

2nd term determines XMLD effect; *Θ* is the angle between E and magnetic axis A; XMLD max for E || A;

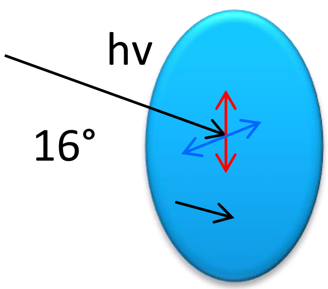

Linear vertical and linear horizontal polarization of the photon beam

Applications of XMCD and XMLD

Direct observation of the alignment of ferromagnetic spins by antiferromagnetic spins

F. Nolting*, A. Scholl*, J. Stöhr†, J. W. Seo‡§, J. Fompeyrine§, H. Siegwart§, J.-P. Locquet§, S. Anders*, J. Lüning†, E. E. Fullerton†, M. F. Toney†, M. R. Scheinfein‖ & H. A. Padmore*

Nature, 405 (2000), 767.

ferromagnet/antiferromagnet
Co/LaFeO3 bilayer
interface exchange coupling
between the two materials

$LaFeO_3$ layer
XMLD Fe L_3

Co layer
XMCD Co L_3/L_2

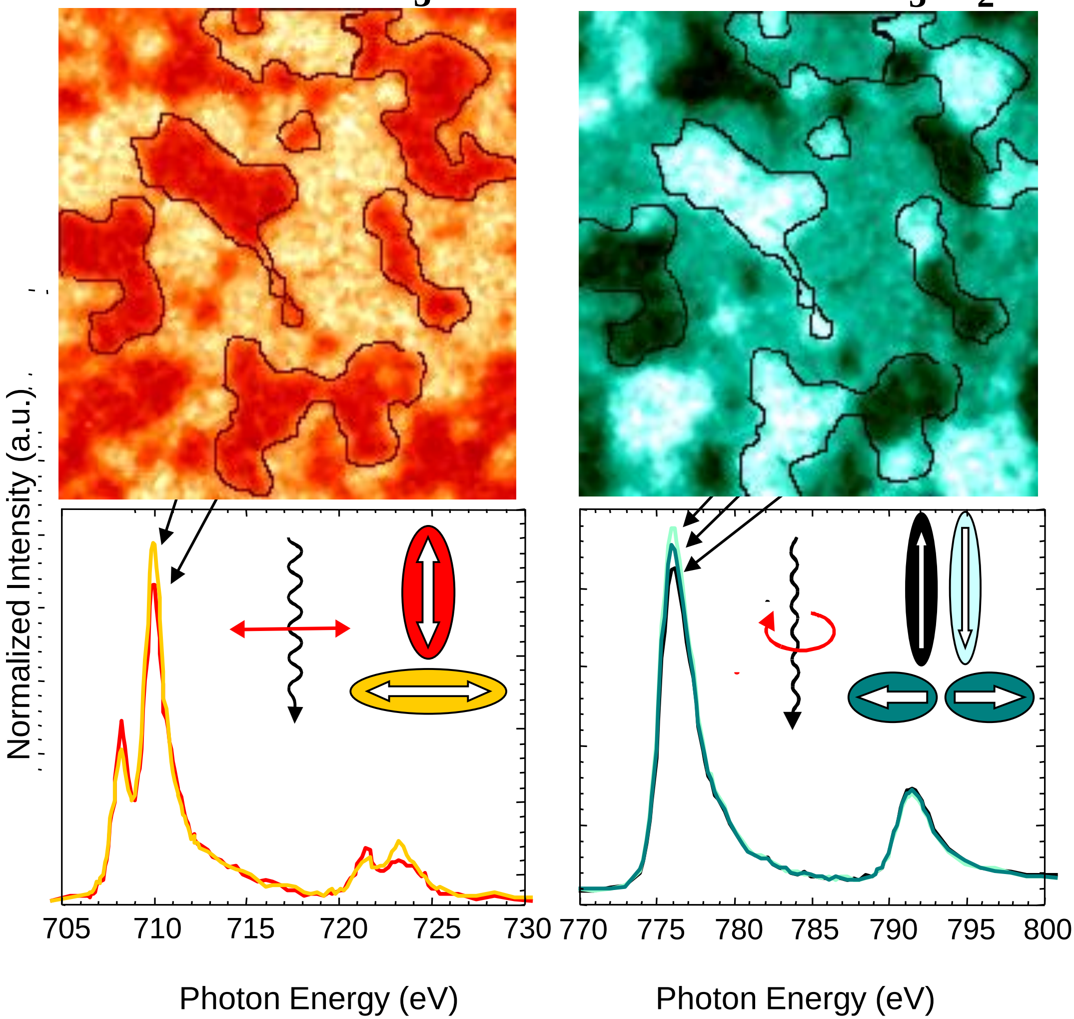

Tomographic imaging in magnetic wires

Observation of Bloch-point domain walls in cylindrical magnetic wir

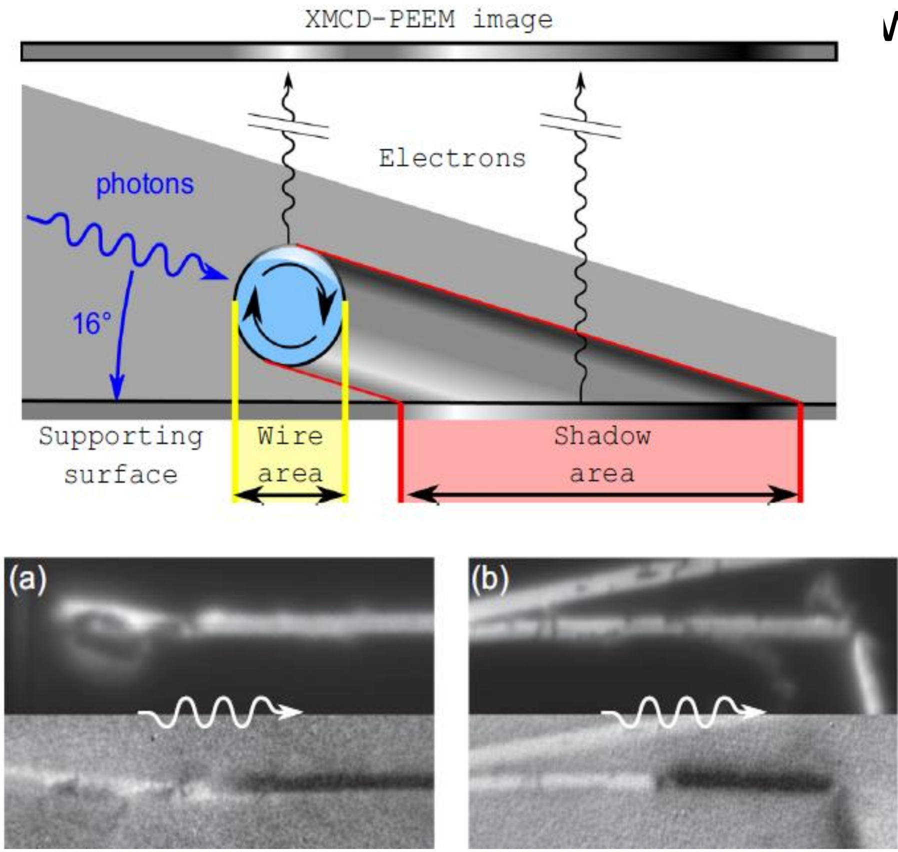

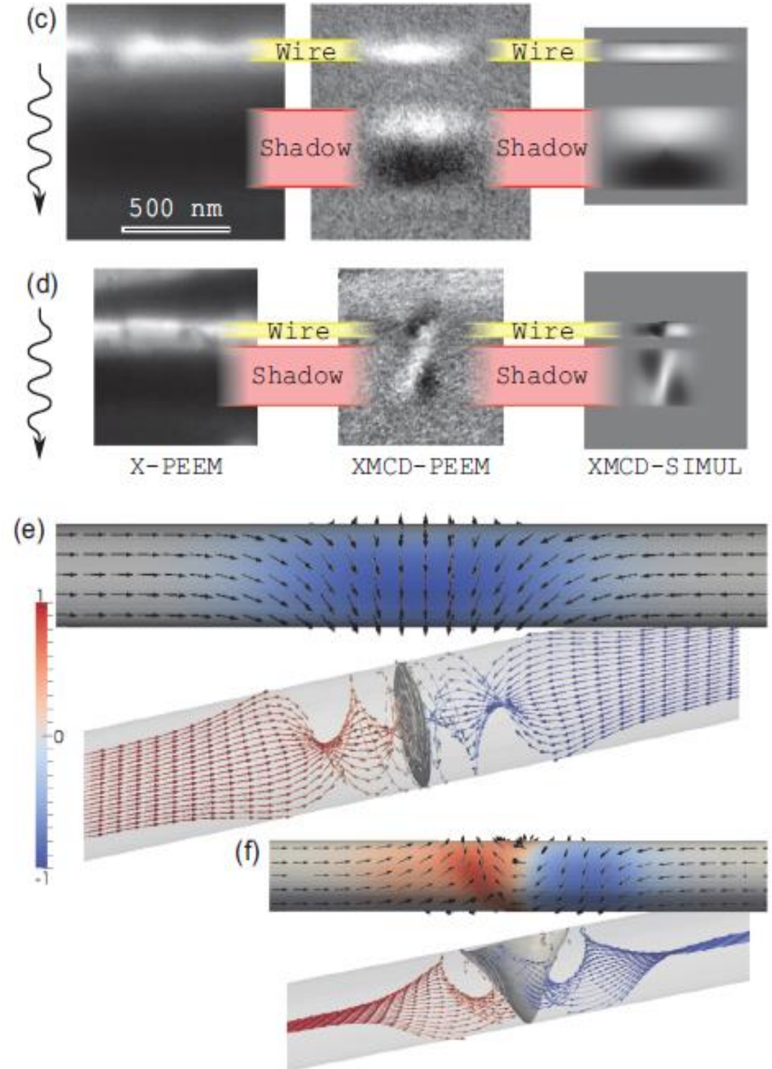

S. Da Col *et al*., Phys. Rev. B**89**, 180405(R) (2014)

Limited probing depth of XMCD: MnAs/GaAs

Elettra Sincrotrone Trieste

Experiment: Straight walls; Head to head domains

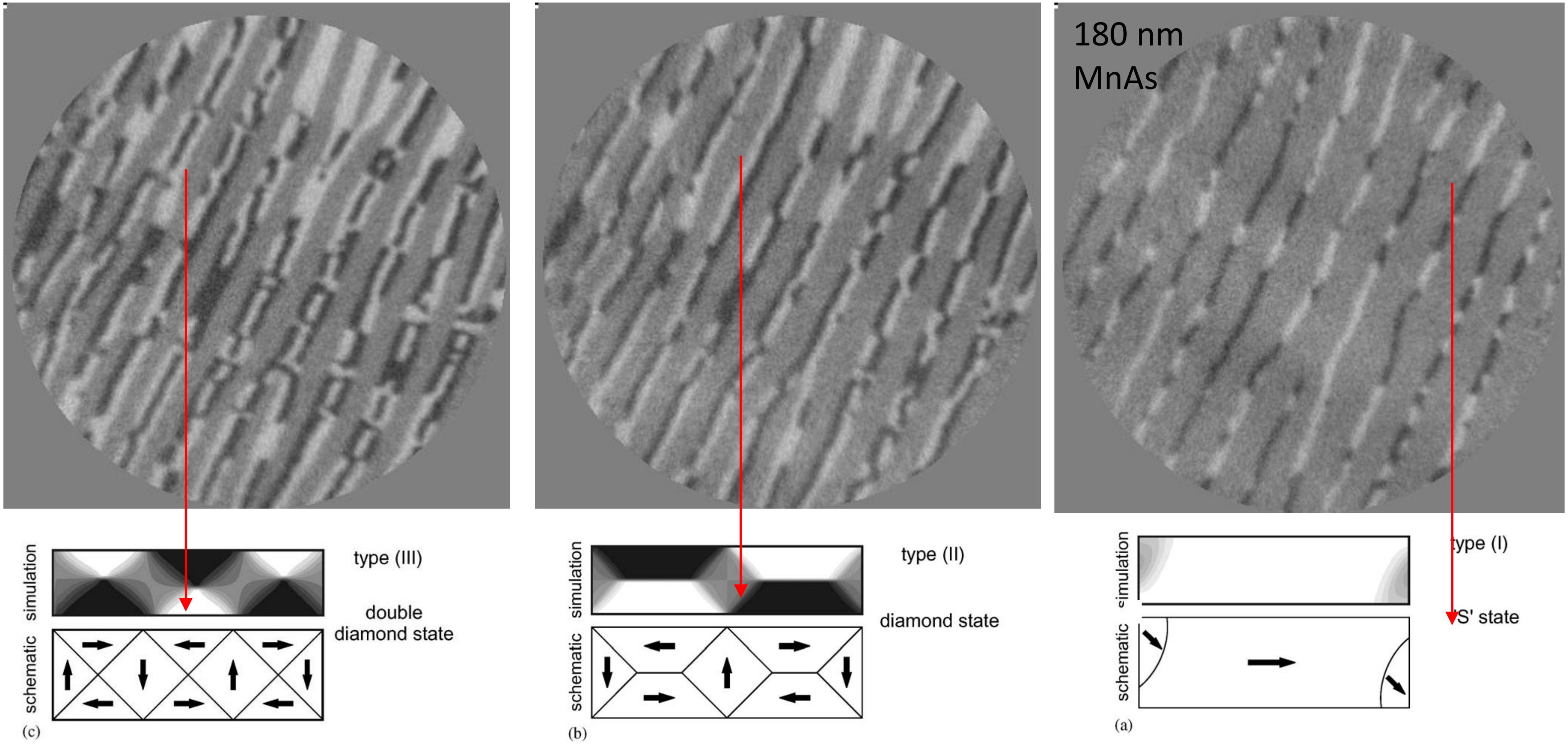

Simulation: Cross sectional cut: diamond state

R. Engel-Herbert et al, J. Magn. Magn. Mater. 305, (2006) 457

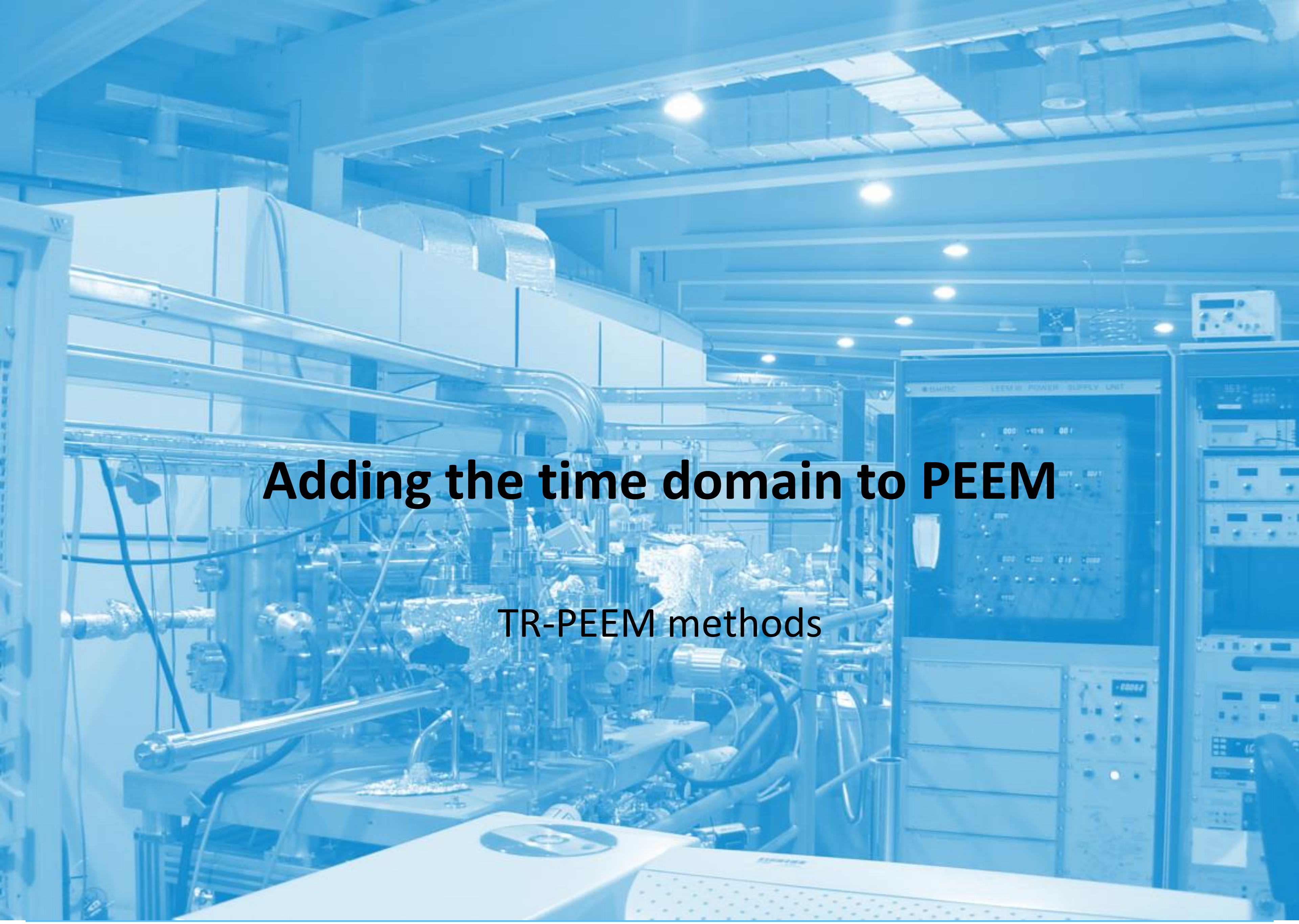

Adding the time domain to PEEM

TR-PEEM methods

Time-resolved PEEM: the stroboscopic approach

Elettra Sincrotrone Trieste

Stroboscopic experiments combine high lateral resolution of PEEM with high time resolution, taking advantage of pulsed nature of synchrotron radiation

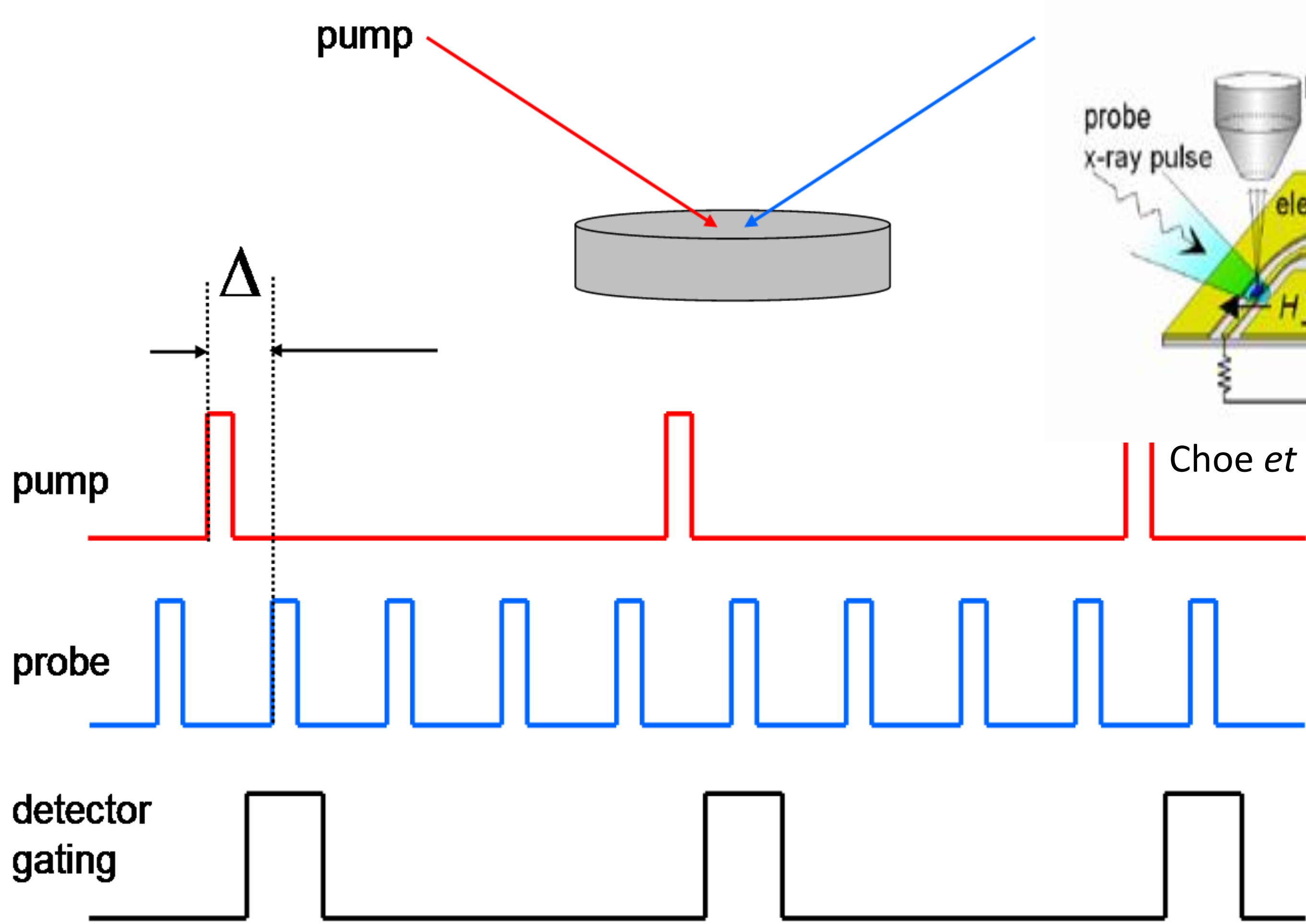

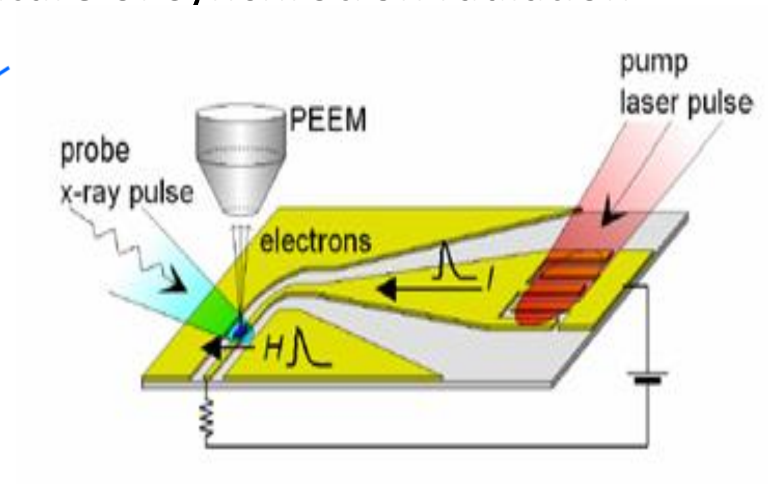

Choe *et al.*, Science 304, 420 (2004)

Time resolved XMCD-PEEM: applications

Elettra Sincrotrone Trieste

- **Switching processes** (magnetisation reversal) in magnetic elements (in spin valves, tunnel junction)
  - Nucleation, DW propagation or both
  - Effect of surface topography, morphology crystalline structure etc.
  - Domain dynamics in Landau flux closure structures.
- response of vortices, domains, domain walls in Landau closure domains in the **precessional regime**
- **Stroboscopic technique**:
  - <u>only reversible processes can be studied by pump – probe experiments</u>
  - Measurements are quantitative

Magnetic excitations in LFC structures

Elettra Sincrotrone Trieste

Quantitative Analysis of Magnetic Excitations in Landau Flux-Closure Structures Using Synchrotron-Radiation Microscopy

J. Raabe,[1,*] C. Quitmann,[1] C. H. Back,[2] F. Nolting,[1] S. Johnson,[1] and C. Buehler[1]

The time dependent magnetization is described by the phenomenological Landau-Lifshitz-Gilbert equation

$$\frac{d}{dt}\vec{M} = -\gamma_0 \vec{M} \times \vec{H}_{\text{eff}} + \frac{\alpha}{M}\left(\vec{M} \times \frac{d}{dt}\vec{M}\right).$$

The first term describes the precession of the magnetization $\vec{M}$ about the total effective field $\vec{H}_{\text{eff}}$. The second term describes the relaxation back into the equilibrium state using the dimensionless damping parameter α.

torque $\vec{T} = -\gamma_0 \vec{M} \times \vec{H}_{\text{eff}}$

xmcd

$t_i - t_0$

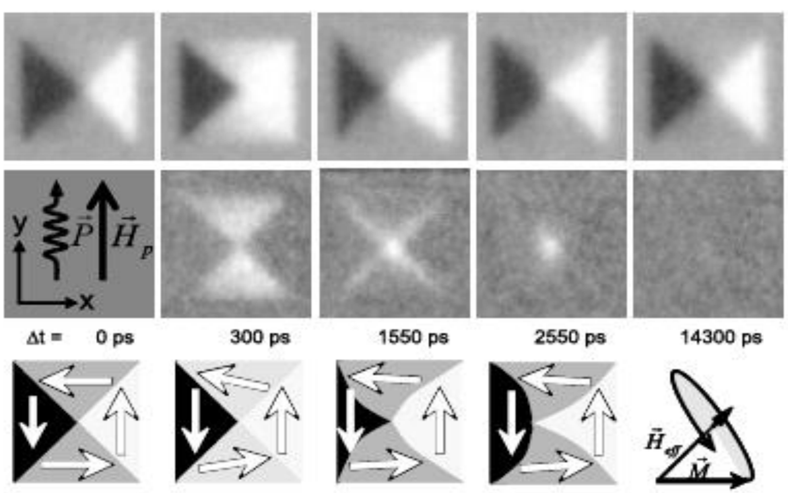

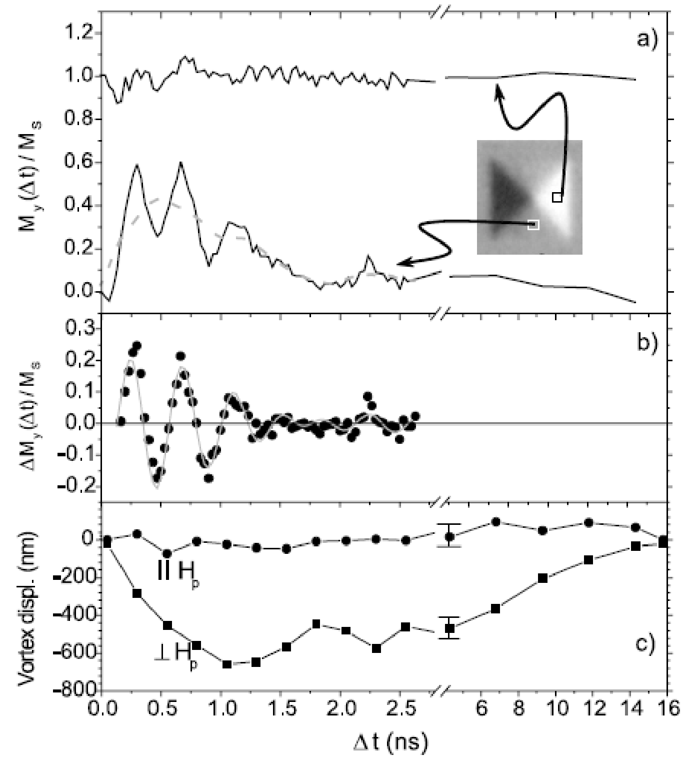

Summary

- XPEEM is a versatile full-field imaging technique. Combined with SR it allows us to implement laterally resolved versions of the most popular x-ray spectroscopies taking advantage of high flux of 3rd generation SR light sources.
- In particular, XAS-PEEM combines element sensitivity with chemical sensitivity (e.g. valence), and, more importantly, magnetic sensitivity. Magnetic imaging has been the most successful application of PEEM (next tutorial lecture!).
- XPEEM or energy-filtered PEEM adds true chemical sensitivity to PEEM. Modern instruments allow to combine chemistry with electronic structure using ARUPS.
- XPEEM can be complemented by LEEM, which adds structure sensitivity and capability to monitor dynamic processes.
- Lateral resolution will approach the nm range as AC instruments become available. Limitations due to space charge are not yet clear
- Novel application field are being approached, such as biology, geology and earth sciences. HAXPES will increase our capabilities to probe buried structures (bulk).

Review work

Elettra Sincrotrone Trieste

Reviews and topical papers on x-ray spectromicroscopy and XPEEM

- S. Guenther, B. Kaulich, L.Gregoratti, M. Kiskinova, *Prog. Surf. Sci.* **70**, 187–260 (2002).
- E. Bauer, *Ultramicroscopy* **119**, 18–23 (2012).
- E. Bauer, *J. Electron. Spectrosc. Relat. Phenom*. (2012): http://dx.doi.org/10.1016/j.elspec.2012.08.001
- G. Margaritondo, *J. Electron. Spectrosc. Relat. Phenom.* **178–179**, 273–291 (2010) .
- A. Locatelli, E. Bauer, *J. Phys.: Condens. Matter* **20**, 093002 (2008) .
- G. Schönhense *et al*., in "*Adv. Imaging Electron Phys.*", vol. **142**, Elsevier, Amsterdam, P. Hawkes (Ed.), 2006, pp. 159–323.
- G. Schönhense, *J. Electron. Spectrosc. Relat. Phenom.* **137–140**, 769 (2004) .
- C.M. Schneider, G. Schönhense, *Rep. Prog. Phys.* **65**, R1785–R1839 (2002) .
- W. Kuch, in "*Magnetism: A Synchrotron Radiation Approach*", Springer, Berlin, E. Beaurepaire et al. (Eds.), 2006, pp. 275–320.
- J. Feng, A. Scholl, in P.W. Hawkes, "*Science of Microscopy*", Springer, New York, J.C.H. Spence (Eds.), 2007, pp. 657–695.
- E. Bauer and Th. Schmidt, in "*High Resolution Imaging and Spectroscopy of Ma-terials*", Springer, Berlin, Heidelberg, F. Ernst and M. Ruehle (Eds.), 2002, pp. 363-390.
- E. Bauer, *J. Electron Spectrosc. Relat. Phenom.* **114-116,** 976-987 (2002).
- E. Bauer, *J. Phys.: Condens. Matter* **13,** 11391-11405 (2001).